2015-02-04

Clumped Isotope Signals of Biogenic and Non-biogenic Carbonates

Deniz Atasoy
University of Miami, atasoy.deniz@hotmail.com

UNIVERSITY OF MIAMI

CLUMPED ISOTOPE SIGNALS OF BIOGENIC AND NON-BIOGENIC CARBONATES

By

Deniz Atasoy

A THESIS

Submitted to the Faculty
of the University of Miami
in partial fulfillment of the requirements for
the degree of Master of Science

Coral Gables, Florida

May 2015

UNIVERSITY OF MIAMI

A thesis submitted in partial fulfillment of
the requirements for the degree of
Master of Science

CLUMPED ISOTOPE SIGNALS OF BIOGENIC AND NON-BIOGENIC CARBONATES

Deniz Atasoy

Approved:

_____	_____
Peter K. Swart, Ph.D. Lewis J. Weeks Professor of Marine Geology and Geophysics	Gregor Eberli, Ph.D. Professor of Marine Geology and Geophysics
_____	_____
Bernard Riegl, Ph.D. Associate Director of National Coral Reef Institute Miami, Florida	M. Brian Blake, Ph.D. Dean of the Graduate School

ATASOY, DENIZ (M.S., Marine Geology and Geophysics)
Clumped Isotope Signals of Biogenic and Non-biogenic Carbonates (May 2015)

Abstract of a thesis at the University of Miami.

Thesis supervised by Professor Peter K. Swart.
No. of pages in text. (130)

The $\delta^{18}O$ of carbonates is most one of the most popular tools used in both marine and terrestrial environments to reconstruct past climate and understand diagenesis. The major problem with the use of the $\delta^{18}O$ is that the value within a carbonate is dependent both upon temperature and the $\delta^{18}O$ of the precipitating fluid. This dilemma is potentially solvable using clumped signatures reported as Δ_{47} which is a direct measure of the temperature of formation only.

This thesis consists of three projects all of which have applied the clumped isotope method. The common thread of all of these projects is to understand the distribution of the Δ_{47} in modern sediments and those which have been influenced by early diagenesis.

The first of these project examines the Δ_{47} in a suite of mainly non-biogenic carbonates from Great Bahama Bank including mudstones, wackestones, packstones, grainstones and rudstone (ooids, pellets, peloids, and grapestone). Such data will serve as a reference for future diagenetic and paleoenvironmental studies involving non-biogenic sediments. In this study a facies control has been observed as the clumped signals

increase and temperature values decrease from muddy facies to grainy facies. Temperatures of formation of the platform carbonates calculated using carbonate clumped isotope paleo-thermometry agree with expected sea surface temperatures on the platform. Oxygen isotopic values of the waters calculated from the $\delta^{18}O$ of the carbonates and the clumped isotope data agree with the values previously measured.

The second study examines the clumped isotopic signature in corals from the island of Tobago. These corals are seasonally bathed by waters originating from the Orinoco and the Amazon rivers and hence the $\delta^{18}O$ of a coral skeleton is influenced by the magnitude of this fluviatile input as well as variations in temperature. Clumped isotope analysis makes it possible to distinguish the temperature induced $\delta^{18}O$ signal from that exerted by the freshwater and consequently calculate the annual variation in the Orinoco discharge.

The last study examines the Δ_{47} of young calcrete complexes. They are frequently used for the reconstruction of paleoclimate and paleoenvironmental conditions and record the $\delta^{18}O$ values of rainfall, but the interpretation is frequently complicated by uncertainty as regards the formation temperature. The clumped isotope method allows to measure formation temperature of the calcrete samples and reveals knowledge of $\delta^{18}O$ of the precipitating water. In the sub-arid conditions of Hog Cay the formation temperatures of calcretes are higher than the mean annual summer temperature, while formation temperature values are consistent with mean annual temperature in New Providence.

ACKNOWLEDGMENTS

This thesis has grown out of over two years of hard work, and would not have been possible without the assistance, encouragement and support of professors, friends and family who have accompanied me while working on my projects.

First and foremost, I would like to express my gratitude to my thesis advisor, Peter K. Swart, whose patience, guidance and suggestions helped me along the way to understand clumped isotopes, shaping my training, and giving ideas to solve scientific problems and unraveling new insights. Always his door was open for discussions when I needed help. I am deeply indebted to my committee members, Dr. Gregor Eberli and Dr. Bernard Riegl for their outstanding contributions to this study. I am also thankful to Dr. Greta Mackenzie for her helpful reading of the document.

I am extremely grateful to Turkish Petroleum Corporation for giving me the invaluable chance to receive a MSc Degree and providing a job position and financial supports. I also want to thank the Stable Isotope Laboratory for financial help.

I sincerely appreciate the help and friendships from all wonderful members of the Stable Isotope Laboratory and particularly sending deepest thanks to Sean Murray and Monica Arienzo for helping me get started on the clumped isotope lab work. I am also thankful to friendship of all of the MGG faculty staff, and students who have made my life at RSMAS more fun and colorful. I would like to thank Deniz Kula, Ergin Karaca, and Emre Havazli who never have made me feel homesick and alone in Miami.

Finally, I am most grateful to my son Demir Atasoy for making my time memorable. I am very thankful to my wife Tulin Atasoy for all her love, patience and encouragement that gave me the energy and confidence to complete this study.

TABLE OF CONTENTS

Page

LIST OF FIGURES

LIST OF TABLES

CHAPTER 1

METHODOLOGY OF CLUMPED ISOTOPE MEASUREMENTS OF CARBONATE SAMPLES

1.1. Introductory Remarks

An understanding of the variations that exist in ancient environments, particularly those related to climate, are crucial for the interpretation of current and future changes in Earth's history. Critical in this regard are various isotopic proxies such as the $^{18}O/^{16}O$ ratio in carbonates and other minerals. Using this ratio, principally in foraminifera, has been a cornerstone of the field of paleooceanography and paleoclimatology. In recent years, it has been recognized that multiply substituted isotopologues from carbonates can provide paleotemperatures independent of the isotopic composition of the water. In the case of carbonates and the CO_2 produced during the reaction of phosphoric acid with the carbonate, the species of interest occur at mass 47, $^{13}C^{18}O^{16}O$. The measurement of ratios of mass 47/44 is referred to as the clumped isotope method.

Although Urey and Bigeleisen examined the measurement of multiply substituted isotolopogues for the first time in the 1950s, analyses were hampered by the limitation of instruments (Bigeleisen and Mayer, 1947; Urey, 1947) which were available at the time and it was not until the 1990s that the first analyses were made (Eiler and Schauble, 2004). Wang et al. (2004) and Schauble et al. (2006) developed a theoretical basis for the applications of carbonate minerals as a carbonate clumped isotope thermometer and

temperature calibration of inorganically precipitated carbonates was published by Ghosh et al. (2006).

Since then, numerous publications have appeared (Ghosh et al., 2007; Came et al., 2007; Affek et al., 2008; Eagle, 2010; Tripati et al., 2010; Thiagarajan et al., 2011; Zaarur et al., 2011; Saenger et al., 2012; Kluge et al., 2012; Dennis et al., 2013; Henkes et al., 2013; Grauel et al., 2013; Zaarur et al., 2013; Eagle et al., 2013; Hill et al., 2013; Wacker et al., 2014; Tang et al., 2014; Fernandez et al., 2014). Although these promising studies have provided valuable contributions to develop theoretically or experimentally its applications and to better understand the limitations, the new field is still evolving. In this regard, this thesis which includes three studies using clumped isotope thermometry will add several more pieces to complete the puzzle.

1.2. Theory of Clumped Isotopes

1.2.1. Principles of the method

Clumped isotope geochemistry basically focuses on multiply substituted isotolopogues and their thermodynamic tendencies such as zero point energies and bond vibration frequencies. When a heavy isotope substitutes with a light isotope, the substitution impacts the thermodynamic properties. In this case, molecular stability of the bond decreases between two atoms and consequently the zero point energy of the bond diminishes. The decreased zero point energy of bond between two heavy isotopes results in more stability than the bond between a heavy and light isotope. In this respect, two heavy isotopes have the lowest zero-point energy and the slowest vibration frequencies (Bigeleisen and Mayer, 1947; Urey, 1947; Eiler, 2007).

Variations in vibrational energy of a bond associated with double heavy isotope substitution is approximately twice that of the single heavy isotope substitution of one atom (Eiler, 2007), which provides the thermodynamic driving effect that causes clumping of the isotopes (Wang et al., 2004; Schauble et al., 2006; Affek, 2012). This assumption is known as the 'rule of means' in stable isotope chemistry (Bigeleisen, 1955). While the driving force can be described as a homogeneous isotope exchange reaction (Reaction 1), it is driven towards the right side owing to the decreasing total zero point energy of the heavier isotope which is more stable.

$$\mathbf{2\ HD = H_2 + D_2} \qquad \mathbf{(1)}$$

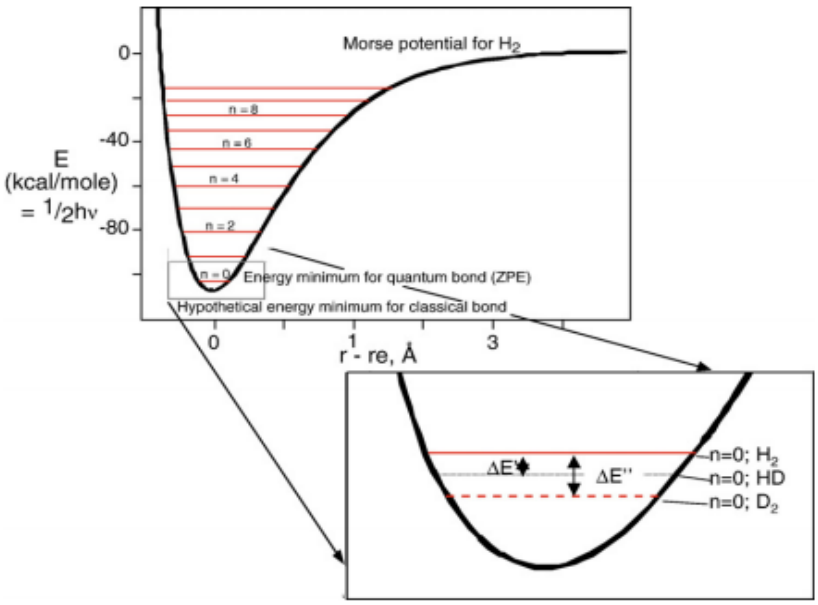

Figure 1.1*: The diagram from Eiler, 2007 is explaining changes in zero point energy for the stable isotopes of hydrogen. Although two heavy isotopes (D_2) have the lower energy, two light isotopes (H_2) show the higher energy based on explanation of Urey, (1947), Bigeleisen et al. (1947).*

The force decreases with increasing temperature. Therefore, the heavy isotopes do not tend to chemically bond to each other due to the effect of the increased temperature

and reach their random isotopic distributions at high temperatures (1000°C). However, a thermodynamically equilibrated abundance of isotolopogues will have a greater population of doubly substituted isotolopogues, this principal forms the basis of carbonate clumped isotope geochemistry.

CO_2 mass	Isotopologues	Relative abundance
44	$^{12}C^{16}O_2$	98.40%
45	$^{13}C^{16}O_2$	1.11%
	$^{12}C^{17}O^{16}O$	748 ppm
46	$^{12}C^{18}O^{16}O$	0.40%
	$^{13}C^{17}O^{16}O$	8.4 ppm
	$^{12}C^{17}O_2$	0.142 ppm
47	$^{13}C^{18}O^{16}O$	44.4 ppm
	$^{12}C^{17}O^{18}O$	1.5 ppm
	$^{13}C^{17}O_2$	1.6 ppb
48	$^{12}C^{18}O_2$	3.96 ppm
	$^{13}C^{17}O^{18}O$	16.8 ppb
49	$^{13}C^{18}O_2$	44.5 ppb

Figure 1.2*: The twelve isotolopogues of CO_2 along with their abundances (modified from Eiler, 2007). Clumped isotopes are analyzed as CO_2 derived from phosphoric acid reaction with carbonates (See section 2.1).*

In the case of carbonates, although there are 12 stable isotopic variants of CO_2 in nature (Figure 1.2.) excluding ^{14}C, eight of these reflect multiply substituted species derived from phosphoric acid digestion of carbonate minerals. Clumped isotope analyses aim to measure the deviation from the expected abundance of multiply substituted isotolopogues if all isotopes had a stochastic distribution. Analysis focuses on mass 47 which consist predominantly of $^{13}C^{16}O^{18}O$ and two more isotolopogues ($^{13}C^{17}O^{17}O$, $^{12}C^{18}O^{17}O$) which cannot be distinguished and are analyzed together by the mass spectrometer.

Although the method has served various applications in many disciplines of geosciences and has been successfully used to solve a number of different problems, the majority of studies utilizing clumped isotopes have focused on applications specific to carbonate clumped isotope thermometry.

1.2.2. Carbonate clumped isotope geothermometry

Clumped isotope thermometry combines aspects of physical chemistry with traditional carbonate–water oxygen paleothermometry which is based on heterogeneous isotope equilibrium (Reaction 2). Traditional paleothermometry has been most widely applied to the reconstruction of past temperatures from carbonates using knowledge of the distribution of $\delta^{18}O$ in both minerals and water (McCrea, 1950; Epstein et al., 1951). Rigorously constraining the oxygen isotopic composition of water is long-standing dilemma in order to determine the temperature of recrystallization of carbonates with a single analysis. This limitation has restricted applications of the conventional oxygen thermometry in deep Earth's history.

$$\mathbf{CaC^{16}O_3 + H_2{}^{18}O = CaC^{18}O^{16}O_2 + H_2{}^{16}O} \qquad \mathbf{(2)}$$

However, the new geothermometer examines homogeneous isotope equilibrium (Reaction 3). The isotope exchange reaction shows clumping of heavy and rare (^{13}C and ^{18}O) isotopes each other with chemical bonds results in the $Ca^{13}C^{18}O^{16}O_2$ ion group (Eiler, 2011). Reaction 3 is temperature dependent and the equilibrium constant increases with decreasing temperature (Schauble et al., 2006).

$$\mathbf{Ca^{13}C^{16}O_3 + Ca^{12}C^{18}O^{16}O_2 = Ca^{13}C^{18}O^{16}O_2 + Ca^{12}C^{16}O_3} \qquad \mathbf{(3)}$$

This geothermometer is based on the enrichment of ^{13}C and ^{18}O bonds in carbonate minerals (Affek, 2012) and is defined as Δ_{47} in the CO_2 extracted from $CaCO_3$ minerals by acid reaction (Details in 2.1). Δ_{47} is a measure of the abundance of clumped isotopes in the carbonate mineral and is independent of $\delta^{13}C$ and $\delta^{18}O$ abundance. This independence makes it possible to calculate the temperature of formation without knowledge of the oxygen and carbon isotopic composition of the fluid (Ghosh et al., 2006; Eiler, 2007, 2011; Affek et al., 2008; Huntington et al., 2009) (Figure 3).

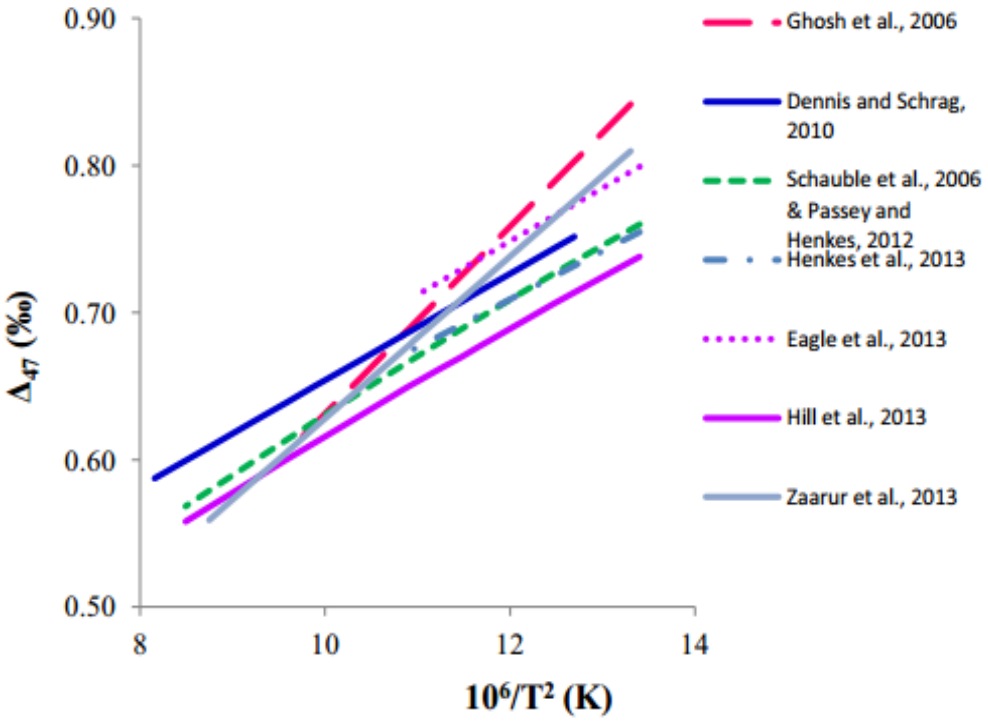

Figure 1.3: *Figure from Tang et al. (2014) displaying an inverse relationship between clumped signals and formation temperatures of both biogenic, abiogenic samples and theoretical calculations. Δ_{47} are reported on the reference framework (Dennis et al., 2011).*

Since the seminal study of Ghosh et al. (2006), a number of other Δ_{47}-temperature calibrations have been published, (Dennis and Schrag, 2010; Zaarur et al., 2013; Tang et al., 2014) including those for biogenic samples (Ghosh et al., 2007; Came et al., 2007; Eagle et al., 2010; Tripati et al., 2010; Thiagarajan et al., 2011; Zaarur et al., 2011; Saenger et al., 2012; Henkes et al., 2013; Grauel et al., 2013; Dennis et al., 2013).

In addition, theoretical calibration studies have been published (Schauble et al., 2006; Guo et al., 2009; Hill et al., 2013). On the other hand, the calibration of recent works of biogenic carbonates (Dennis et al., 2013; Henkes et al., 2013; Eagle et al., 2013) are similar to the calibration proposed by Dennis and Schrag et al. (2010). As it appears, the issue of calibration is a cornerstone of carbonate clumped isotope thermometry. The following section will discuss recently published temperature calibrations utilized in this study.

Discrepancies among these can be considered to be a result of several factors, for example, standardization or analytical problems, ambiguity of formation temperature and kinetic effects (Tang et al., 2014).

In an attempt to standardize the results of different laboratories and minimize possible analytical artifacts Dennis et al. (2011) proposed a reference framework to standardize carbonate clumped isotope measurements. Thus, the clumped isotope data of this study is normalized to the Dennis et al. (2011) scale which is given in section 2.3.

1.3. Experimental Part of Clumped Isotopes

1.3.1. Acid digestion and purification of CO_2

Approximately 8±0.3 mg of powdered carbonate samples are reacted for 30 minutes with 103% phosphoric acid (H_3PO_4) at 90°C in the vessel using the common acid method (Swart, 1991) (Equation 4) with released CO_2 collected in a U-trap by liquid nitrogen at -196°C. After the reaction time, methanol at 90°C is placed under the first U-trap to get rid of H_2O and $CaHPO_4$ by high vacuum.

$$CaCO_3 + H_3PO_4 \leftrightarrow CaHPO_4 + CO_2 + H_2O \quad (4)$$

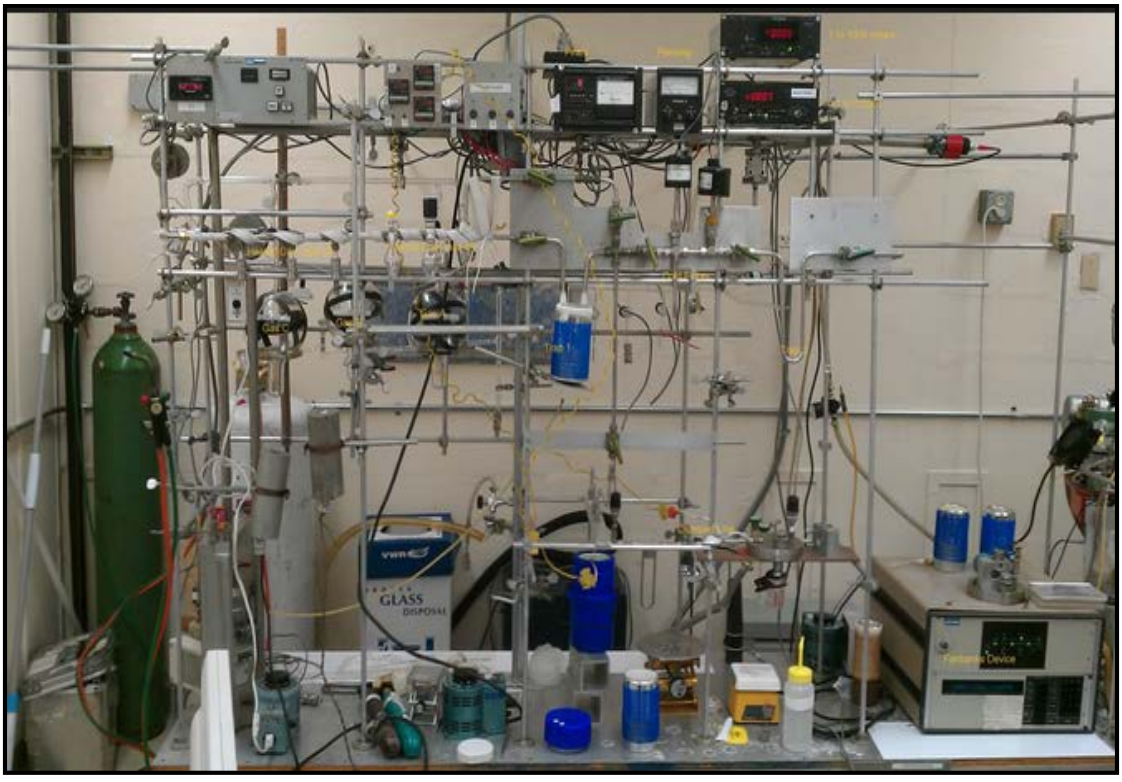

Figure 1.4: *Gas purification line, stable isotope laboratory, University of Miami, RSMAS*

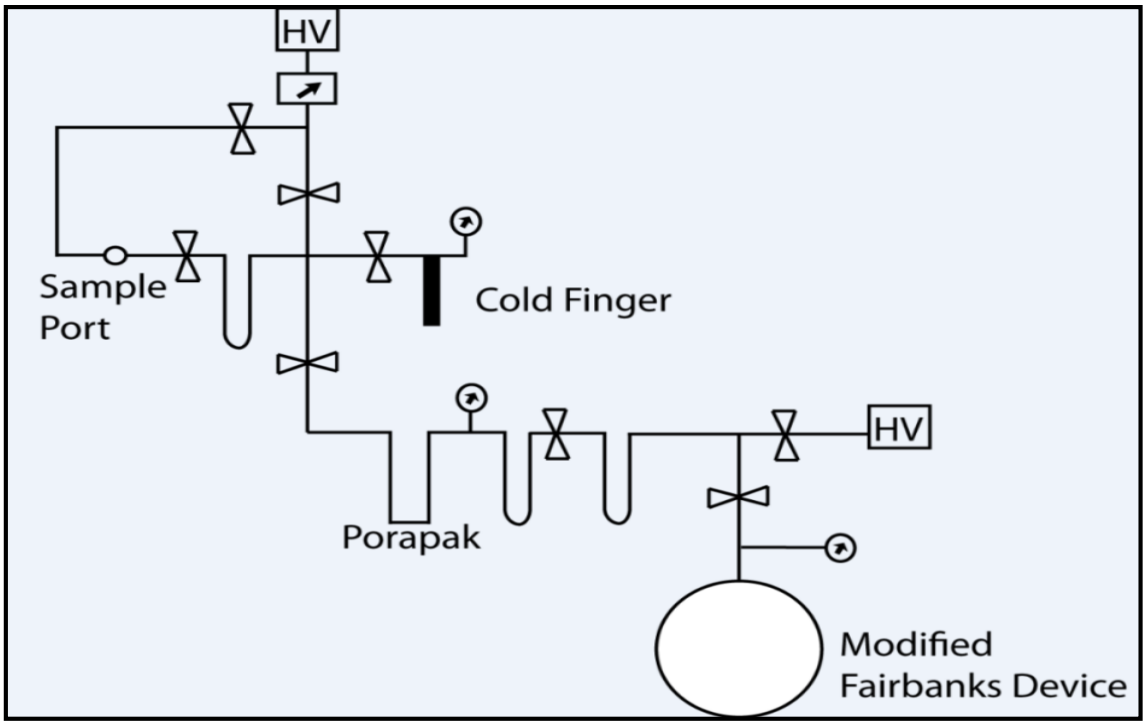

Figure 1.5: *A simple schematic of the gas purification line (HV denotes high vacuum).*

The CO_2 which is transferred to a second U-trap and collected with liquid nitrogen with the CO_2 then transferred through a PoroPak trap held between -30°C and -27°C. While CO_2 diffuses through the second U-trap and PoroPak, unwanted gases are pumped away. Liquid nitrogen is removed from the second U-trap and put under a third U-trap. This step takes an average of 45 minutes. Purified CO_2 is then transported to the mass spectrometer (MAT 253). The Poropak is baked out at 200°C over a period of 20 minutes to clean up the purification line using low and high vacuum for each individual sample. The final step requires that the line cool down for 10 minutes prior to analysis of next sample.

1.3.2. Mass spectrometric measurements of extracted CO_2

The clean CO_2 sample is measured using a MAT 253 (Figure 1.6) The MAT 253 is configured to measure 44 ($^{12}C^{16}O_2$), 45 ($^{13}C^{16}O_2$ and $^{12}C^{16}O^{17}O$), 46 ($^{12}C^{18}O^{16}O$, $^{13}C^{16}O^{17}O$ and $^{12}C^{17}O_2$), 47 ($^{13}C^{18}O^{16}O$, $^{12}C^{18}O^{17}O$ and $^{13}C^{17}O_2$), 48 ($^{12}C^{18}O_2$, $^{13}C^{17}O^{18}O$) and 49 ($^{13}C^{18}O_2$). Masses 48 and 49 are applied as internal monitoring of contamination such as hydrocarbon (Eiler et al., 2004).

Figure 1.6 *The Thermo Scientific MAT 253 stable isotope ratio mass spectrometer in SIL.*

The sample gas and reference gas are performed at a bellows pressure corresponding to 12 V. Oxygen isotope values of carbonate samples $\delta^{18}O$ of carbonates are reported with respect to Vienna Pee-Dee Belemnite (V-PDB) according to the standard notation, while water samples $\delta^{18}O_w$ are calculated relative to Vienna Standard Mean Ocean Water (V-SMOW). Temperatures are quoted as T (Δ_{47}) in °C.

1.3.3. Standardization of CO_2

This study has followed a calibration regime specific to the Stable Isotope Laboratory (SIL) at the University of Miami, RSMAS to normalize the data (Murray et al., in prep.). The reference framework of the SIL instrument was determined by combining two suites of low temperature equilibrated gases 25°C and 50°C and a suit of heated gases (1000°C) to document the measured Δ_{47} on a common reference scale (Dennis et al., 2011). A regime of three sets of heated and equilibrated gas samples have been rigorously maintained once every month to correct Δ_{47} values.

1.3.3.1. Heated gases

The carbon dioxide is prepared using quartz break seals and equilibrated at 1000°C in a muffle furnace for two hours (Wang et al., 2004). Thereafter, CO_2 is quickly quenched at 25°C (room temperature) to avoid isotopic exchange during cooling. The heated gas needs to be purified as outlined in section 2.1 before being transferred to the mass spectrometer.

A set of heated gases containing a range of bulk C and O isotopic compositions are measured to correct non-linearity and scale compression resulting from dissociation-recombination reactions of CO_2 in the ion resource (Huntington et al., 2009).

1.3.3.2. Equilibrated gases

At the SIL, University of Miami, analyses of two equilibrations at 25°C and 50°C are performed by equilibrating CO_2 with water (Dennis et al., 2011). The procedure is not always carried out at the same temperatures in all laboratories.

1.3.3.3. In-house standard

One sample of Carrera marble is measured daily as an internal standard using the same analytical protocol (as presented in section 2.1) (10 cycles consists of 6 working-sample gas changeovers) as employed with the samples. Standards are dispersed at regular intervals between the samples. The standard has a Δ_{47} value of 0.399±0.03‰ which results in a calculated temperature of approximately 115±5°C. These values are consistent with the mean Δ_{47} values measured in other laboratories (Dennis et al., 2011; Fernandez et al., 2014).

1.3.3.4. Conversion of raw data to corrected data

The Δ_{47} values have been calculated from measured ratios of mass 45, 46, and 47 relative to mass 44 using equation 5. In other words, Δ_{47} is a measure of the deviation between the measured ratio of R^{47} and the expected value of R^{47} if all isotopes of oxygen and carbon were stochastically distributed among all possible isotolopogues (Wang et al., 2004; Ghosh et al., 2006; Affek et al., 2008; Huntington et al., 2009; Dennis et al., 2010).

$$\Delta_{47} = \left[\frac{R_{47}}{2R_{13}XR_{18}+2R_{17}XR_{18}+R_{13}+R_{17}^2} - \frac{R_{46}}{2R_{18}+2R_{13}XR_{17}+R_{17}^2} - \frac{R_{45}}{R_{13}+2R_{17}} + 1 \text{ X } 1000 \right] \quad (5)$$

In the following section, the raw Δ_{47} values will be modified using the calibration slope of Δ_{47} with regard to $\delta 47$ values obtained from a combination of the heated gases (25°C, 50°C and 1000°C). In the equation below, Δ_{47} [SG vs WG] (Δ_{47} sample gas-working gas) values have been determined by calculating average slopes of the heated and equilibrated gases (25°C, 50°C and 1000°C) in the SIL, RSMAS, University of Miami. The theoretical calculation of $\delta 47$ is described in Wang et al. (2004) (Equation 6).

$$\Delta_{47\,[SG\ vs\ WG]} = \Delta_{47} - \delta 47 \text{ X Slope Average (0.028)} \quad (6)$$

The values of Δ_{47} [SG vs WG] calculated in the previous step can be reconstructed on the common scale proposed by Dennis et al. (2011). The empirical transfer function (ETF) slope and intercept is calculated experimentally from a determination of the slope and intercept of equilibrated and heated gases.

$$\Delta_{47-RF} = \Delta_{47\,[SG\ vs\ WG]} \text{ X Slope}_{ETF} \text{ (1.058) + Intercept}_{ETF} \text{ (0.966)} \quad (7)$$

1.3.4. Acid correction of the corrected Δ_{47}

The Δ_{47} values require correction for an acid fractionation factor where carbonate samples react with phosphoric acid at temperatures other than 25°C in clumped isotope measurements. While some calibrations were made using acid digestion at 25°C (Ghosh

et al., 2006; Came et al., 2007; Tripati et al., 2010; Thiagarajan et al., 2011), other authors used temperatures of 90°C (Dennis and Schrag, 2010; Henkes et al., 2013). Several acid fractionation factors have been proposed by theoretical work of Guo et al. (2009) and empirical studies of Passey et al. (2010) and Henkes et al. (2013).

The study has analyzed the samples using common acid method at 90°C and then have used acid fractionation factor of 0.092‰ as represented below (Henkes et al., 2013) for calcite samples. However, the aragonite samples have been corrected by acid fractionation factor of 0.112 as determined in house (Murray, unpublished) (Equation 8).

$$\Delta_{47-AC} = \Delta_{47} + 0.112 \quad (8)$$

1.3.5. Temperature calibrations

As previously stated, temperature estimates of carbonate samples can be determined using a calibration equation obtained from the inverse correlation between the clumped isotope composition of carbonates and temperature when Δ_{47} values are normalized using standardization processes.

Many calibration studies have been published since the first was performed by Ghosh et al. (2006) (Dennis and Schrag, 2010; Dennis et al., 2011; Zaarur et al., 2013; Wacker et al., 2013; Henkes et al., 2013; Fernandez et al., 2014; Tang et al., 2014).

Although determination of the most suitable calibration is still controversial, it will depend on the type and nature of the carbonate under investigation. In this thesis a number of biogenic and non-biogenic samples from various locations have been analyzed using the clumped isotope method. While suitable calibration equations exist for some

samples, for others none are available. For this reason, five temperature calibrations, in conjunction with additional supporting evidence, have been discussed in subsequent chapters to determine which sample is most appropriate.

The seminal temperature calibration has been used to convert clumped signals to temperature estimates of carbonates (Dennis et al., 2011) (Equation 9).

$$\Delta_{47} = \frac{0.00362 \times 10^6}{T^2} \quad (9)$$

Numerous calibrations have been tested using a wide range of carbonates consisting of various combinations of calcite, aragonite, and dolomite. The most recent of these analyzed pedogenic siderites to develop a new temperature calibration (Fernandez et al., 2014) (Equation 10).

$$\Delta_{47} = \frac{0.00356 \pm 0.0018 \times 10^6}{T^2} + (0.172 \pm 0.019) \quad (10)$$

Other recent work has addressed the temperature sensitivity of biogenic samples, specifically mollusk and brachiopod shells (Henkes et al., 2013) (Equation 11).

$$\Delta_{47} = \frac{0.00327 \times 10^6}{T^2} + (0.3286) \quad (11)$$

While the empirical calibration of a number of inorganic calcites precipitated under certain conditions was presented in the recent work (Tang et al., 2014) (Equation 12).

$$\Delta_{47} = \frac{0.00387 \pm 0.0072 \times 10^6}{T^2} + (0.2532 \pm 0.0829) \quad (12)$$

Temperature calibrations of several calcites of various origins (foraminifera, bivalve, brachiopod, cold seep and eggshell of ostrich) collected from different locations were carried out in an attempt to generate a 'universal' temperature calibration (Wacker et al., 2013) (Equation 13).

$$\Delta_{47} = \frac{0.00327 \pm 0.0026 \text{ X } 10^6}{T^2} + (0.3030 \pm 0.0308) \qquad (13)$$

CHAPTER 2

CLUMPED ISOTOPIC COMPOSITION OF SKELETAL AND NON-SKELETAL SURFACE MARINE SEDIMENTS ON GBB

2.1. Summary

A number of skeletal and non-skeletal samples were selected from the surface of Great Bahama Bank for clumped isotope analyses. These provided a data set of original surface marine samples for comparison to diagenetically altered slope samples found in the subsurface. Formation temperatures obtained from clumped isotopes and $\delta^{18}O_W$ values are close to equilibrium with observed sea surface temperature and water data from previous studies.

2.2. Perspective

Numerous studies have examined the geochemistry of shallow water carbonate sediments to investigate environmental changes and the nature of the depositional environment. However, the primary textures, mineral compositions, and rock properties of carbonates such as porosity and permeability are altered by diagenetic processes as sea-level rises and falls over geologic time (Gross, 1964; Gross and Tracey, 1966; Allan and Matthews, 1977, 1978).

The clumped isotope technique is one of the most promising methods which have been developed to investigate the stable isotope geochemistry of carbonates since the early 1950s. It permits the temperature of recrystallization to be determined as well as the oxygen isotopic composition of the fluid involved in the formation of carbonate. Although the application of the clumped isotope technique to diagenetic studies is still in

the early stages, there have been a number of papers (Dennis and Schrag, 2010; Bristow et al., 2011; Ferry et al., 2011; Van De Velde et al., 2013) and presentations which have suggested that promising results could be obtained. However, there have been no studies as of yet which have examined the behavior of clumped isotopes in well constrained diagenetic settings. While previous clumped isotope calibration studies have been carried out using skeletal carbonates, there have been no studies of non-skeletal carbonates.

2.3. Field Sites, settings and goals

Great Bahama Bank (GBB) is an isolated, flat topped carbonate platform located in the Bahama archipelago. It is comprised of more than 103,000 km^2 of shallow and submarine plateau capped by an irregularly shaped nearly pure carbonate platform surrounded on all sides by the open ocean (Figure 2.1).

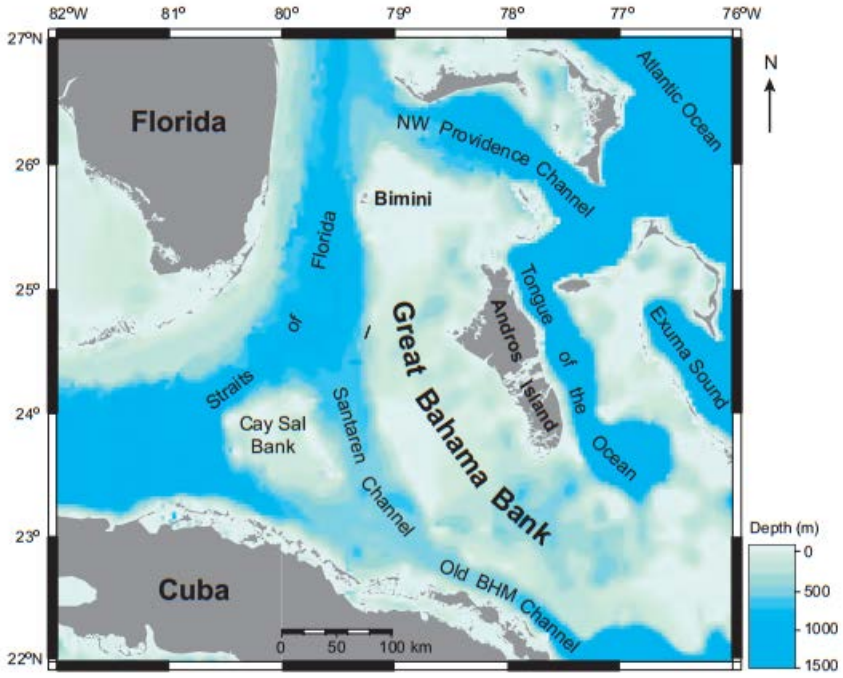

Figure 2.1: *Map of study area showing water depth (Reijmer et al., 2009)*

Surface sediments and depositional facies of GBB have been widely studied since the 1950s and are discussed in the classic papers of Illing, (1954), Newell et al. (1957), Ginsburg et al. (1958), Cloud, (1962), Purdy, (1963), Ball, (1967) and Enos, (1974).The depth of water over most of the bank is less than 10 m. Many islands are located on the east side of the GBB, the majority of these islands are made up of Pleistocene age oolitic and pelletal limestones formed as eolianites and sand banks (Newell et al., 1957, 1959; Cloud, 1962; Traverse and Ginsburg, 1966; Harris et al., 2014).

Although several studies have been conducted on the origin, geochemical variations and distribution of surface sediments on GBB (Lowenstam and Epstein, 1957; Morse et al., 1985; Shinn et al., 1989; Milliman et al., 1993), the grain size, organic and inorganic mineralogy, and composition of surface sediments were re-assessed for the first time in detail using approximately 300 GPS-located samples (Reijmer et al., 2009; Swart et al., 2009). Samples range from mud-rich wackestone to rudstone and are predominantly non-skeletal in origin (ooid, pelloids).

The first goal of this study will be to document the original (diagenetically unaltered) clumped isotope signals Δ_{47} of non-biologically produced marine surface sediments from Great Bahama Bank prior to diagenetic processes.

The second goal of this study is to determine if there is any facies control on the clumped isotope signature (Δ_{47}) using approximately 25 samples of recent non-biologically produced surface sediments selected from the range of depositional facies encountered (mudstone through grainstone) and from 9 different types of skeletal

sediments (*Rudstone*, *Halimeda sp*., *Acetabularia sp*., *Udotea sp., Penicillus sp., Penicillus capitatus, Penicillus fibrosa., Penicillus dumentosus*, *Cerithium sp*).

On average, water temperatures on GBB vary from 18.5°C in winter through 28.5°C during the summer (Fugilister, 1947; Cloud, 1962; Bathurst, 1975), due to shallowness of the platform and limited mixing with open ocean waters. Although waters on the platform show little lateral variation in temperature, significant sea surface temperature changes were observed at or near the edges of GBB where platform water mixes with ocean surface water (Smith, 1940; Purdy, 1963a). Finally, this study attempts to determine whether temperatures of formation of the platform carbonates calculated using carbonate clumped isotope paleo-thermometry agree with expected sea surface temperatures on the platform.

2.3.1. Climate

Great Bahama Bank is bathed by warm ocean water, thus it reflects a mild subtropical climate. Although winter temperatures average 21°C in the region, temperatures range from 27°C to 32°C during summer months (Newell et al., 1957).

Temperature and rainfall on GBB are intensively affected by seasonal atmospheric circulation as it reacts to variations in the location and magnitude of high and low pressure systems. The Intertropical Convergence Zone (ITCZ) and the Subtropical Divergence Zone (STDZ) are linked to trade winds. As the ITCZ and STDZ move northward, high precipitation ensues over the northern part of the Bahamas. However, the position of the ITCZ moves toward the equator during the winter season causing colder and drier days (Smith, 1995).

The annual amount of precipitation over the platform is 1355 mm (Carew and Mylroie, 1997), most of this rainfall occurs during the period from May to December (Smith, 1940) and reaches a maximum between September and October (Gebelein, 1974). Conversely, winter months are comparatively dry from December through April (Miller et al., 1983).

2.3.2. Sea surface temperature and salinity

Annual SST on the platform averages 25°C (Fugilister, 1947; Cloud, 1962, Bathurst, 1975) with some variation depending on the season. The temperatures between bank and ocean water deviate by as much as 3.6°C (Smith, 1940).

The salinity of the shallow bank waters has a tendency to be relatively low and changes from 36‰ close to the margin of the bank to 46‰ in the platform interior during the summer season when evaporation is at maximum (Black, 1933; Smith, 1940; Cloud, 1955; Ginsburg et al., 1958; Newell et al., 1959). The maximum salinity reaches 38‰ during winter season (Gebelein, 1974).

2.3.3. Age of surface sediments

Several authors demonstrated with the radiocarbon dating method that the unconsolidated recent surface sediments on the western portion of GBB formed during a period of rising sea level during the retreat of the Wisconsin Ice Age (Newell et al., 1959; Cloud, 1962). The modern sediments were determined by radiocarbon age experiments of less than a few thousand years (Newell and Rigby, 1957).

2.3.4. Carbonate mineralogy

The carbonate sediments on GBB are dominated by aragonite (about 94%) across the bank top, with minor amount of high magnesium calcite (HMC) and low magnesium calcite (LMC). However, the contribution of aragonite falls to about 89% for sediments on the western slope (Purdy, 1963(a); Husseini et al., 1972; Milliman, 1974; Mullins, 1986; Milliman et al., 1993; Reijmer et al., 2009).

The source of the finest grained carbonate sediments on the platform has been controversial since the 1930s (Black, 1933; Smith, 1940; Cloud, 1962). These sediments are considered to be primarily a product of the decomposition of calcifying green algae (Lowenstam and Epstein, 1957; Neumann and Land, 1975), or as a result of aragonitic mud which has precipitated directly from seawater (Cloud, 1962; Shinn et al., 1989).

2.4. Methodology

2.4.1. Material

Between 2001 and 2004 291 samples were collected from the surface sediments of GBB during a research cruise undertaken by the RV Bellows (Figure 2.2) (Reijmer et al., 2009). The samples were classified using a modified Dunham scale (Dunham, 1962). Mudstone, wackestone, packstone, grainstone and rudstone classifications were designated respectively with numbers from 1 through 5. Three intermediate divisions were added into the classification. Mud-rich wackestone, mud–rich packstone and mud-containing grainstone were assigned facies numbers 1.5, 2.5 and 3.5 (Reijmer et al., 2009).

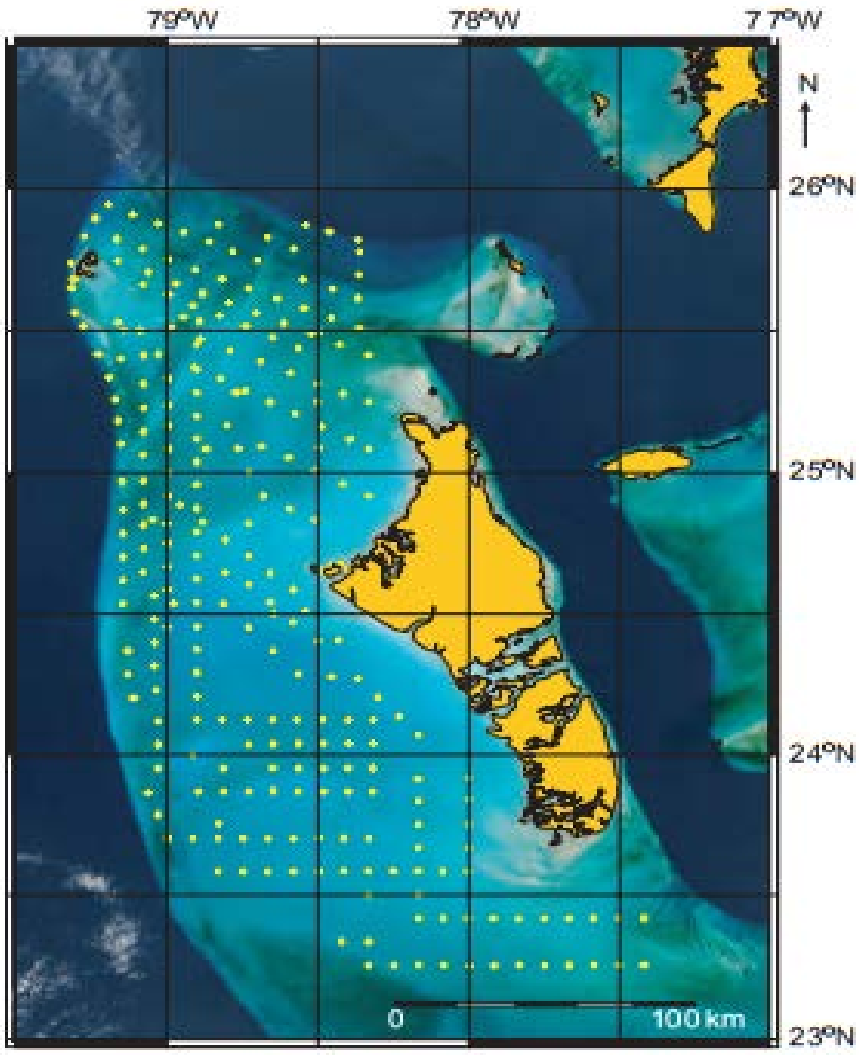

Figure 2.2: *Map of GPS located samples from the study of Reijmer et al., 2009.*

For this study, nearly 25 non-biologically produced carbonate samples were chosen from the samples collected by Reijmer et al. (2009). The mineralogy of these samples is dominated by aragonite which ranges in composition from 89.4% to 100.0%, with a mean of 94.0% (Table 2.1). Sample mineralogy was measured using the technique of Swart and Melim (2000). The low-Mg calcite content of these samples varies between 0% and 10.6%.

No	Sample	Facies	Depth	Aragonite	Low Mg-calcite	Ooids	Peloids	Pellets	Grapestone	Skeletal
	ID		(m)	%	%					
1	**GBB0903-08**	1.5	14.7	94.4	5.6		x			
2	**GBB0903-11**	1.5	11.8	92.7	7.3		x			x
3	**GBB0902-02**	1.5	14.4	99.8	0.2			x		x
4	**GBB0902-09**	1.5	13	93.9	6.1		x			x
5	**GBB0902-16**	1.5	20.1	89.4	10.6		x	x		
6	**GBB0903-06**	2.0	13.1	93.9	6.1		x			x
7	**GBB0903-18**	2.0	20	94.7	5.3		x			x
8	**GBB0902-13**	2.0	12.2	94.5	5.5			x		
9	**GBB0903-19**	2.5	19.9	94.7	5.3		x			
10	**GBB0903-21**	2.5	17.8	94.7	5.3		x			
11	**GBB0903-47**	2.5	17.2	93.3	6.7		x			x
12	**GBB0903-20**	2.5	17.8	95.2	4.8		x			
13	**GBB0903-14**	3.0	16.5	93.8	6.2		x			x
14	**GBB0903-15**	3.0	17.9	92.0	8.0		x			x
15	**GBB0903-28**	3.0	14.9	92.5	7.5		x			x
16	**GBB0903-36**	3.0	13.9	91.8	8.2		x			x
17	**GBB0903-03**	3.5	13.4	94.7	5.3		x			x
18	**GBB0902-27**	3.5	17	93.1	6.9	x	x			x
19	**GBB0902-05**	3.5	9.5	89.7	10.3		x		x	x
20	**GBB0903-05**	3.5	13	95.5	4.5		x			x
21	**GBB0903-02**	4.0	11.7	100.0	0.0		x			x
22	**GBB0903-04**	4.0	11.9	94.2	5.8	x	x			x
23	**GBB0902-46**	4.0	22	94.3	5.7		x		x	x
24	**GBB0902-52**	4.0	39.4	92.0	8.0		x			x
25	**GBB0902-39**	5.0	140	97.5	2.5					x
26	**GBB0902-41**	5.0	502	91.2	8.8					x

Table 2.1: *Facies types, mineralogy and composition of analyzed from mudstone through rudstone samples along with their names.*

The majority of the non-biogenic samples consists of peloids together with pellets, ooids and grapestone, and contain minor amount of skeletal material (Table 2.1). In addition, the clumped isotope signals (Δ_{47}) have been determined for different types of calcareous green algae that are significant producers of carbonate sediments within coral reef environments (Milliman, 1993). These biologically produced materials are the dominant component of the sediments in a narrow belt along the edges of the GBB (Swart et al., 2009) while skeletal sands dominate around islands and reefs. The skeletal component decreases from the GBB margins towards the interior of the platform (Kornicker, 1963).

2.4.2. Preparation

The biologically produced skeletal carbonate samples were bleached for 24 hours and then subsequently rinsed with distilled water to remove the organic component. After cleaning, samples were dried in the oven at 40°C for at least 24 hours.

Both biogenic and non-biogenic samples were finely ground using a mortar and pestle. For each clumping measurement approximately 8±0.3 mg of sample was weighed out into small copper boats.

2.4.3. Analytical

2.4.3.1. Clumped isotope method

As previously discussed (see Chapter 1), CO_2 extracted from samples by reaction with phosphoric acid using the common acid method (Swart et al., 1991) was introduced to a MAT 253 for analysis of skeletal and non-skeletal modern surface samples collected

from GBB. The clumped signals were determined utilizing the equation of numerous workers (Eiler, 2007; Affek et al., 2008; Huntington et al., 2009). Thereafter, the Δ_{47} values were normalized to the reference framework (Dennis et al., 2011) and subsequently they were adjusted by the acid fractionation factor of 0.112‰ (Murray, 2014 unpublished). A regime of daily in-house (Carrera marble) and monthly inter-laboratory calibration proposed by Dennis et al., 2011 has been applied to standardize the results in the Stable Isotope Laboratory at the University of Miami, RSMAS.

2.4.2.2. Determining oxygen composition and salinity of the water

One of the most notable benefits of the carbonate clumped isotope method is that it non empirically allows us to calculate the $\delta^{18}O$ of the fluid using the appropriate paleo-temperature equation (Grossman and Ku, 1986).

$$\delta^{18}O_w = \delta^{18}O_{aragonite} - (19.7 - T) / 4.34 \quad (14)$$

In this equation, $\delta^{18}O_w$ = oxygen isotopic composition of water (SMOW), $\delta^{18}O_{aragonite}$ = oxygen isotopic composition of aragonite (PDB) and T= temperature (°C). To solve this equation, temperature and $\delta^{18}O_{aragonite}$ values were obtained as a result of clumped isotope measurements performed on a MAT 253.

The equation was developed through measurements of modern specimens of aragonitic foraminifera, gastropods and mollusks collected from the continental margins off southern USA and Mexico across a range in ambient temperature of 2.6-22.0°C.

$$\text{Salinity} = (\delta^{18}O_w + 5.57) / 0.1926 \quad (15)$$

After obtaining $\delta^{18}O_{w,}$ the salinity can be readily calculated using the data from Swart et al. (2009) (Equation 15).

2.5. Results

2.5.1. Clumped isotopes

No	Sample ID	Facies	Mean Δ 47	sd	Dennis Temp.	sd	Fernandez Temp.	sd	Walker Temp.	sd	Tang Temp.	sd	Henkes Temp.	sd	replicates
			‰		°C		°C		°C		°C		°C		
1	GBB0903-08	1.5	0.686	0.010	30.29	2.26	31.43	3.78	19.05	3.93	25.88	9.83	29.34	4.35	3
2	GBB0903-11	1.5	0.707	0.019	25.89	3.99	24.23	6.48	11.60	6.70	19.08	7.87	21.10	7.40	3
3	GBB0902-02	1.5	0.683	0.012	31.06	2.69	32.73	4.5	20.40	4.68	27.10	10.42	30.84	5.19	3
4	GBB0902-09	1.5	0.704	0.022	26.55	4.58	25.33	7.46	12.73	7.71	20.12	8.37	22.35	8.51	3
5	GBB0902-16	1.5	0.697	0.026	27.95	5.59	27.65	9.11	15.14	9.42	22.30	9.61	25.03	10.40	3
6	GBB0903-06	2.0	0.666	0.016	34.91	3.64	39.31	6.23	27.27	6.51	33.27	12.81	38.49	7.26	3
7	GBB0903-18	2.0	0.706	0.018	26.00	3.75	24.41	6.13	11.77	6.34	19.25	7.94	21.29	7.01	4
8	GBB0902-13	2.0	0.693	0.039	28.93	8.70	29.43	14.6	17.03	15.24	23.96	11.35	27.15	16.93	3
9	GBB0903-19	2.5	0.715	0.015	24.23	3.03	21.52	4.88	8.79	5.04	16.53	6.88	18.00	5.55	3
10	GBB0903-21	2.5	0.699	0.017	27.52	3.59	26.88	5.91	14.33	6.12	21.59	8.66	24.12	6.77	3
11	GBB0903-47	2.5	0.713	0.021	24.56	4.37	22.08	7.03	9.38	7.25	17.05	7.40	18.66	7.98	2
12	GBB0903-20	2.5	0.672	0.009	33.53	2.10	36.91	3.59	24.76	3.75	31.03	11.94	35.68	4.17	2
13	GBB0903-14	3.0	0.713	0.043	24.78	9.00	22.59	14.5	9.93	14.98	17.52	9.12	19.29	16.51	3
14	GBB0903-15	3.0	0.713	0.016	24.63	3.31	22.17	5.34	9.46	5.51	17.14	7.14	18.74	6.08	3
15	GBB0903-28	3.0	0.687	0.013	30.21	2.80	31.32	4.7	18.93	4.89	25.77	9.96	29.21	5.42	3
16	GBB0903-36	3.0	0.689	0.028	29.74	6.25	30.65	10.5	18.26	10.91	25.12	10.70	28.49	12.12	3
17	GBB0903-03	3.5	0.689	0.011	29.70	2.43	30.46	4.06	18.04	4.22	24.96	9.52	28.22	4.69	4
18	GBB0902-27	3.5	0.720	0.016	23.11	3.19	19.73	5.08	6.94	5.22	14.83	6.40	15.97	5.74	3
19	GBB0902-05	3.5	0.711	0.005	24.89	1.02	22.56	1.65	9.86	1.71	17.51	6.62	19.17	1.88	3
20	GBB0903-05	3.5	0.706	0.022	26.11	4.79	24.61	7.84	11.99	8.12	19.44	8.16	21.54	8.97	3
21	GBB0903-02	4.0	0.693	0.019	28.76	4.06	28.95	6.75	16.48	7.00	23.53	9.39	26.50	7.76	5
22	GBB0903-04	4.0	0.695	0.008	28.34	1.73	28.20	2.85	15.69	2.95	22.83	8.63	25.61	3.27	3
23	GBB0902-46	4.0	0.705	0.020	26.23	4.23	24.79	6.85	12.17	7.08	19.61	8.27	21.74	7.80	3
24	GBB0902-52	4.0	0.693	0.007	28.68	1.45	28.76	2.39	16.27	2.48	23.36	9.06	26.26	2.74	3
25	GBB0902-39	5.0	0.730	0.034	21.32	7.01	17.02	11.2	4.19	11.52	12.26	7.41	12.97	12.68	3
26	GBB0902-41	5.0	0.708	0.019	25.73	3.87	23.96	6.24	11.31	6.44	18.83	7.93	20.78	7.09	3

Table 2.2: *Mean temperature estimates using five equations and* Δ_{47} *values of* CO_2 *of mostly non-skeletal Bahamian samples performed by phosphoric acid digestion at 90°C versus facies types. n denotes number of analyses of the samples.*

The clumped signals (Δ_{47}) of the biogenic and non-biogenic carbonate samples were assigned to the reference framework suggested by Dennis et al. (2011). These values have been recorded along with their standard deviations in Table 2.2 and Table 2.3. Although the clumped isotope signatures of the non-biogenic samples range between 0.666±0.016‰ and 0.720±0.016‰ (Table 2.2), the Δ_{47}values of the biogenic samples typically show higher values ranging between 0.692‰ and 0.754‰ (Table 2.3).

The signals, modified to temperatures of recrystallization typical of modern bank top sediments, using a series of temperature equations are shown in Table 2.2 and Table 2.3 (Dennis et al., 2011; Henkes et al., 2013; Fernandez et al., 2014; Wacker et al., 2014; Tang et al., 2014). In the following section, five different temperature calibrations will be employed in order to determine the most accurate equation for the biogenic and abiogenic samples in this study.

No	Sample ID	Mean Δ 47	Dennis Temp.	Fernandez Temp.	Walker Temp.	Tang Temp.	Henkes Temp.	18Oxygen	sd	13Carbon	sd
		‰	°C	°C	°C	°C	°C	‰		‰	
27	**Penicillus Dumetosus**	0.754	16.46	9.30	-3.754	4.95	4.2412	-0.67	0.009	1.88	0.006
28	**Halimeda**	0.701	27.14	26.21	13.63	20.96	23.333	-1.62	0.009	1.21	0.005
29	**Penicillus Capitatus**	0.729	21.28	16.80	3.9289	12.07	12.651	-0.87	0.009	2.56	0.005
30	**Penicillus**	0.722	22.63	18.94	6.1252	14.09	15.063	-1.19	0.010	0.46	0.006
31	**Acetabularia**	0.706	25.98	24.31	11.666	19.17	21.165	-1.32	0.009	-1.27	0.005
32	**Penicillus Fibrosa**	0.729	21.35	16.91	4.0423	12.17	12.775	0.10	0.010	0.27	0.005
33	**Cerithium**	0.692	29.03	29.33	16.859	23.89	26.905	0.82	0.010	2.57	0.005
34	**Udotea**	0.729	21.17	16.63	3.7504	11.90	12.455	-0.50	0.009	3.77	0.005

Table 2.3: *Average clumped signals values of the surface skeletal samples analyzed in this study, along with converted temperature estimates derived from equations of five recent published studies and results of stable isotope analyses.*

2.5.2. Stable isotopes

No	Sample ID	Facies Types	Depth	18Oxygen	sd	se	13Carbon	sd	se
			(m)	‰			‰		
1	**GBB0903-08**	1.5	14.7	0.34	0.010	0.001	4.55	0.006	0.001
2	**GBB0903-11**	1.5	11.8	0.27	0.010	0.001	4.47	0.006	0.001
3	**GBB0902-02**	1.5	14.4	0.16	0.010	0.001	4.41	0.007	0.001
4	**GBB0902-09**	1.5	13.0	0.32	0.010	0.001	4.40	0.007	0.001
5	**GBB0902-16**	1.5	20.1	-0.16	0.010	0.001	4.31	0.006	0.001
6	**GBB0903-06**	2.0	13.1	0.21	0.010	0.001	4.57	0.006	0.001
7	**GBB0903-18**	2.0	20.0	0.09	0.012	0.001	4.36	0.007	0.001
8	**GBB0902-13**	2.0	12.2	0.27	0.011	0.001	4.56	0.007	0.001
9	**GBB0903-19**	2.5	19.9	0.06	0.009	0.001	4.42	0.006	0.001
10	**GBB0903-21**	2.5	17.8	0.15	0.012	0.001	4.44	0.007	0.001
11	**GBB0903-47**	2.5	17.2	0.13	0.012	0.001	4.35	0.006	0.001
12	**GBB0903-20**	2.5	17.8	0.05	0.009	0.001	4.43	0.006	0.001
13	**GBB0903-14**	3.0	16.5	0.10	0.010	0.001	4.41	0.007	0.001
14	**GBB0903-15**	3.0	17.9	0.07	0.010	0.001	4.40	0.006	0.001
15	**GBB0903-28**	3.0	14.9	0.14	0.010	0.001	4.53	0.006	0.001
16	**GBB0903-36**	3.0	13.9	0.13	0.010	0.001	4.45	0.006	0.001
17	**GBB0903-03**	3.5	13.4	0.28	0.011	0.001	4.83	0.006	0.001
18	**GBB0902-27**	3.5	17.0	0.00	0.011	0.001	4.80	0.006	0.001
19	**GBB0902-05**	3.5	9.5	0.62	0.010	0.001	4.96	0.006	0.001
20	**GBB0903-05**	3.5	13.0	0.50	0.010	0.001	4.93	0.006	0.001
21	**GBB0903-02**	4.0	11.7	0.26	0.010	0.001	4.97	0.006	0.001
22	**GBB0903-04**	4.0	11.9	0.41	0.011	0.001	5.03	0.006	0.001
23	**GBB0902-46**	4.0	22.0	-0.10	0.011	0.001	4.83	0.006	0.001
24	**GBB0902-52**	4.0	39.4	-0.18	0.011	0.001	4.33	0.006	0.001
25	**GBB0902-39**	5.0	140.0	-0.38	0.010	0.001	3.39	0.006	0.001
26	**GBB0902-41**	5.0	502.0	-0.16	0.010	0.001	3.65	0.006	0.001

Table 2.4: *Stable isotope analyses are summarized including facies types and depth of the measured samples.*

All non-biologically produced aragonite samples from mud-rich wackestone (1.5) to grainstone (4.0) show narrow ranges in $\delta^{13}C$ from 4.31‰ to 5.03‰ and in $\delta^{18}O$ ranging from -0.18‰ to 0.62‰, therefore all samples tend to have similar $\delta^{18}O$ and $\delta^{13}C$

values. This situation is thought to be related to the genetic of the carbonates on GBB (Swart et al., 2009). However, the biogenic samples have much lower $\delta^{13}C$ (-1.27 to 3.65‰) and $\delta^{18}O$ (-1.62 to 0.82‰) values.

2.5.3. Estimates of oxygen composition of seawater

No	Sample ID	Facies	Depth	δ18O-measured	δ18Ow-Dennis Temp.	sd	δ18Ow-Fernandez Temp.	sd	δ18Ow-Wacker Temp.	sd	δ18Ow-Tang Temp.	sd	δ18Ow-Henkes Temp.	sd
			(m)		‰		‰		‰		‰		‰	
1	GBB0903-08	1.5	14.7	1.57	2.78	0.62	3.05	0.97	0.19	1.00	1.77	0.92	2.56	1.36
2	GBB0903-11	1.5	11.8	1.44	1.70	0.85	1.32	1.42	-1.60	1.47	0.13	1.34	0.59	1.63
3	GBB0902-02	1.5	14.4	1.41	2.77	0.66	3.16	1.08	0.32	1.12	1.86	1.02	2.72	1.44
4	GBB0902-09	1.5	13.0	1.56	1.90	0.97	1.62	1.63	-1.28	1.68	0.42	1.53	0.94	1.78
5	GBB0902-16	1.5	20.1	1.19	1.74	1.33	1.67	2.14	-1.21	2.21	0.44	2.02	1.07	2.18
6	GBB0903-06	2.0	13.1	1.71	3.71	0.95	4.73	1.54	1.95	1.61	3.34	1.46	4.54	1.80
7	GBB0903-18	2.0	20.0	1.61	1.55	0.86	1.18	1.40	-1.73	1.45	-0.01	1.32	0.46	1.62
8	GBB0902-13	2.0	12.2	1.25	2.40	2.00	2.51	3.37	-0.35	3.51	1.25	3.17	1.99	3.23
9	GBB0903-19	2.5	19.9	1.17	1.10	0.77	0.48	1.20	-2.45	1.23	-0.67	1.13	-0.33	1.46
10	GBB0903-21	2.5	17.8	1.40	1.95	0.82	1.80	1.35	-1.09	1.40	0.58	1.27	1.17	1.59
11	GBB0903-47	2.5	17.2	1.44	1.24	0.92	0.67	1.53	-2.25	1.58	-0.48	1.44	-0.12	1.70
12	GBB0903-20	2.5	17.8	1.30	3.24	0.56	4.02	0.90	1.22	0.94	2.66	0.85	3.74	1.35
13	GBB0903-14	3.0	16.5	1.74	1.27	2.05	0.76	3.32	-2.15	3.42	-0.40	3.13	0.00	2.87
14	GBB0903-15	3.0	17.9	1.15	1.21	0.82	0.64	1.29	-2.28	1.33	-0.52	1.22	-0.15	1.53
15	GBB0903-28	3.0	14.9	1.26	2.56	0.64	2.82	1.07	-0.03	1.12	1.54	1.01	2.33	1.43
16	GBB0903-36	3.0	13.9	1.51	2.44	1.46	2.65	2.44	-0.20	2.54	1.38	2.30	2.16	2.45
17	GBB0903-03	3.5	13.4	1.91	2.58	0.63	2.76	1.01	-0.10	1.05	1.49	0.96	2.24	1.40
18	GBB0902-27	3.5	17.0	1.81	0.78	0.75	0.00	1.19	-2.94	1.22	-1.13	1.13	-0.86	1.45
19	GBB0902-05	3.5	9.5	1.41	1.81	0.13	1.27	0.27	-1.65	0.29	0.11	0.25	0.49	1.02
20	GBB0903-05	3.5	13.0	1.71	1.97	1.02	1.63	1.73	-1.28	1.79	0.43	1.62	0.92	1.86
21	GBB0903-02	4.0	11.7	1.75	2.30	0.89	2.29	1.51	-0.59	1.56	1.05	1.42	1.70	1.75
22	GBB0903-04	4.0	11.9	1.86	2.40	0.32	2.36	0.57	-0.52	0.60	1.13	0.54	1.77	1.15
23	GBB0902-46	4.0	22.0	1.28	1.40	0.97	1.07	1.57	-1.84	1.62	-0.12	1.48	0.37	1.73
24	GBB0902-52	4.0	39.4	2.21	1.89	0.34	1.91	0.56	-0.97	0.58	0.67	0.52	1.33	1.14
25	GBB0902-39	5.0	140.0	1.13	0.00	1.49	-0.99	2.46	-3.95	2.53	-2.09	2.32	-1.93	2.42
26	GBB0902-41	5.0	502.0	1.02	1.23	0.88	0.82	1.43	-2.09	1.48	-0.36	1.35	0.09	1.63

Table 2.5: *Actual values of $\delta^{18}O_w$ measured and average estimates of $\delta^{18}O_w$ of the surface samples based on paleotemperature equation of Grossmann and Ku, (1986) using various calculated temperatures obtained from clumped isotopes.*

2.6. Discussion

2.6.1. Δ_{47} proxy of the recent marine sediments as a baseline

This study is the first to record Δ_{47} values of non-diagenetically altered modern surficial platform carbonates on GBB and will provide a baseline for future studies.

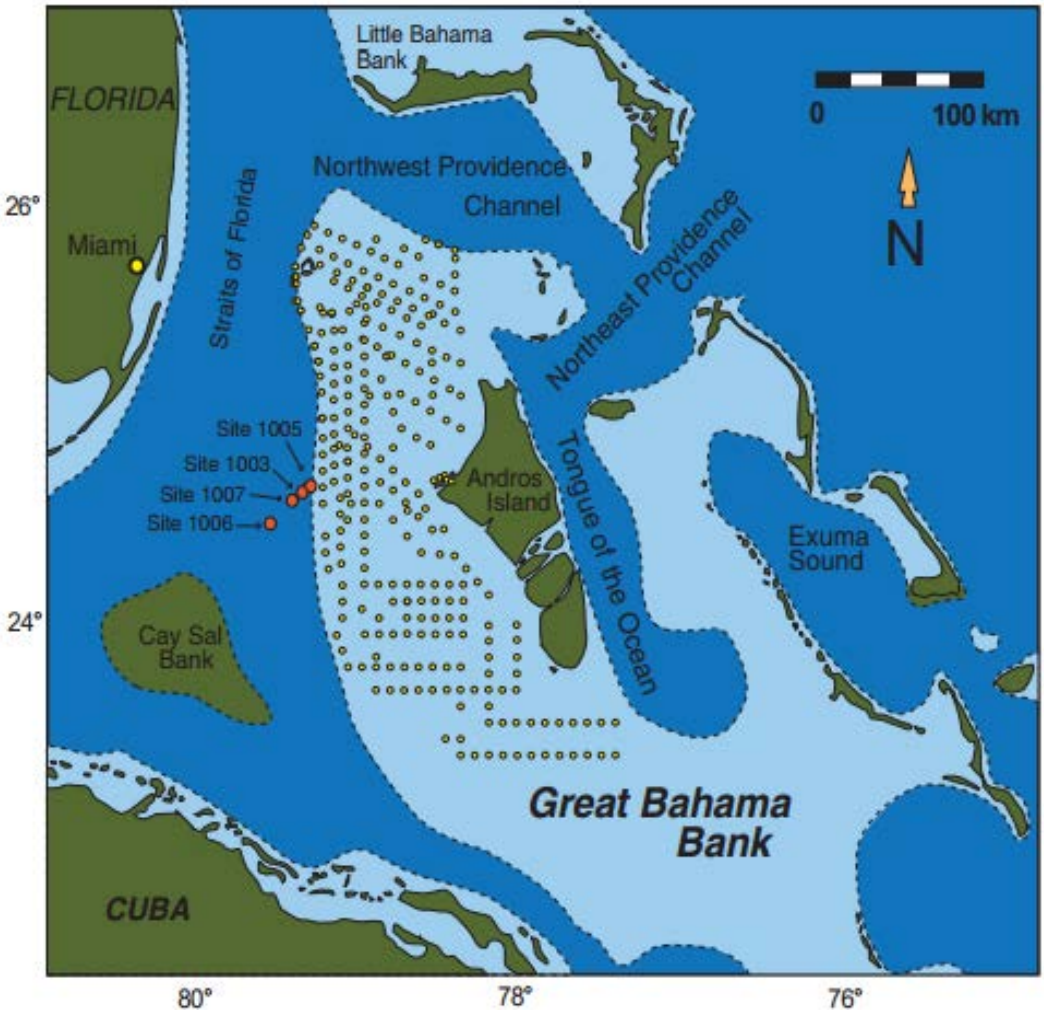

Figure 2.3: *The map of study area along with locations of seven drill sites for Ocean Drilling Program Leg 166 (Oehlert et al., 2012)*

For example, two shallow water cores (Clino and Unda) were drilled on the western portion of the GBB, to be followed later by five deep water cores during Ocean Drilling Program Leg 166 (Figure 2.3). The deepest core (1003) penetrates earliest Miocene deposits at a depth of 1300 m. While the amount of recrystallization is highest in the upper section of the core, it decreases with depth (Oehlert et al., 2012).

High Δ_{47} values should be observed in the top part of the core due to the bottom water temperatures which average 8°C, however the clumped signatures tend to decrease with depth. In this respect, a comparison between the diagenetic responses of the clumped isotopic signals in periplatform sediments during marine burial diagenesis with known rates of recrystallization and the Δ_{47} values of the recent sediments will allow us to ascertain influences of diagenetic processes on Δ_{47} in marine environments.

2.6.2. Relationship between Δ_{47} and facies variations

A number of studies have produced maps of the spatial distribution of recent surficial marine sediments throughout the GBB (Illing, 1954; Newell and Rigby, 1957; Newell et al., 1959; Traverse and Ginsburg, 1966; Ball, 1967). In particular, the maps of Purdy (1963b) and Enos, (1974) have been widely used by geologists.

These earlier studies were based on limited sampling sites (less than 50), without GPS-located samples, using a Van-Veen grab sampler or hand collected resulting in the loss of the fine fraction. However, the distribution of surface sediments along with evaluation of their grain-size, mineralogy and composition were re-examined in nearly 300 specimens collected across GBB using a Shipek sampler (to ensure retention of the

fine sediment fraction) while using precision positioning systems (Reijmer et al., 2009; Swart et al., 2009) (Figure 2.4).

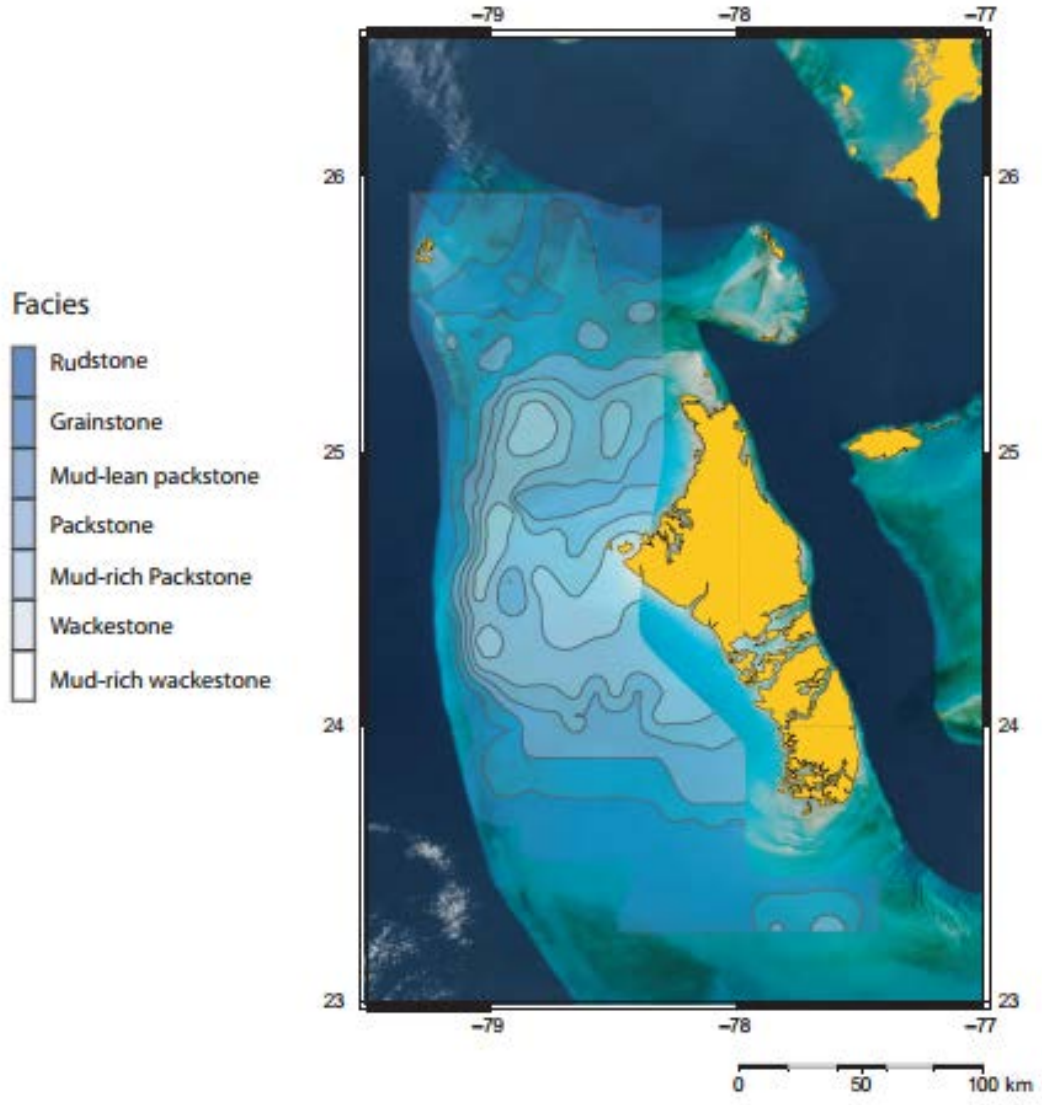

Figure 2.4: *Map of based on facies types assigned to a modified Dunham classification scheme (Reijmer et al., 2009). Light colored regions are dominated by fine-grained materials in the inner platform, dark colored regions represent coarse-grained sediment at the outer edge of the GBB.*

The study of Reijmer et al. (2009) provided a detailed map of the surface bank sediments and is reasonably similar to the facies distribution map of Purdy (1963a,b), also conforming roughly to the map of Traverse and Ginsburg (1966). Accordingly, the

more recent and more detailed map of Reijmer et al. (2009) has been employed in this study.

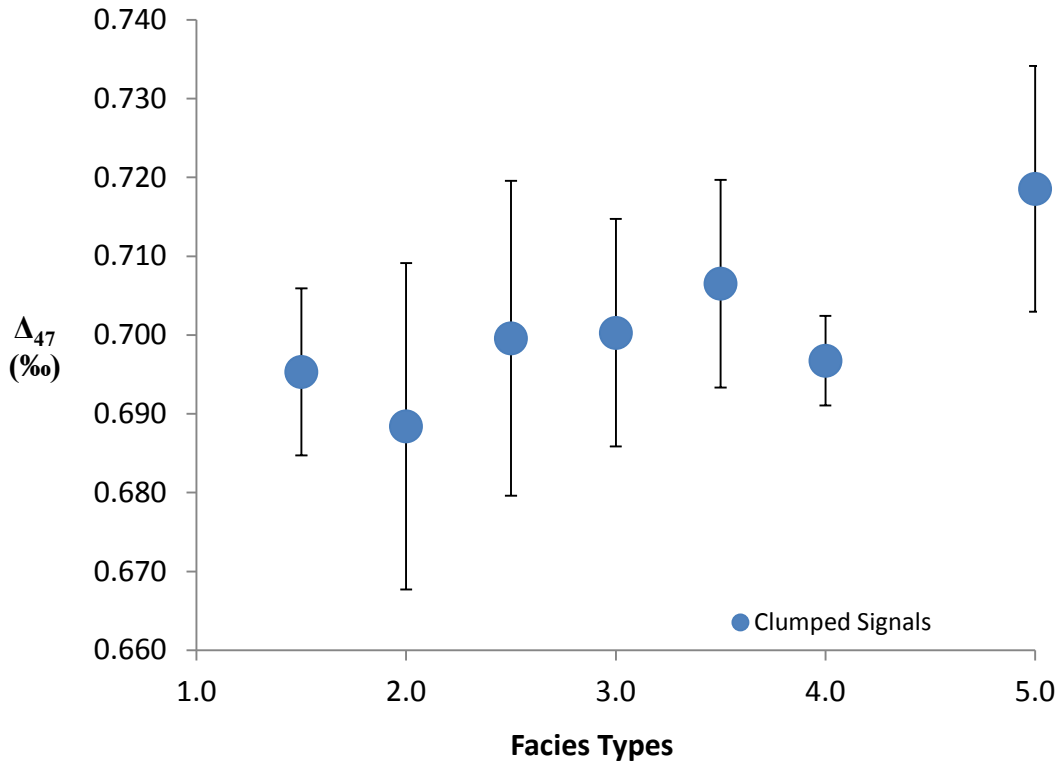

***Figure 2.5**: Relationship between clumped signals of the carbonate samples and facies variations (1= Mud, 1.5= Mud-rich wackestone, 2= Wackestone, 2.5= Mud-rich packestone, 3= Packstone, 3.5= Mud-lean packstone, 4= Grainstone, 5= Rudstone). Error bars represent +/- one standard deviation.*

In spite of their differences all maps show that biologically produced sediments dominate at the edge of the platform while non-biologically produced sediments (pellets, peloids, mud and grapestone) (facies types from 1.5 to 4.0) occur towards the interior of the GBB. In other words, the amount of mud within the sediments decreases significantly moving away from the interior of the bank towards the platform margin (Figure 2.4) (Swart et al., 2009). Note that in Figure 2.5 the apparent positive correlation is driven by the inclusion of the rudstones which are actually composed predominantly of the green algae *Halimeda*. There is no statistically significant variations in Δ_{47} between the non-

skeletal facies. A full comparison of the mean Δ_{47} values between each facies is shown in Table 2.6.

	MRW	W	MRP	P	MRG	G
MRW						
W	0.36					
MRP	0.36	0.25				
P	0.30	0.22	0.48			
MRG	0.11	0.13	0.29	0.26		
G	0.30	0.27	0.41	0.35	0.12	
R	0.12	0.08	0.15	0.14	0.23	0.13

Table 2.6: *Significance of t-test comparison between various facies types. The rudstone and wackestone facies are significantly different at the > 90% confidence limits.*

While there is a general trend between facies types (from 1.5 to 5.0) and clumped signals (Δ_{47}) of marine surface sediments on GBB, no statically relationship has been observed (Figure 2.5). Thus, the clumped isotopic compositions of the sediments gradually tends to increase from 1.5(inner platform) through 5.0 (outer platform), however, the variations in clumped signals cannot be said to be directly controlled by facies distributions.

Since Δ_{47} is inversely proportional to temperature of formation or alteration of carbonates, coarse-grained sediment types tend to have lower values with respect to temperature than the finer-grained sediment types. A 0.064‰ range in clumped signals was observed throughout the various facies of the non-skeletal samples (Figure 2.5) indicating an estimated range in growth temperature of 21°C through 35°C based on the temperature calibration equation of Dennis et al. (2011).

2.6.3. Temperature considerations

The clumped isotopic compositions of the non-skeletal and skeletal samples have been converted to temperatures using the appropriate temperature equations (Dennis et al., 2011; Henkes et al., 2013; Tang et al., 2014; Wacker et al., 2014 and Fernandez et al., 2014).

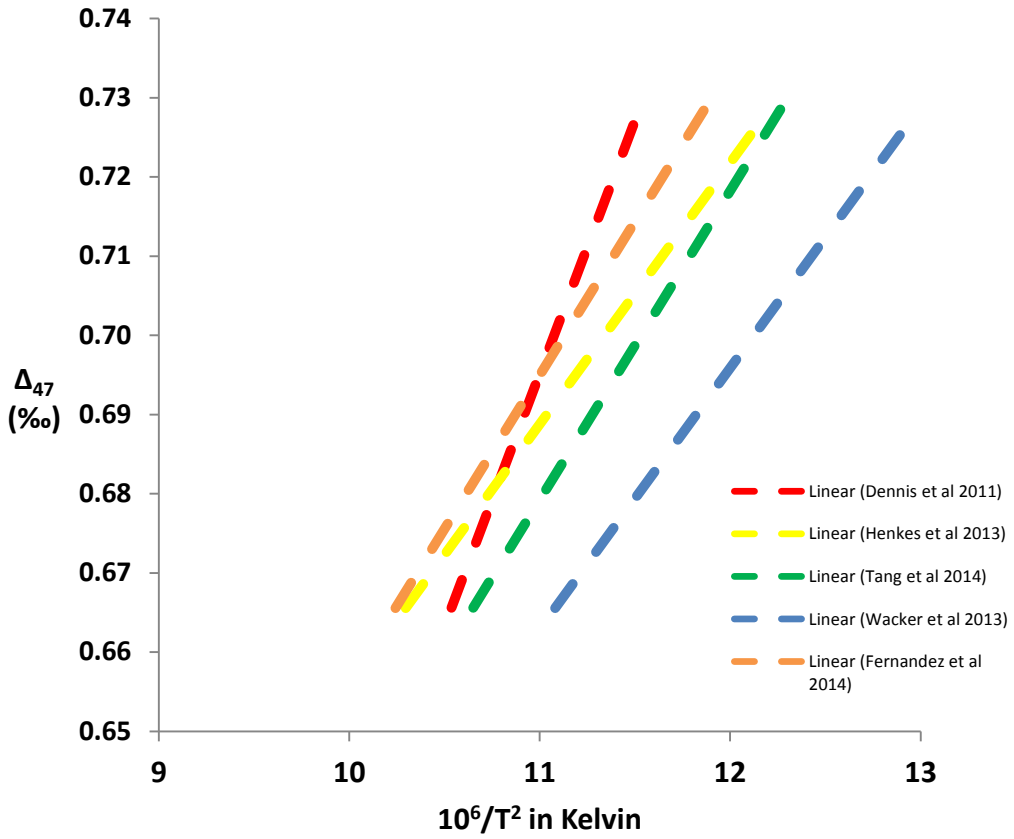

Figure 2.6: *Linear relationship between estimated temperatures derived from five recent published equations (Dennis et al., 2011; Tang et al., 2014; Wacker et al., 2014; Fernandez et al., 2014; Henkes et al., 2013) and Δ47 values of CO_2 produced by acid digestion of the modern mainly non-skeletal samples from GBB.*

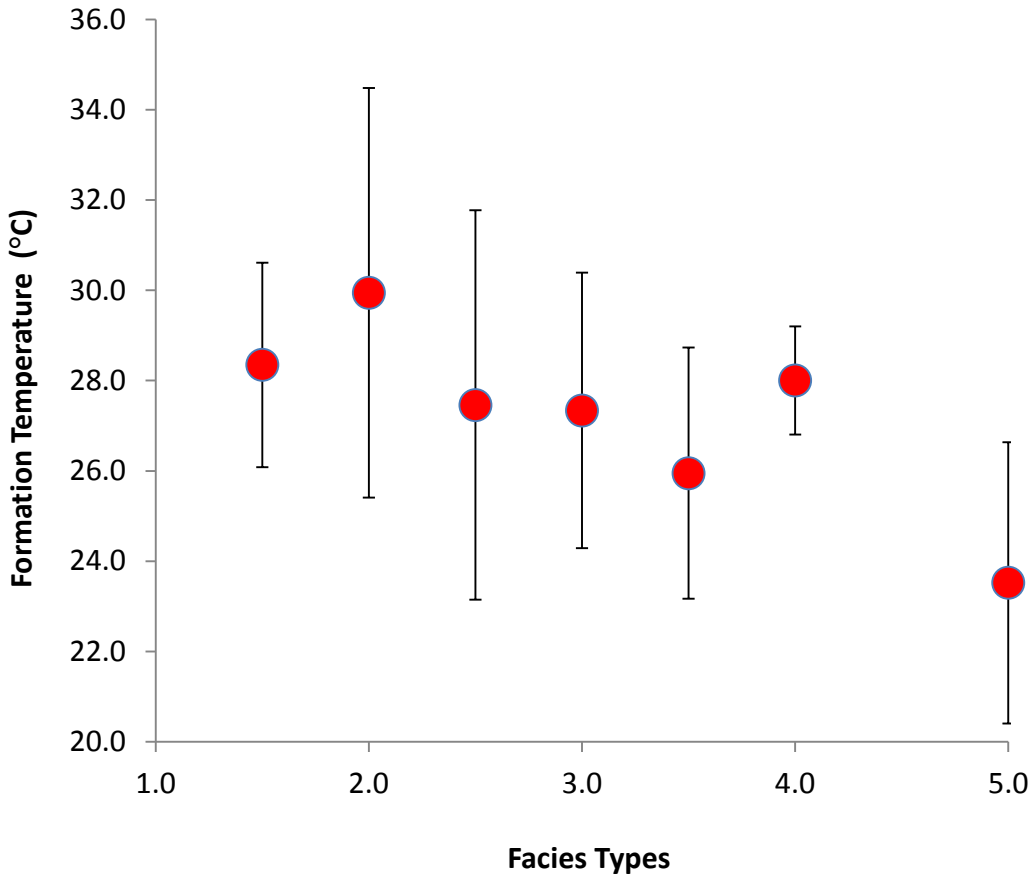

Figure 2.7: *Relationship between mean temperatures of formation of the surface samples and facies variations using equation of Dennis et al., 2011 (1= Mud, 1.5= Mud-rich wackestone, 2= Wackestone, 2.5= Mud-rich packestone, 3= Packstone, 3.5= Mud-lean packstone, 4= Grainstone, 5= Rudstone).*

Of these the (Figure 2.6), equation of Dennis et al. (2011) produces the narrowest range of temperature estimates of the sediments with low standard deviations and agrees closely to the actual measured SST (Table 2.2 and Figure 2.7). Temperature estimates based on the non-biogenic samples from Wacker et al. (2014) not only appear to be much colder with respect to annual SST values on the platform, but also show significant standard deviations (Table 2.2). However, the equations of Henkes et al. (2013) and Fernandez et al. (2014) define that the non-skeletal samples reflecting a wide range in temperature of 13-38°C and 17-39°C respectively with high standard deviations (Table 2.2).

On the other hand, because of their higher Δ_{47} values, the clumped signatures of the biogenic samples result in lower temperatures than the non-biogenic samples. Once again, the equation of Wacker et al. (2014) leads to unrealistic temperatures in the biogenic samples (Table 2.3). The equations of Henkes et al. (2013) and Tang et al. (2014) result in lower temperatures when compared with surface platform waters. However, the temperature estimates of the skeletal materials provided by the equations of Dennis et al. (2011) and Fernandez et al. (2014) appear to be ideal equations for the biogenic samples of this study.

2.6.4 Estimates of the formation temperatures

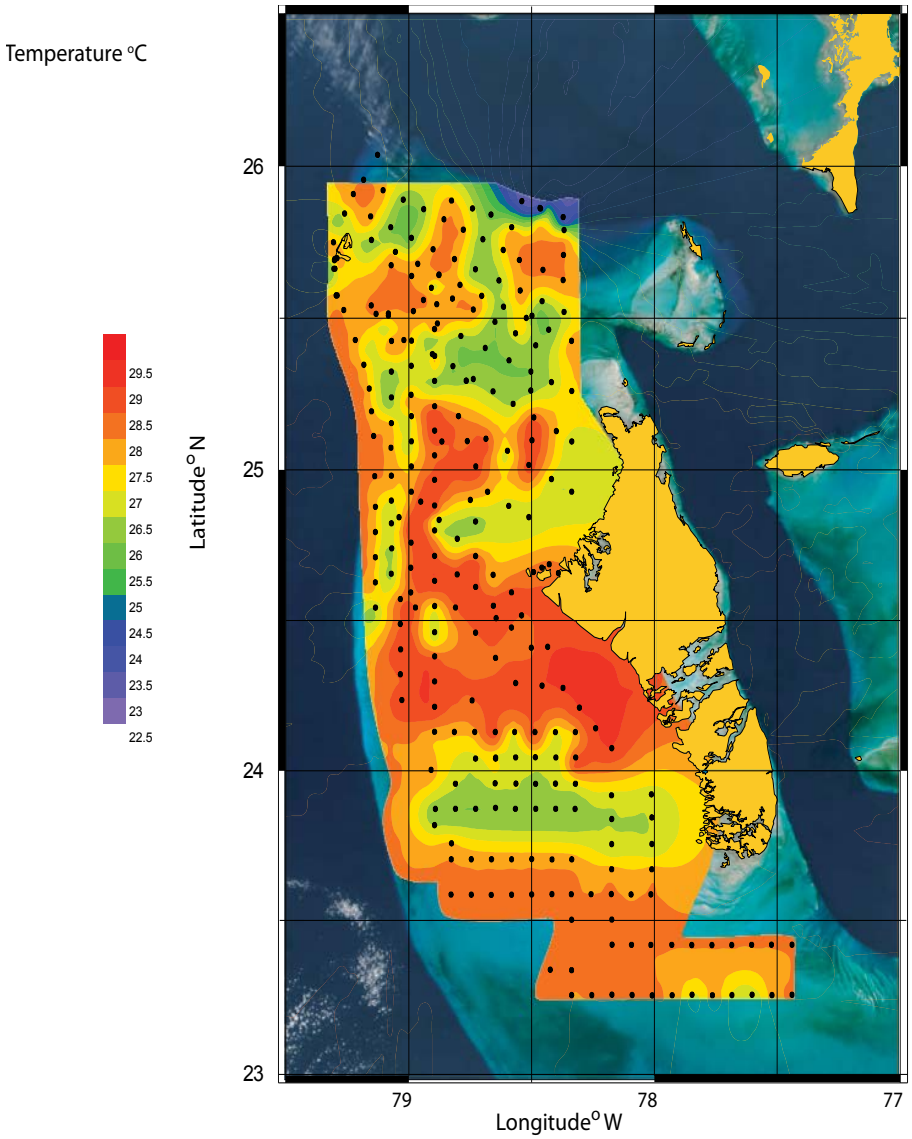

Figure 2.8*- Distribution map of average SST estimates obtained from clumped isotopes based on the equation of Dennis et al., 2011 on Great Bahama Bank.*

Using the average values of each facies it is possible to calculate the average temperature recorded by the sediments using the facies distribution of Reijmer et al (2009) (Figure 2.8).

The contour map of predicted SST exhibits variation across the bank. In other words, higher SST values were determined in the interior of the platform, however, SST values decrease by few degree along the edges of the platform.

2.6.5. Calculation of the $\delta^{18}Ow$

The oxygen isotopic composition of the waters ($\delta^{18}Ow$) varies between +0.75‰ and +2.93‰ across the GBB (Swart et al., 2009), values which are comparable with the $\delta^{18}O$ determined using the clumped isotope temperatures. However, the calculated water values reflect a wider range from -3.95‰ to +4.73‰ depending on the temperature equation employed (Table 2.5).

Both actual and calculated $\delta^{18}O_w$ values exhibit a slightly reverse correlation from mud-dominated facies to mud-lean facies and the correlation cannot be observed from the inner platform to the outer platform everywhere on GBB (Figure 2.9). Although the $\delta^{18}O_w$ values determined using the equations of Dennis et al. (2011) and Fernandez et al. (2014) agree fairly closely with the actual data, the $\delta^{18}O_w$ results calculated employing the method of Wacker et al. (2014) are much more negative. The calculated $\delta^{18}O_w$ estimates which result from the equations of Henkes et al. (2013) and Tang et al. (2014) agree roughly with measured $\delta^{18}O_w$ values. Therefore, despite small discrepancies, the equations of Dennis et al. (2011) and Fernandez et al. (2014) can be considered to be the most suitable for calculating temperature based on the oxygen isotopic composition of the water.

As stated in section 3.2.2, Grossmann and Ku, (1986) analyzed biologically produced carbonates to develop a paleotemperature equation. While a species specific correction would normally be considered most appropriate in order to generate the most accurate results (Grossmann, 2012), a paleotemperature equation for the non-skeletal carbonates utilized in this study is unavailable. This partially explains the discrepancies between $\delta^{18}O_{w\text{-measured}}$ and $\delta^{18}O_{w\text{-calculated}}$ observed in this study.

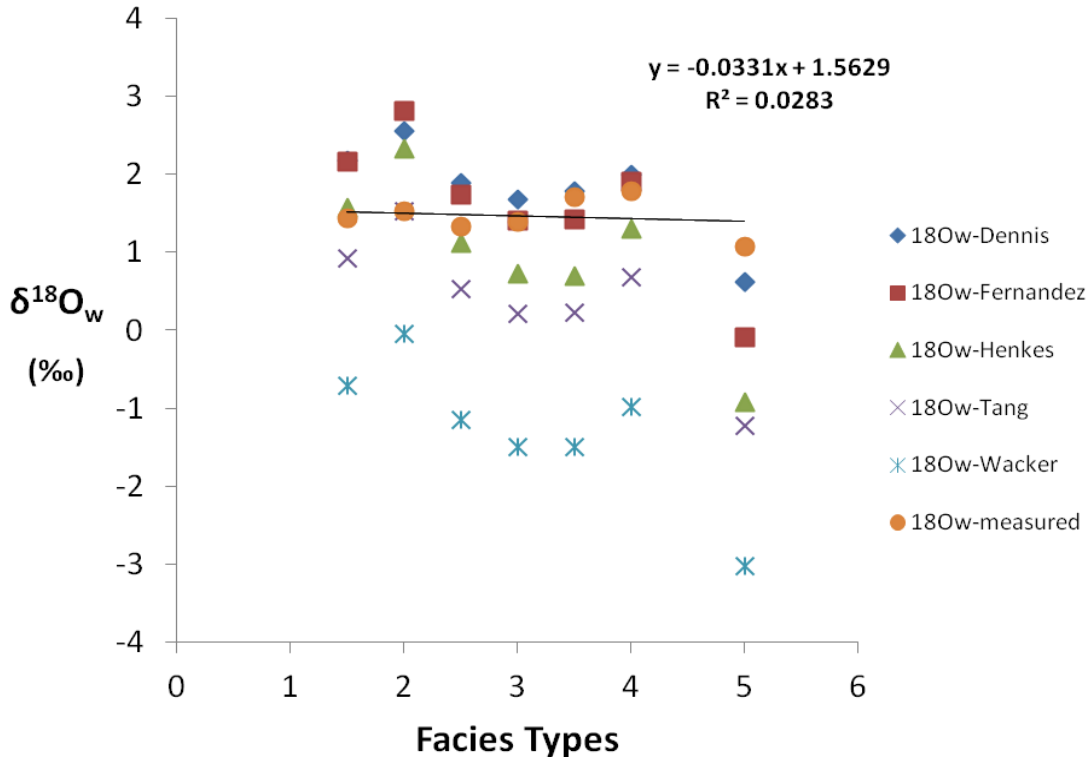

Figure 2.9: *Relationship between actual $\delta^{18}O_w$ and $\delta^{18}O_w$ estimates with facies types (1= Mud, 1.5= Mud-rich wackestone, 2= Wackestone, 2.5= Mud-rich packestone, 3= Packstone, 3.5= Mud-lean packstone, 4= Grainstone, 5= Rudstone).*

Another possible explanation is that the observed discrepancies could result from the mineralogy of the non-skeletal samples, typically ~94% aragonite with a mean

contribution of low-Mg calcite of ~6% (Table 2.1). The discrepancies can be minimized through the use of a better temperature calibration equation.

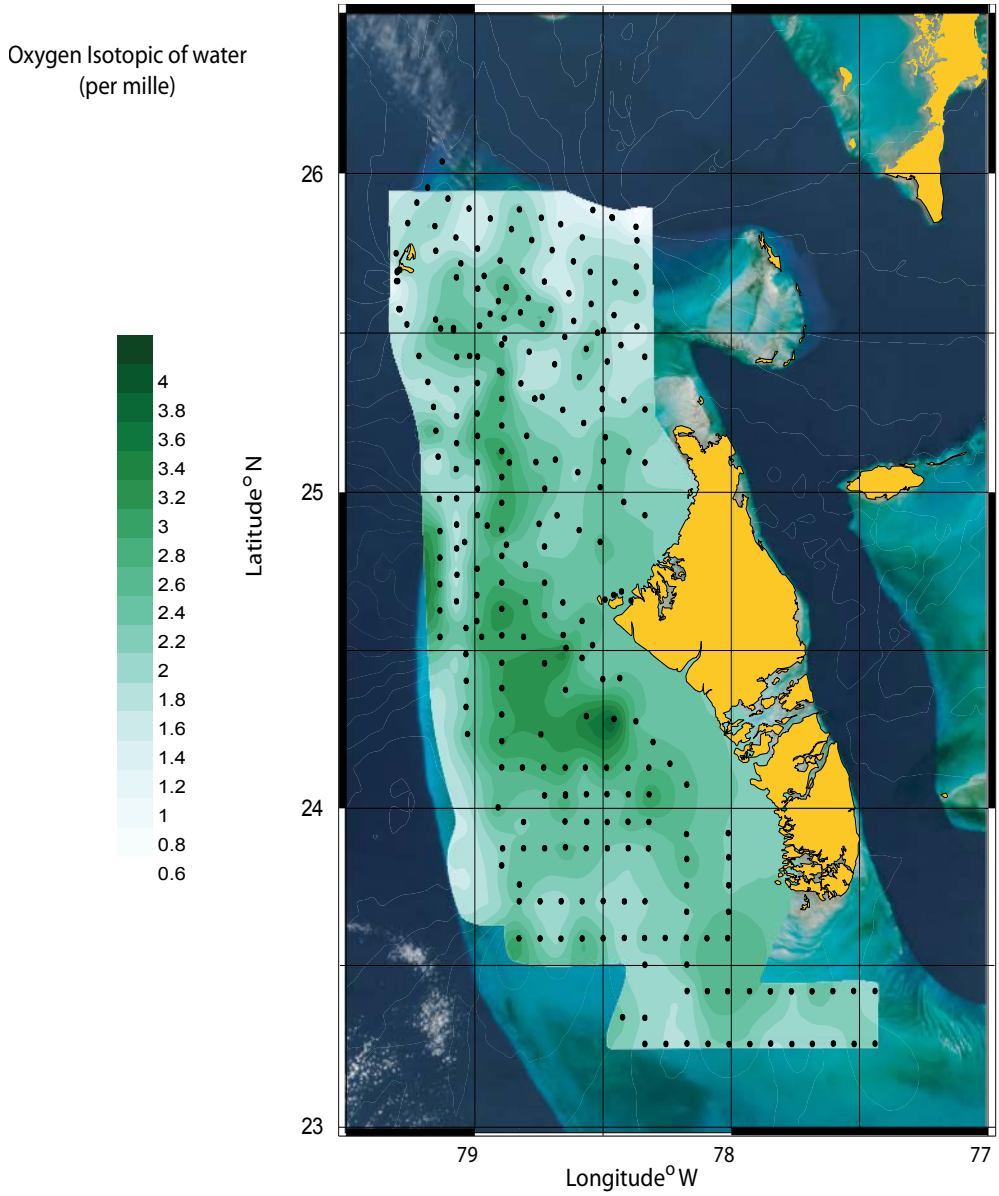

Figure 2.10: *Spatial map of average oxygen isotopic composition calculated for water on GBB.*

2.6.6. Calculation of the salinity

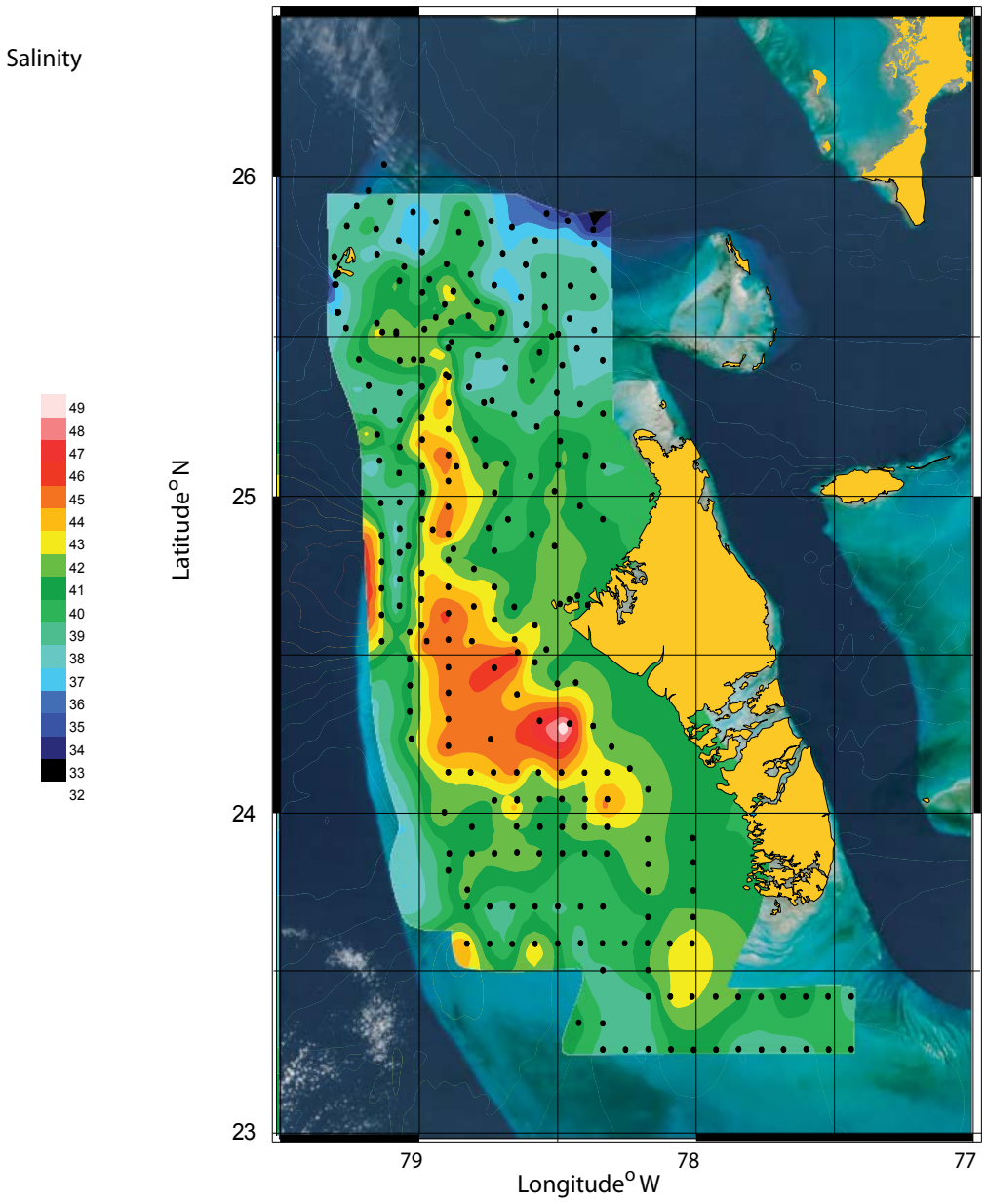

Figure 2.11: *Salinity distribution along the Great Bahama Bank.*

Using the previously determined relationship between $\delta^{18}O$ and salinity (Swart et al., 2009), it is possible to calculate the average salinity represented by the $\delta^{18}O$ of the samples and the calculated $\delta^{18}O_w$ (Figure 2.11). The salinity tends to increase from the

margins of the bank towards the inner of the bank as suggested in previous studies (Black, 1933; Smith 1940b; Cloud, 1962; Shinn et al., 1989).

Low saline surface waters can be explained by mixing between open ocean and bank waters at the margins of the platform and seasonally high amount of precipitation around Andros Island (Cloud, 1962). On the other hand, high evaporation and limited movement of the bank waters leads to exist high saline waters in the middle of the platform.

2.7. Final considerations

The work presented in this thesis is the first to record the clumped isotopic compositions of approximately 35 non-diagenetically altered recent biogenic and non-biogenic carbonate samples collected from GBB. Such data are expected to serve as a reference line for future diagenetic studies and is crucial to determine the influence of early diagenesis on clumped signatures Δ_{47} in marine environments.

There is a correlation between clumped signals and temperature estimates in the original mainly non-biogenic sediments of GBB. However, there may also be some facies control as the clumped signals increase and temperature values decrease from muddy facies to grainy facies.

In this study, the equation of Dennis et al. (2011) was proved as the most suitable equation to employ based on a comparison of results obtained from four other calibration studies and knowledge of the oxygen isotopic composition of the ambient seawater temperatures.

Although the calculated oxygen isotopic composition of water on GBB exhibits a wide range of values when compared to the actual measurements, these calculated $\delta^{18}O_w$ values are fairly consistent with those of the actual data using one of the temperature equations. Realistic salinity estimates, which were determined as a result of calculation of $\delta^{18}O$ of water, generally increase away from the edge of the platform towards the interior. In conclusion, use of the Dennis et al. (2011) equation allowed the expected sea surface temperatures on the GBB to be determined using the clumped isotope method.

CHAPTER 3

CLUMPED ISOTOPE SIGNATURES IN CORALS FROM THE ISLAND OF TOBAGO

3.1. Summary

The island of Tobago is seasonally bathed by water originating from the Orinoco and the Amazon rivers. The $\delta^{18}O$ of a coral skeleton influenced by the magnitude of this fluviatile input responds annually to a change in temperature of approximately 4°C, and precipitation associated with the ITCZ. Clumped isotope analysis makes it possible to distinguish the temperature induced $\delta^{18}O$ signal from that exerted by the freshwater. In order to investigate the efficacy of this technique a specimen of *Diploria Stirgosa* collected in 1991 was analyzed. An extension rate of about 2 cm/yr allowed between 4-5 samples to be collected within each yearly growth increment.

The clumped isotope data underestimates sea surface temperature values by as much as 8°C when compared to the actual values obtained from COADS. This is consistant with previous studies on corals. Once the temperature offset was taken into account, it is possible to extract the reasonable $\delta^{18}O$ of the water using one of the paleotemperature equations established for corals and compare these data to discharge records from the Orinoco River. Reverse correlations have been observed between $\delta^{18}O_{coral}$, $\delta^{18}O_w$ and salinity versus discharge of the Orinoco River over the annual growing interval represented by the modern coral allowing the historical outflow of the Orinoco River to be calibrated through time.

3.2. Overview

Global climate is influenced by fluctuations of sea surface temperatures (SST) and ocean-atmosphere interactions in the tropical realm. An understanding of ancient SST of these regions can help in the reconstruction of past and future climate changes (Allison et al., 2005).

The environmental parameters such as temperature, salinity, freshwater discharges, upwelling and movements of oceans are reflected in the minor and trace element composition and isotopic signature of aragonite coral skeletons (Yu et al., 2004; Allison et al., 2005; Eakin and Grotoli, 2006). Despite a number of limitations, scleractinian corals have been widely utilized to monitor sea surface chemistry and paleoenvironmental conditions in the shallow water tropical oceans of the world (Fairbanks and Dodge, 1979; Swart, 1983; Wellington and Dunbar, 1995; Leder et al., 1996). Corals are particularly useful for several reasons. First, the corals contain density bands which reflect an annual chronology and therefore they can be easily dated. Second, $\delta^{18}O$ and the Sr/Ca values in the skeleton contain a record of seawater surface salinity (SSS) and SST. Lastly, they can live between 200 to 500 years.

The corals from the island of Tobago provide a particularly interesting case study in which the ability of the clumped isotope method can be used to extract the competing influences of salinity and temperature from the $\delta^{18}O$ record of the skeleton. It is known that the island is seasonally influenced by the outflow of fresh water from the Orinoco and the Amazon rivers. The corals therefore show therefore both an annual signal related

to temperature superimposed on a signal derived from the riverine input. Hence using the Δ_{47} both SST and SSS can be ascertained and a long term record of Orinoco discharge obtained.

3.3. Proxies for determining of sea surface temperature

The concentration or abundance of numerous chemical constituents, from trace elements to isotopes, is affected by variations in sea temperature therefore proxies of these parameters will elucidate SST (Correge, 2005). The challenge here is to determine what influences SST and to how much, and to separately identify the effects of each tracer.

In the following section, traditional tools such as Sr/Ca and $\delta^{18}O$ will be briefly discussed along with the advantages of using carbonate clumped isotope paleothermometry for this study.

3.3.1. Oxygen isotope paleothermometry

Traditional oxygen isotope paleothermometry is based on the temperature dependence of oxygen isotope fractionation between carbonate minerals and ambient waters (McCrea, 1950; Epstein et al., 1953). Calibration of the applications are required and are based on the mineral-water oxygen fractionation measurements at high temperatures, mineral precipitation analyses at low temperatures and natural experiments using minerals grown under certain conditions (Anderson and Arthur, 1983; Pearson, 2012) (Leder et al., 1996 - Equation 16).

$$T\ (°C) = 5.33 - 4.519\ (\pm 0.19)\ X\ (\delta^{18}O_{aragonite} - \delta^{18}O_{water}) \qquad (16)$$

Urey (1947) theorized and McCrea, (1950) & Epstein et al., (1951) analytically proved the temperature dependency of carbonate-water oxygen isotopic exchanges, therefore they provided the first oxygen isotope temperature equations using non-biogenic and biogenic carbonates (Epstein and Lowenstam, 1953; Epstein and Mayeda, 1953).

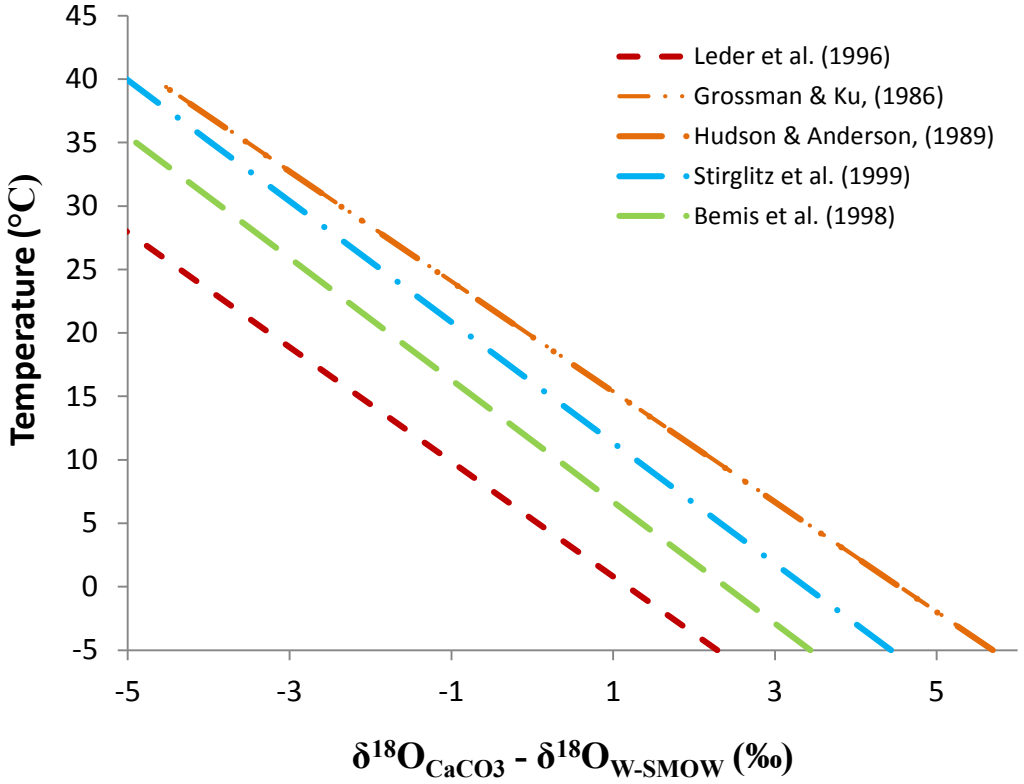

Figure 3.1: *A linear relationship between calcite-water and aragonite-water fractionations using various paleotemperature equations.*

Additional conventional oxygen paleothermometries have been developed analyzing synthetic calcite (Shackleton, 1974; Bemis et al., 1998), biogenic aragonite

(Anderson and Arthur, 1983; Grossman and Ku, 1986; Hudson and Anderson, 1989) and foraminiferal calcite (Erez and Luz, 1983; Bemis et al., 1998).

The most appropriate equation for use in calculating past temperatures is still uncertain (Grossman, 2012). Generally, the equation obtained from material most similar to the subject samples is applied, for example, investigation of the recrystallization temperatures of biogenic aragonite can be derived from equation of Grossman and Ku, (1986).

The essential limitation of the conventional carbonate oxygen thermometry is that the equation contains two unknowns to calculate temperature (See equation 16). Oxygen isotope paleothermometry can be used to calculate past temperatures using high precision calibrations in certain environments. On the other hand, such as unrestricted open surface ocean water, the $\delta^{18}O$ of ambient waters is difficult to estimate. In addition to evaporation (Le Grande and Schmidt, 2006), freshwater input (Swart and Price, 2002), precipitation, river discharge (Gentry et al., 2008), carbonate ion concentrations (Zeebe, 1999) can impact the $\delta^{18}O$ of water. These factors can all contribute to the oxygen isotopic composition of ambient water and limit traditional oxygen paleothermometry.

3.3.2. Sr / Ca proxy

Aragonite skeletons of reef corals contain minor amount of elements such as strontium (Lowenstam, 1963, 1964; Milliman et al., 1967, 1974). Weber, (1973) demonstrated that a possible temperature component existed in Sr/Ca ratios. Although the $\delta^{18}O$ of coral aragonite is strongly affected by SST and the $\delta^{18}O$ composition of seawater, the ratio of Sr/Ca in coral aragonite is a proxy for SST alone independent of

salinity (Beck et al., 1992), being inversely proportional to SST (Kinsman and Holland, 1969). Subsequent works of Houck et al. (1977) and Smith et al. (1979) reported the first equations to explain the relationship between Sr/Ca and SST to be followed by other workers who used the relationship between Sr/Ca and SST as a paleothermometer (Swart, 1981; Schneider and Smith, 1982). The use of Sr/Ca in coral skeletons was published for the first time with high precision (0.5°C) using thermal ionization mass spectrometry to reconstruct SST by Beck et al. (1992). Traditionally, many studies have been carried out to test the robustness of this proxy and understand better mechanisms of Sr incorporation into coral aragonite (Linsley et al., 2000; Correge et al., 2000; Allison et al., 2001; Cohen et al., 2001).

As discussed above, SST is directly related to the Sr/Ca ratio in coral skeletons at the time the skeleton forms; therefore it should theoretically reflect ancient sea temperature fluctuations (Flannery et al., 2013). However, in practice, the better precision of Sr/Ca ratio of coral skeletons versus SST have not been observed with respect to that of Beck et al. (1992) despite many studies (Swart et al., 2002).

Discrepancies in composition may be introduced because the Sr/Ca ratio may vary between different skeletal elements (Smith et al., 2006), skeletal elements can have secondary thickening after initial formation (Cohen et al., 2004), the skeletal growth rate itself may vary (de Villiers et al., 1995).

3.3.3. Carbonate clumped isotope thermometry

As stated in section 2.1, traditional oxygen isotope carbonate-water paleothermometry is based on heterogeneous equilibrium of ^{18}O between carbonate

mineral and water (Epstein et al., 1953; Kim and O'Neil, 1997). Hence, temperatures of formation of carbonates can be measured where ^{18}O values of both phases are known. However, the oxygen isotopic composition of waters is fairly ambiguous over much of the geological record. If the oxygen isotopic composition of coexisting water is uncertain, it may not be possible to calculate carbonate growth temperature using conventional paleothermometry.

3.3.3.1. Previous coral studies using clumped isotope thermometry

Detailed work on modern deep water corals was completed by Thiagarajan et al. (2011) using 11 samples of three species of deep water corals, as well as one species of shallow water coral, from a variety of locations and depths to calibrate carbonate clumped isotopes values in modern deep water corals. As a result of the study, deep sea corals showed a temperature-dependent trend in the clumped signature (Δ_{47}) value that is coincident with the slope and intercept of the inorganic calcite calibration of Ghosh et al. (2006) and demonstrated that clumped isotopes can be utilized as an accurate paleothermometer in deep water corals. Despite considerable vital effects on ^{18}O, Thiagarajan et al. (2011) did not find any vital effects on Δ_{47} and demonstrated that pH effects explained observed changes in $\delta^{18}O$ and Δ_{47}. The shallow water coral sample exhibited no vital effects and differed from the method of Ghosh et al. (2006) in using mean annual bands rather than seasons. Thus, the clumped isotope technique can be considered as the most appropriate tool for SST studies (Thiagarajan et al., 2011).

The first systematic study of clumped signals (Δ_{47}) in shallow water corals was published by Saenger et al. (2012) using a suite of hermatypic/ahermatypic and symbiotic/asymbiotic corals collected from the Red Sea, Pacific and Atlantic Oceans to explore variations in Δ_{47} linked with vital effects. Although the results from ahermatypic corals are generally consistent with the inorganic calibration of Ghosh et al. (2006), hermatypic corals display higher than predicted Δ_{47} values that result in temperature underestimates of ~8°C. They concluded that the clumped isotope signals (Δ_{47}) in shallow water corals reflect temperature dependence and may be used as a novel proxy (Saenger et al., 2012).

3.4. Hypothesis and goals

3.4.1. Hypothesis

The island of Tobago is located just off the northern coast of South America (Mallela et al., 2010). Around the island of Tobago, water temperature changes between 25°C to 29°C (COADS) and is seasonally bathed by waters from the Orinoco and the Amazon rivers (Moses et al., 2006). While it has been suggested that the $\delta^{18}O$ of the corals changes in response to the magnitude of the outflow of the Orinoco River (Risk et al., 1992), detailed work by Moses et al (2006) showed that while there was some fluviatile influence, the magnitude of the outflow was not recorded in deviations of the $\delta^{18}O$ signal from expected values (Moses et al., 2006). In fact it was concluded that variations in the ITCZ (Intertropical Converge Zone) caused the Orinoco and Amazon rivers to periodically influence reefs growing around island of Tobago. If this hypothesis

is correct, it should be possible to measure SST using the clumped isotope signal and then correct the $\delta^{18}O$ value to determine the signal of the water.

3.4.2. Goals

The first purpose of this study is to examine how well scleractinian corals record the clumped isotope signal. The second aim of the study is to determine past SST and SSS. The last goal is to reveal any relationship between the magnitudes of the freshwater input originating from the Orinoco and Amazon rivers, and if this affects the position of the ITCZ and the oxygen isotopic composition of the corals.

3.5. Study site and settings

3.5.1. Study site

Trinidad and Tobago are the southernmost of the Caribbean Islands. The island of Tobago lies nearly 30 km north-east of Trinidad has an area of approximately 300 km^2 (Figure 3.2). Although the island is geologically distinct from the islands of the Lesser Antilles, it is characterized as a fragment of the Antillean Cretaceous island arc (Frost and Snoke, 1989; Jackson and Donovan, 1994).

Jackson et al. (1988) described the island in terms of three geological units with the surface geology made up of sedimentary, igneous and metamorphic rocks. The sedimentary layer consists of coral limestone overlying the siliciclastic Rockly Bar Formation which is Pliocene in age (Donovan, 1989), which in turn overlies Cretaceous volcanic. The study area falls within the Speyside marine area (11°10'N, 60°51'W),

incorporating one of the largest reefs systems around Tobago and located on the northeastern point of the island.

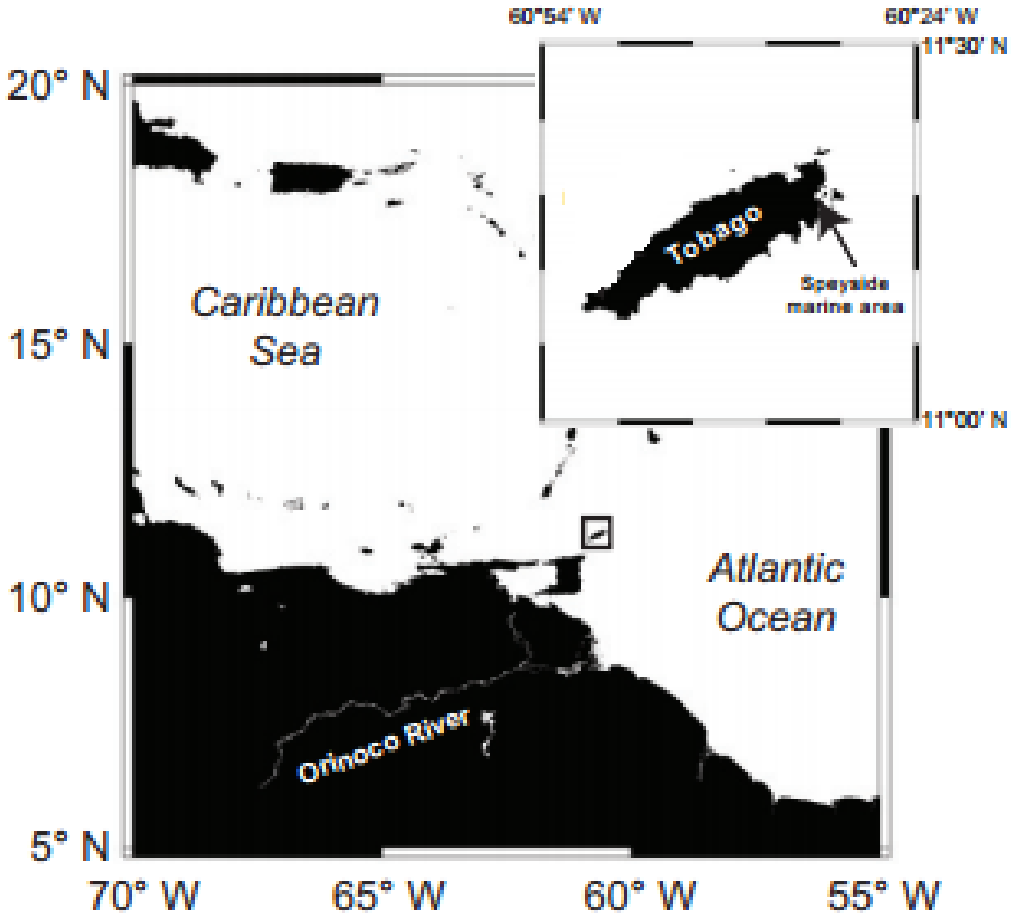

Figure 3.2: *Map of the island of Tobago showing the location of sampling site (Moses et al., 2006).*

3.5.2. Settings

The North Atlantic trade winds undergo latitudinal displacements with seasonal movement of the ITCZ throughout a gradient from the Amazon River Basin and the Orinoco River Basin into the Central Caribbean (Lewis et al., 1995). These events cause a dry season from January to May with low rainfall and warm days. The rainy season,

characterized by high rainfall and hot humid days, extends from June to December (Tobago and Trinidad Meteorological Service, 2009). Once the northern part of the ITCZ is centered over the Caribbean and Northern South America, both abundant rainfall and terrestrial runoff results in freshwater discharges to the eastern part of the Caribbean.

The discharges play a significant role in the hydrological cycle of the Caribbean Sea which is strongly affected by both the Orinoco and Amazon rivers (Hu et al., 2004). The Amazon is described as the largest river in the world in terms of fresh water outflow (175-300 x $10^3 m^3 s^{-1}$) (Milliman et al., 1983; Perry et al., 1996). The discharge of the Amazon disperses northwestward along the north Brazilian coast, offshore into the Caribbean Sea and eastward into the north Atlantic (Muller-Karger et al., 1988, 1995; Johns et al., 1990; Hu et al., 2004).

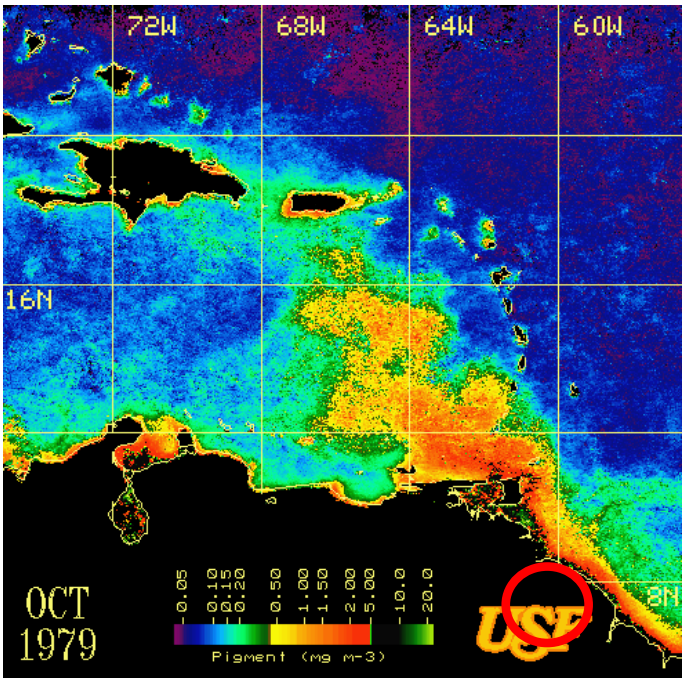

Figure 3.3: *Dispersion of discharge of freshwater from Orinoco River into Caribbean as shown by the satellite image using the coastal zone color scanner (Muller and Karger et al., 1988). Trinidad and Tobago are shown by red circle*

The Orinoco River meanwhile is the fourth largest of the world's rivers in terms of discharge with a mean outfall of 20 x 10^3 m^3s^{-1}fresh water into the southern Caribbean Sea near Venezuela (Muller-Karger et al., 1994; Perry et al., 1996) (Figure 3.3) and is a the prevailing factor affecting development of marine life on Tobago has been the outflow from the Orinoco River (UNEP/IUCN, 1988) with as much as half of the $\delta^{18}O$ signature of coral heads reflecting the low salinity (Risk et al., 1992). The seasonal floods of the Orinoco River (August-September) affect the northward movement of the ITCZ and South American Moonson (SAM) (Lewis and Saunders, 1989; Wang and Fu, 2002).

3.6. Methodology

3.6.1. Samples

Diploria Strigosa (Dana, 1846), (brain coral) is an important reef-building, shallow water coral (Bak, 1977) forming large colonies in the Caribbean Sea (Woodley et al., 1981; Scheffers et al., 2006). The coral generates distinct annual density bands (Helmle et al., 2000) that have been demonstrated to correspond with climate variations in the Tropical Atlantic Ocean based on Sr/Ca and $\delta^{18}O$ values (Hetzinger et al., 2006, 2008, 2010; Kuhnert et al., 2005). As a result, this species is a potential recorder of ancient SST in the Southern Caribbean (Giry et al., 2010).

This study analyzed a modern specimen of *Diploria Strigosa* (Figure 3.4) collected from the island of Tobago (Speyside; February, 1991) at a depth of 14 feet. Counting of the density bands determined that the sample formed from 1983 to 1991.

Four to five subsamples were cut annually giving a total of 38 samples. After extraction the samples were dried in an oven at 40°C and then finely ground using a mortar and pestle in preparation for clumped isotope analyses. For each sample approximately 8 mg of powder was placed into individual small copper boats with each sample being analyzed either in triplicate or in duplicate.

Figure 3.4: *The shallow water coral from Speyside marine area.*

3.6.2. Analytical

As explained in the first chapter, the CO_2 generated from the coral samples by reaction with 103% phosphoric acid using the gas purification line (Swart et al., 1991), was subsequently delivered to the advanced mass spectrometer (MAT 253). The clumped signals (Δ_{47}) were calculated using the equation identified by several authors (Eiler, 2006; Affek et al., 2008; Huntington et al., 2009) and then converted to the reference frame proposed by Dennis et al. (2011). Eventually, Δ_{47} values were adapted using an acid fractionation factor of 0.112‰ (Murray, 2014 unpublished). A regime of daily in-house standards (Carrera marble) and monthly inter-laboratory calibrations (Dennis et al., 2001) was applied to check for instrumental errors or problems with sample preparation.

In order to acquire high resolution $\delta^{18}O$ data from the coral, 12 samples were taken from each annual extension during the 8 years encompassing 1983 to 1991. These 96 samples were analyzed using a Kiel III attached to a Finnigan Delta Plus. Data obtained was corrected for isobaric interferences using the procedures outlined in Craig (1957) modified for a triple collector mass spectrometer. Data were reported relative to Vienna Pee Dee Belemnite (V-PDB) using the traditional notation. Average standard deviation based on replicate analyses of internal standards was less than 1%.

The SST data for a grid centered on 11^{o}N, 61^{o}W comes from the Comprehensive Atmospheric Data Set (COADS) due to the limited availability of regional documentation pertaining to the island of Tobago (Slutz et al., 1985). The SST varies annually by approximately 4°C near the sample site. Equivalent *in situ* SST data is not available for Speyside marine area. Utilization of this dataset is intended to show how well carbonate clumped isotope thermometry works to measure SST values between 1983 and 1991 using a modern shallow water coral in Tobago.

The Orinoco River discharge data set was recorded using a flood gauge located on the Orinoco River at Ciudad Bolivar, Venezuela from 1983-1991. Between 1985 and 1986, there is no documented discharge data from the mouth of Orinoco River.

3.6.2.1. Calculation of oxygen composition of seawater

One of the most remarkable features of the clumped isotope technique is that it theoretically enables the determination of the $\delta^{18}O$ of the water. For this study, the coral-based equation of Leder at al. (1996) was believed to be the most appropriate paleotemperature equation (Equation 17).

$$\delta^{18}O_w = \delta^{18}O_c - (5.33 - T) / 4.23 \quad (17)$$

In this equation $\delta^{18}O_w$ = isotopic composition of water (V-SMOW), $\delta^{18}O_c$ = oxygen composition of coral (V-PDB) and T= temperature (°C). Temperature and $\delta^{18}O_c$ values were obtained from the clumped isotope measurements. With knowledge of these parameters, the oxygen isotopic composition of the water can be readily gathered.

3.6.2.2. Calculation of sea surface salinity

Oxygen isotopic composition of seawater ($\delta^{18}O_w$) and SSS co-varies in the surface ocean waters on a global scale (Schmidt et al., 1999). The relationship between SSS and $\delta^{18}O_w$ has been paid considerable attention over the last five decades (Craig and Gordon, 1965; Schmidt, 1999; Delaygue et al., 2000).

$$\delta^{18}O_w = 0.204\ (\pm 0.03)\ X\ SSS - 6.54\ (\pm 0.68) \quad (18)$$

When $\delta^{18}O_w$ has been calculated based on the equation of Leder et al. (1996), SSS can be easily acquired from Equation 18 (Watanabe et al., 2001). In the equation, $\delta^{18}O_w$ and SSS refer to the oxygen isotopic composition of seawater (V-PDB) and SSS (psu).

3.7. Results

The Δ_{47} values were normalized to the common scale determined by Dennis et al. (2011). The calculated Δ_{47} values are shown in Table 6 with their standard deviations. The Δ_{47} variability displays ranges from 0.716±0.03‰ to 0.753±0.01‰. These clumped signals have been modified to temperature estimates using the recent

various equations (Dennis et al., 2011; Fernandez et al., 2014; Henkes et al., 2013; Tang et al., 2014; Wacker et al., 2014).

No	Sample ID	Mean Δ 47	sd	Dennis Temp.	sd	Fernandez Temp.	sd	Henkes Temp.	sd	Tang Temp.	sd	Wacker Temp.	sd	replicates
Unit		‰		°C		°C		°C		°C		°C		
1	**TC 01.01**	0.717	0.02	23.69	2.26	20.65	3.62	17.01	4.10	15.70	3.42	7.89	3.73	2
2	**TC 01.02**	0.742	0.01	18.62	1.92	12.65	2.97	7.98	3.33	8.12	2.82	-0.33	3.04	2
3	**TC 01.03**	0.732	0.02	20.70	3.01	15.91	4.71	11.65	5.30	11.21	4.46	3.01	4.83	3
4	**TC 01.04**	0.716	0.03	23.98	5.61	21.20	8.98	17.67	10.18	16.21	8.49	8.47	9.25	3
5	**TC 01.05**	0.738	0.01	19.52	2.18	14.05	3.41	9.56	3.83	9.45	3.23	1.10	3.49	3
6	**TC 02.01**	0.745	0.02	18.22	3.65	12.06	5.65	7.34	6.32	7.57	5.36	-0.93	5.78	3
7	**TC 02.02**	0.738	0.00	19.58	0.68	14.12	1.06	9.64	1.19	9.53	1.01	1.18	1.09	2
8	**TC 02.03**	0.750	0.01	17.12	2.00	10.32	3.07	5.38	3.43	5.92	2.92	-2.72	3.14	2
9	**TC 02.04**	0.731	0.02	21.00	4.78	16.43	7.57	12.26	8.54	11.71	7.16	3.56	7.78	3
10	**TC 02.05**	0.739	0.01	19.27	2.07	13.66	3.21	9.12	3.60	9.08	3.05	0.70	3.29	3
11	**TC 03.01**	0.739	0.01	19.37	2.04	13.81	3.18	9.29	3.57	9.23	3.01	0.86	3.26	3
12	**TC 03.02**	0.719	0.00	23.33	0.31	20.05	0.50	16.32	0.56	15.14	0.47	7.27	0.51	2
13	**TC 03.03**	0.728	0.00	21.53	0.00	17.19	0.00	13.08	0.00	12.43	0.00	4.32	0.00	1
14	**TC 03.04**	0.722	0.01	22.81	3.65	19.26	5.81	15.44	6.58	14.39	5.50	6.46	5.98	2
15	**TC 03.05**	0.721	0.01	22.91	1.71	19.39	2.72	15.58	3.08	14.52	2.57	6.59	2.80	3
16	**TC 04.01**	0.725	0.01	22.04	2.85	18.03	4.55	14.04	5.15	13.22	4.30	5.19	4.68	3
17	**TC 04.02**	0.741	0.02	18.99	2.99	13.23	4.68	8.65	5.26	8.68	4.44	0.27	4.80	3
18	**TC 04.03**	0.736	0.01	19.92	1.73	14.68	2.70	10.26	3.03	10.05	2.56	1.75	2.77	3
19	**TC 04.04**	0.722	0.00	22.67	0.66	19.00	1.06	15.13	1.20	14.14	1.00	6.19	1.09	3
20	**TC 05.01**	0.733	0.01	20.41	1.38	15.43	2.17	11.11	2.44	10.76	2.05	2.52	2.23	3
21	**TC 05.02**	0.728	0.01	21.49	1.07	17.13	1.68	13.02	1.90	12.37	1.59	4.26	1.73	2
22	**TC 05.03**	0.736	0.01	19.82	1.58	14.51	2.47	10.08	2.78	9.90	2.34	1.58	2.54	2
23	**TC 05.04**	0.753	0.01	16.56	1.74	9.46	2.67	4.42	2.98	5.10	2.54	-3.60	2.73	3
24	**TC 06.01**	0.728	0.00	21.37	0.96	16.95	1.51	12.81	1.71	12.20	1.43	4.08	1.55	2
25	**TC 06.02**	0.729	0.01	21.24	1.42	16.74	2.24	12.58	2.53	12.01	2.12	3.87	2.30	3
26	**TC 06.03**	0.743	0.01	18.45	2.25	12.39	3.49	7.70	3.91	7.88	3.31	-0.60	3.57	3
27	**TC 06.04**	0.725	0.01	22.01	2.11	17.96	3.33	13.97	3.76	13.16	3.15	5.12	3.42	3
28	**TC 06.05**	0.730	0.01	21.03	2.41	16.42	3.80	12.23	4.28	11.70	3.60	3.54	3.90	3
29	**TC 07.01**	0.716	0.01	23.84	2.98	20.90	4.75	17.30	5.38	15.94	4.50	8.15	4.89	3
30	**TC 07.02**	0.721	0.02	22.90	3.24	19.40	5.15	15.60	5.83	14.52	4.88	6.61	5.31	3
31	**TC 07.03**	0.735	0.01	20.10	1.63	14.95	2.56	10.57	2.88	10.31	2.42	2.03	2.62	3
32	**TC 07.04**	0.721	0.00	22.83	0.31	19.26	0.50	15.42	0.56	14.39	0.47	6.45	0.51	2
33	**TC 07.05**	0.732	0.01	20.59	1.35	15.73	2.12	11.44	2.39	11.04	2.01	2.82	2.18	3
34	**TC 08.01**	0.730	0.02	21.15	4.40	16.65	6.98	12.51	7.89	11.92	6.61	3.79	7.18	3
35	**TC 08.02**	0.731	0.03	21.07	6.07	16.59	9.60	12.46	10.84	11.85	9.09	3.73	9.87	3
36	**TC 08.03**	0.718	0.01	23.60	1.31	20.49	2.09	16.82	2.37	15.55	1.98	7.72	2.15	3
37	**TC 08.04**	0.726	0.00	21.81	0.57	17.64	0.90	13.60	1.02	12.86	0.85	4.79	0.93	2
38	**TC 08.05**	0.727	0.02	21.76	3.43	17.59	5.41	13.56	6.09	12.81	5.12	4.75	5.55	3

Table 3.1: *Average clumped signals values and temperature estimates of replicates of the coral with standard deviations. Although TC 01.01 represents the top of the coral dated 1991, TC 08.05 reflects the bottom of the coral formed in 1983. n denotes number of analyses of the samples.*

No	Sample	δ18Owater	sd	Salinity	sd	No	Sample	δ18Owater	sd	Salinity	sd
Unit	ID	‰					ID	°C			
1	**TC 01.01**	2.28	0.9	43.22	4.2	20	**TC 05.01**	1.61	0.3	39.96	1.3
2	**TC 01.02**	1.14	0.4	37.65	1.9	21	**TC 05.02**	1.68	**0.3**	40.31	1.3
3	**TC 01.03**	1.74	0.7	40.56	3.6	22	**TC 05.03**	1.50	0.4	39.44	2.1
4	**TC 01.04**	2.14	1.3	42.54	6.4	23	**TC 05.04**	0.47	0.3	34.37	1.7
5	**TC 01.05**	1.32	0.6	38.52	2.7	24	**TC 06.01**	1.76	0.2	40.69	1.1
6	**TC 02.01**	0.97	0.8	36.83	4.0	25	**TC 06.02**	1.56	0.3	39.73	1.6
7	**TC 02.02**	1.27	0.1	38.28	0.6	26	**TC 06.03**	0.95	0.5	36.74	2.5
8	**TC 02.03**	0.74	0.5	35.70	2.2	27	**TC 06.04**	1.94	0.5	41.58	2.4
9	**TC 02.04**	1.57	1.1	39.77	5.5	28	**TC 06.05**	1.76	0.6	40.69	2.8
10	**TC 02.05**	1.16	0.5	37.73	2.4	29	**TC 07.01**	2.37	0.7	43.65	3.6
11	**TC 03.01**	1.27	0.5	38.28	2.2	30	**TC 07.02**	2.06	0.8	42.18	3.9
12	**TC 03.02**	2.13	0.0	42.50	0.2	31	**TC 07.03**	1.51	0.4	39.47	1.9
13	**TC 03.03**	1.90	0.0	41.38	0.0	32	**TC 07.04**	2.01	0.1	41.92	0.5
14	**TC 03.04**	1.96	0.5	41.67	4.4	33	**TC 07.05**	1.60	0.3	39.91	1.7
15	**TC 03.05**	2.22	0.4	42.96	1.9	34	**TC 08.01**	1.78	1.0	40.81	5.1
16	**TC 04.01**	1.92	0.7	41.48	3.2	35	**TC 08.02**	1.60	1.4	39.91	6.7
17	**TC 04.02**	1.24	0.7	38.11	3.7	36	**TC 08.03**	2.31	0.3	43.40	1.3
18	**TC 04.03**	1.56	0.3	39.71	1.7	37	**TC 08.04**	1.91	0.1	41.40	0.3
19	**TC 04.04**	2.01	0.2	41.90	0.8	38	**TC 08.05**	1.71	0.8	40.42	4.1

Table 3.2: *The estimates of $\delta^{18}O$ of ambient seawater based on Leder et al. 1996 and SSS values using equation of Watanabe et al. 2001 together with their standard deviations.*

A 0.036‰ range in clumped signals was calculated among the samples having an estimated range in growth temperature of 16.56-23.98°C depending on the equation employed (Dennis et al., 2011), 9.46-21.20°C (Fernandez et al., 2014), 11.20-25.10°C (Henkes et al., 2013), 4.42-11.65°C (Tang et al., 2014), -3.60-8.47°C (Wacker et al., 2014) (Table 3.1). The standard deviations are markedly higher using the equation of Fernandez et al. (2014), Henkes et al. (2013), Tang et al. (2014) and Wacker et al. (2014), relative to the standard deviation obtained from the equation of Dennis et al. (2011).

No	Year	δ13Carbon	δ18Oxygen	No	Year	δ13Carbon	δ18Oxygen	No	Year	δ13Carbon	δ18Oxygen
Unit		‰	‰			‰	‰			‰	‰
1	1991	-0.79	-3.64	33	1988	-0.76	-3.76	65	1985	0.21	-3.28
2	1990	-0.27	-2.90	34	1988	-1.76	-3.08	66	1985	-0.73	-3.53
3	1990	-0.72	-2.83	35	1988	-0.70	-3.61	67	1985	0.26	-3.03
4	1990	-1.47	-2.82	36	1988	0.01	-3.03	68	1985	-0.05	-2.66
5	1990	-0.78	-3.98	37	1987	0.08	-3.06	69	1985	-0.76	-3.01
6	1990	-1.60	-3.20	38	1987	-1.30	-3.80	70	1985	-0.43	-2.32
7	1990	-1.38	-2.49	39	1987	-0.78	-3.73	71	1985	-1.29	-3.15
8	1990	-0.70	-3.23	40	1987	0.43	-2.24	72	1985	-0.69	-3.17
9	1990	-1.69	-3.69	41	1987	-0.11	-2.15	73	1984	-0.88	-3.26
10	1990	-1.56	-3.43	42	1987	0.00	-2.20	74	1984	-0.34	-3.66
11	1990	-2.51	-2.74	43	1987	-0.39	-2.44	75	1984	-1.84	-1.83
12	1990	-0.57	-3.65	44	1987	0.42	-2.96	76	1984	-0.58	-3.90
13	1989	-1.96	-3.12	45	1987	-0.16	-3.22	77	1984	-1.44	-3.36
14	1989	-1.57	-3.87	46	1987	0.04	-3.00	78	1984	-0.65	-3.89
15	1989	-1.30	-3.10	47	1987	-0.46	-2.73	79	1984	-0.62	-3.17
16	1989	-1.00	-2.97	48	1987	-1.29	-3.54	80	1984	0.06	-3.45
17	1989	-0.99	-2.30	49	1986	0.07	-3.80	81	1984	-1.12	-3.62
18	1989	-1.24	-3.83	50	1986	-0.18	-2.54	82	1984	-0.19	-3.60
19	1989	-1.56	-2.62	51	1986	-1.33	-3.59	83	1984	0.30	-3.38
20	1989	-0.69	-3.88	52	1986	0.26	-2.80	84	1984	-0.15	-2.71
21	1989	-1.54	-2.62	53	1986	-0.39	-3.50	85	1983	-0.76	-3.39
22	1989	-0.85	-3.20	54	1986	-0.84	-2.34	86	1983	-0.22	-3.97
23	1989	-0.78	-2.92	55	1986	-0.25	-3.76	87	1983	-0.52	-3.30
24	1989	-1.53	-2.72	56	1986	-0.62	-2.66	88	1983	-0.39	-3.64
25	1988	-1.13	-3.81	57	1986	-1.57	-4.04	89	1983	0.18	-3.57
26	1988	-1.28	-3.07	58	1986	-0.30	-3.60	90	1983	0.14	-3.04
27	1988	-1.73	-3.21	59	1986	-0.41	-3.42	91	1983	-0.59	-4.15
28	1988	-0.54	-3.63	60	1986	-0.57	-2.87	92	1983	-0.05	-3.69
29	1988	-1.28	-3.25	61	1985	-1.01	-3.14	93	1983	-0.34	-3.87
30	1988	-0.98	-3.55	62	1985	-0.70	-2.89	94	1983	-0.03	-3.97
31	1988	-1.43	-2.05	63	1985	-0.69	-1.81	95	1983	-0.37	-3.94
32	1988	-1.35	-3.67	64	1985	-0.16	-3.76	96	1983	-0.29	-2.42

Table 3.3: *Stable isotope analyses of 96 subsamples from each annual growth band from 1983 to 1991.*

Using temperature estimates (Table 3.2) the oxygen isotopic composition of water has been calculated based on the paleotemperature equation of Leder et al. (1996) (See 4.2.1) The $\delta^{18}O_w$ changes from -0.73±0.3‰ to 1.13±0.7‰ during the sampling period 1983 through 1991. Although the $\delta^{18}O$ of the coral varies from -4.15‰ to -1.83‰, the $\delta^{13}C$ of the coral displays a wider range varying between -2.51‰ and 0.43‰ over this time period.

3.8. Discussions

3.8.1. Temperature estimates

As stated in section 2.3.1, two previous papers, the deep water coral study of Thiagarajan et al. (2011) and the shallow water coral study of Saenger et al. (2012), have used the first temperature calibration of Ghosh et al. (2006) to estimate growth temperature. Generally speaking, coral aragonite formed over a certain temperature range agrees with the calibration of Ghosh et al. (2006), which although based on inorganic calcite has been frequently applied to both non-biogenic and biogenic carbonate minerals.

However, while the synthetic calibration studies of Ghosh et al. (2006) and Dennis and Schrag et al. (2010) suggested that the effects of recombination and fragmentation reactions were insignificant, subsequent work by Dennis et al. (2011) to establish an absolute reference frame has demonstrated that this is not in fact the case.

For this reason, the clumped signatures (Δ_{47}) obtained from the coral are needed to be normalized to the reference frame outlined by Dennis et al. (2011). The coral displays seasonal variability in clumped signals that ranges from 0.716±0.03‰ to

0.753±0.01‰.These values are given in Table 3.1 and have been converted to temperature estimates using recently published temperature equations (Dennis et al., 2011; Fernandez et al., 2014; Henkes et al., 2014; Tang et al., 2014; Wacker et al., 2014) instead of using equation of Ghosh et al. (2006).

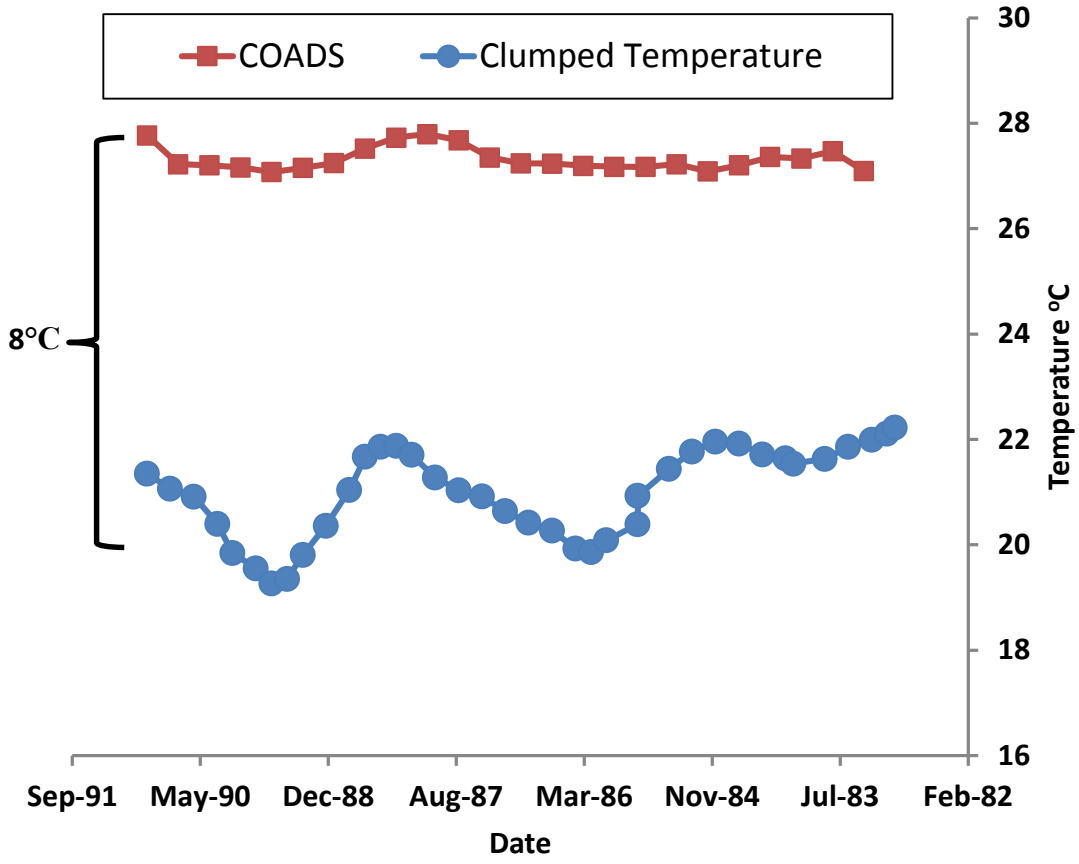

Figure 3.5: *The actual SST data obtained from COADS and SST estimates measured from the shallow water coral using clumped isotope method between 1983 and 1991.*

Typically, there is insignificant variation in COADS offshore SST values between 1983 and 1991 (Figure 3.5). When compared to the actual measurements, Table 3.1 undoubtedly exhibits that temperature calibration of Dennis et al. (2011) were determined as a most suitable equation among five recent calibration studies. Whereas the seasonal

temperature amplitude of nearly 3°C was observed as a result of calibration of Dennis et al. (2011), seasonal variation in 1°C was determined from the COADS (Figure 3.5).

While the hermatypic corals showed higher clumped signature values and temperature estimates which were lower by approximately 8°C (Saenger et al., 2012), values for ahermatypic corals were consistent with the inorganic calcite temperature calibration of Ghosh et al. (2006). On the other hand, deep water corals can be utilized to determine SST using the clumped isotope method with high precision (0.5°C) in spite of having large vital effects in $\delta^{18}O$ (Thiagarajan et al., 2011).

In the study area, the seasonal variability of SST, a characteristic feature of shallow marine environments, is expected to produce temperatures several degrees warmer than the open ocean SST reported in COADS. However, the SST estimates of clumped isotopes from the specimen of *Diploria Strigosa* analyzed in this study leads to an underestimation of about 8°C relative to the open ocean data and confirm results of shallow water coral determined by the first systematic survey of Saenger et al. (2012). This disagreement is unlikely to be due to laboratory processes such as sample preparation, in house standardization and analysis artifacts.

3.8.2. Possible correlations between outflow of Orinoco, $\delta^{18}O_{water}$, $\delta^{18}O_{coral}$ and SST

There is no simple correlation between $\delta^{18}O_{Coral}$ and average monthly input from the river from 1983 through 1991 in the study area (Figure 3.6). The influence of discharge is supposed to consider as small effect on $\delta^{18}O_{coral}$. For this reason, the $\delta^{18}O_{coral}$ should be strongly affected by variation in SST around the Speyside marine area

according to the hypothesis. When underestimation of SST values was remedied, the SST dependency of oxygen isotopic composition of the coral skeleton was verified by a positive correlation as described Figure 3.7. Therefore, more positive oxygen values are associated with high SST values.

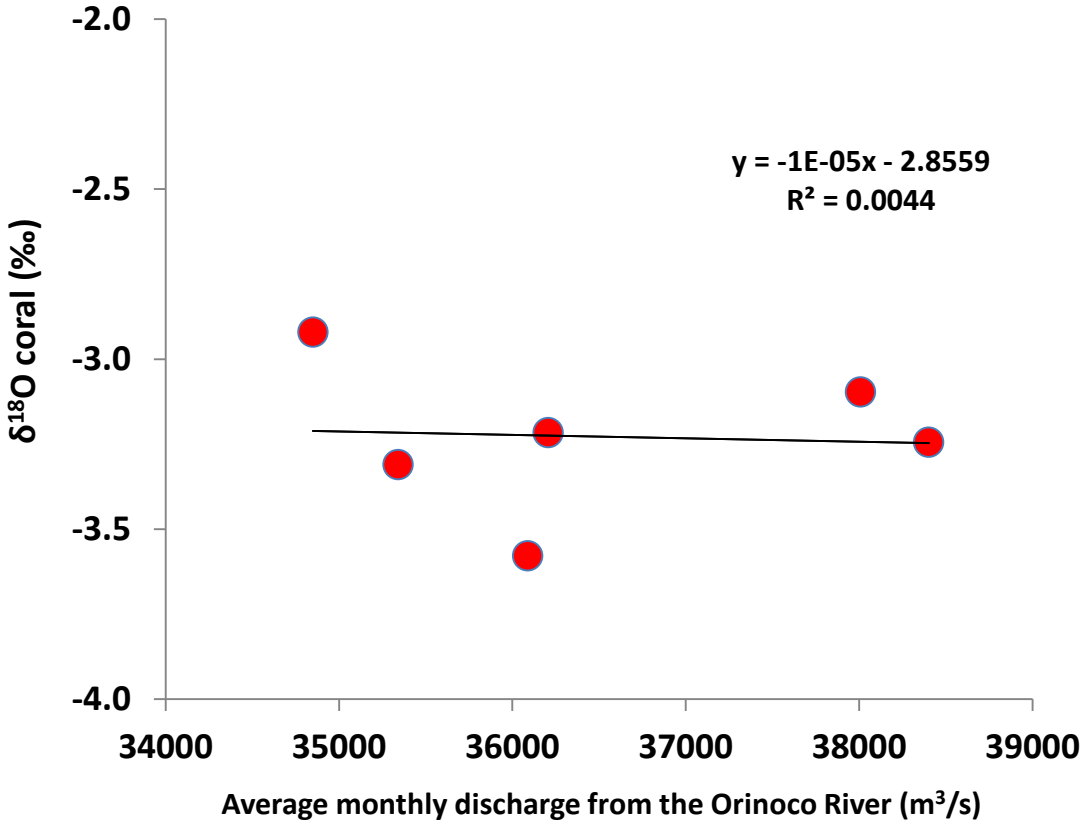

Figure 3.6: *No simple correlation in this study between oxygen isotopic composition of coral skeleton and average monthly discharge from Orinoco River of Venezuela.*

One of the most promising aspects of the clumped isotope revolution is that it allows for the theoretical calculation of the oxygen isotopic composition of water (Ghosh et al., 2006a,b; Eiler, 2007; 2011; Affek et al., 2008; Henkes et al., 2012). At the start of this study, this advantageous feature was expected to be a strong tool to extend the detailed study of Moses and Swart, (2006).

In this respect, correlations between the discharge of the Orinoco River and $\delta^{18}O_w$ are essential in order to understand the influence that the freshwater discharge of the Orinoco River has on the $\delta^{18}O$ of the coral skeleton. After calculating realistic $\delta^{18}Ow$ values, it is inversely associated with the output of the Orinoco River (Figure 3.8). This correlation would be expected with the largest fluviatile input corresponding to intervals characterized by more negative oxygen isotopic water compositions.

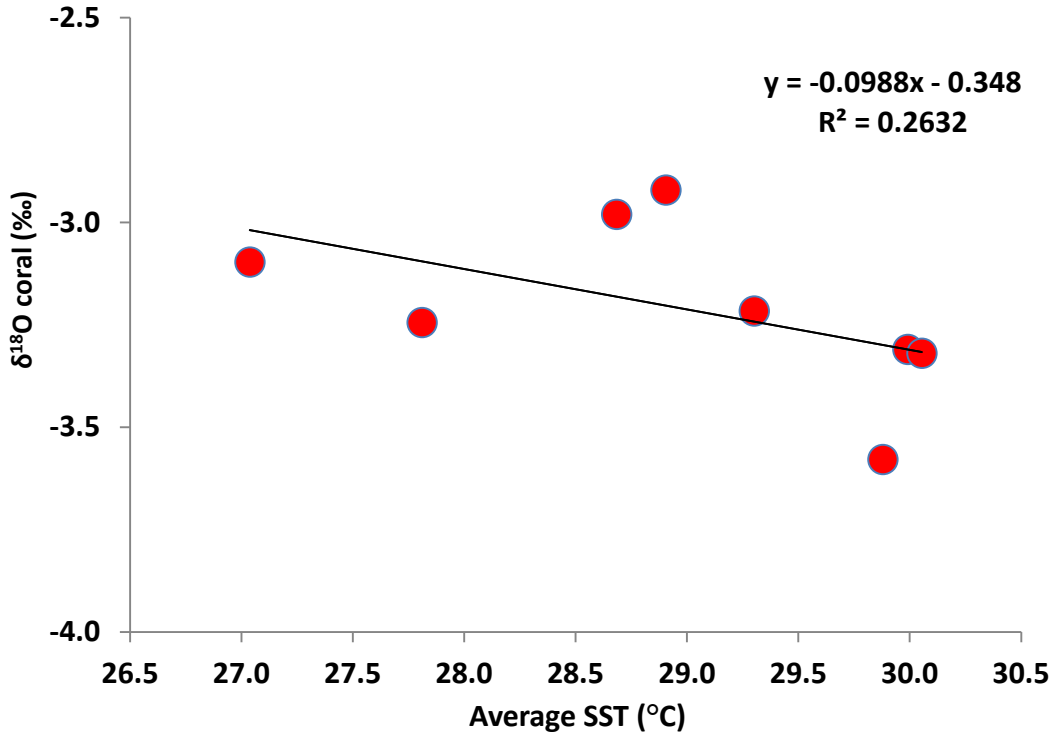

Figure 3.7: *Inverse relationship between average oxygen isotopic compositions of coral skeleton and average sea surface temperature estimates modified from the clumped isotope measurements during study time.*

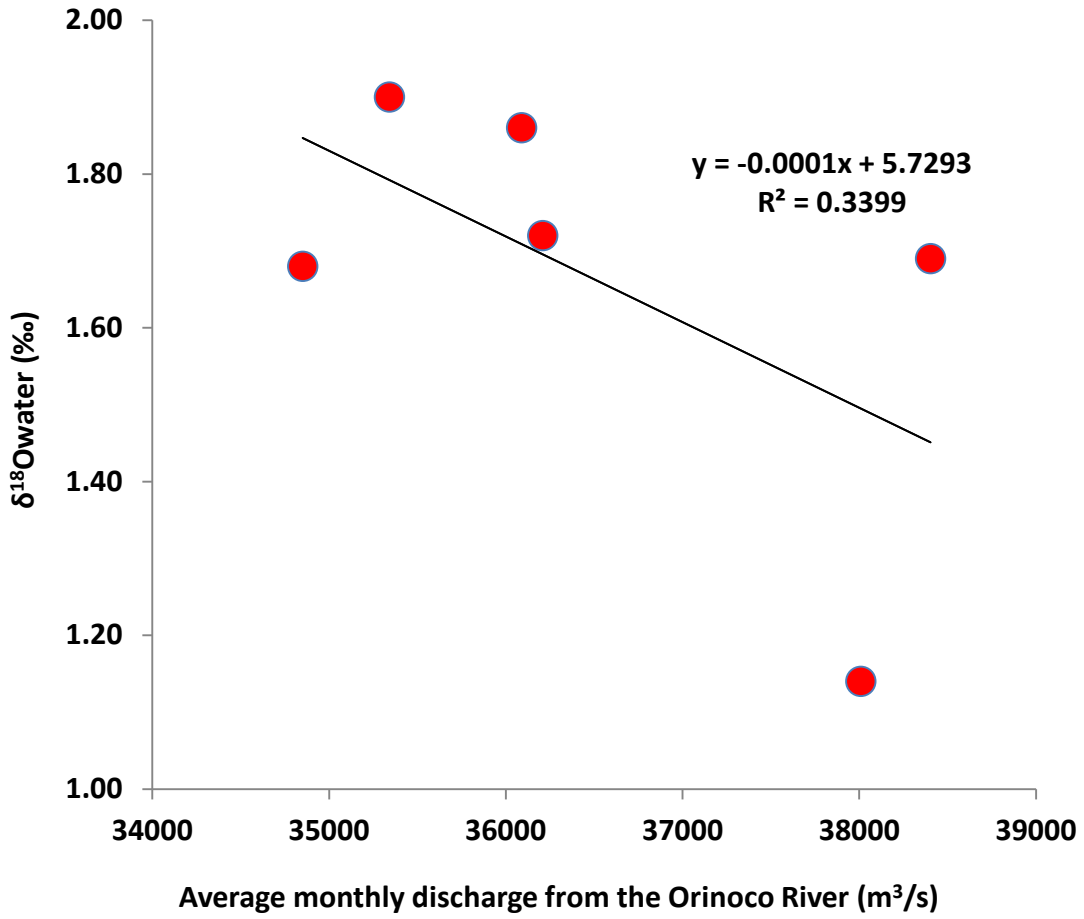

Figure 3.8: *A linear in this study between oxygen isotopic composition of water and average monthly discharge from Orinoco River of Venezuela.*

3.8.3. Salinity

Oxygen isotopic composition of coral aragonite is a combined function of SST and $\delta^{18}O_w$ which is linearly related to salinity (Epstein et al., 1953; Weber et al., 1972; Leder et al., 1996; Watanabe et al., 2001). The detailed study of Moses et al. (2006) in Tobago demonstrated that $\delta^{18}O_c$ is dependent on SST change and noticeable variability in salinity from one year to the next. There is no well documented salinity record, however, the salinity-$\delta^{18}O_w$ equation of Watanabe et al. (2001) in section 4.2.2 was used to provide the data on SSS shown in Table 3.2.

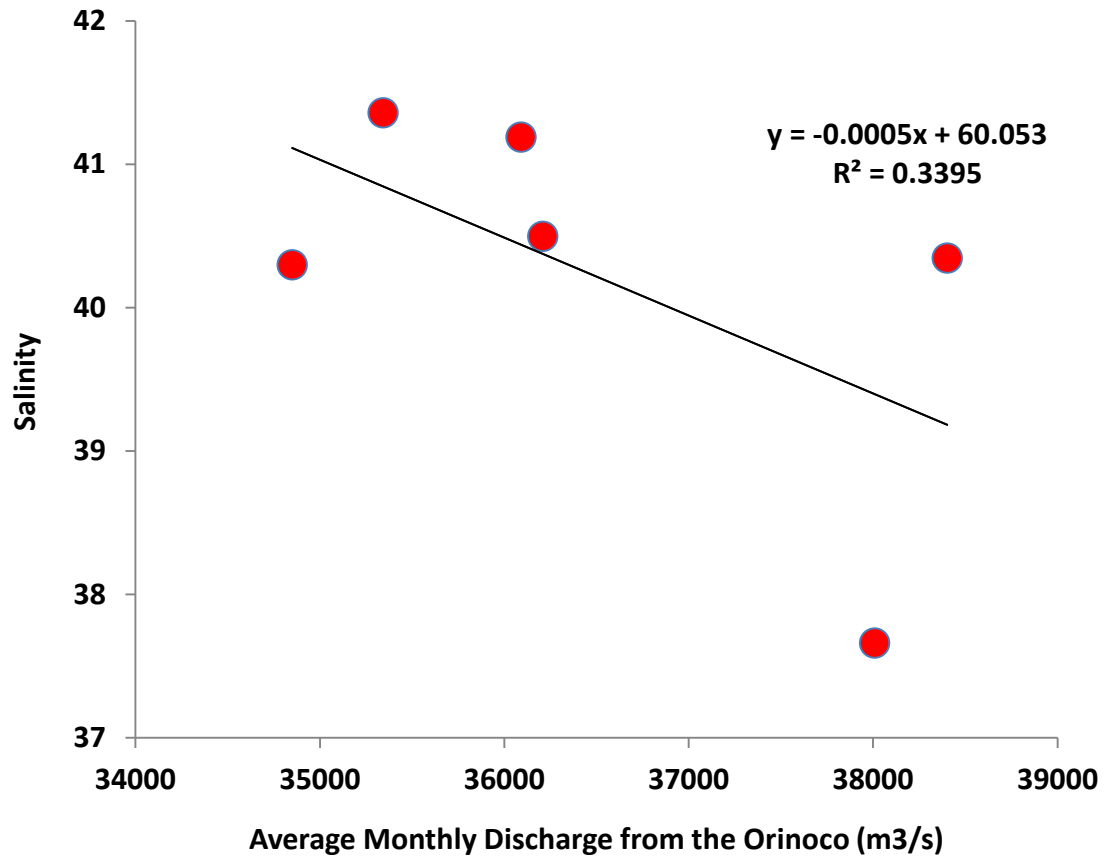

Figure 3.9: *SSS estimates based on equation of Watanabe et al. (2001) versus average monthly output from Orinoco River of Venezuela*

The archive detailing low salinity output from the Orinoco River (Risk et al., 1992) was accepted as an indicator of the magnitude of salinity variations around the island of Tobago, since the main driver of salinity variations was considered to be the fresh water outflow of the Orinoco River (Moses et al., 2006).

In this regard, depletion in the $\delta^{18}O$ of coral aragonite skeletons should result from increased Orinoco discharge and its concomitant effect on salinity (Zeebe, 2007). Saenger et al. (2012) analyzed corals that were formed at elevated and normal salinities in the Red Sea and then concluded that clumped signals of shallow water corals are not affected by salinity.

In the wet season, all surface waters around the island of Tobago have lower salinity than oceanic waters which average 36 (Kenny, 2000). Around the island of Tobago, the seasonal fluctuation of shallow water salinity has been observed to vary by 3 psu between the dry and wet seasons (Levitus et al., 1994). The calculated SSS data is partly consistent with observed values.

Although the range of SST data supports the actual measurements from Levitus et al. (1994), the SSS estimates are lower than expected due to colder SST estimates from the clumped isotopes. If we take into account the offset (approximately 8°C) between SST estimates and the COADS, reasonable salinity values can be obtained from the coral sample.

The SSS exhibits a significant reverse correlation with the outflow of the Orinoco River throughout the study period (Figure 3.9). This is the type of relationship which would be expected with the minimum amount of discharge corresponding to more saline seawater at surface. The SSS variability can be explained not only by the direct effect of the discharge from the Orinoco River but also by a combination of several factors such as local precipitation, evaporation and influence of the ITCZ which increases seasonal freshwater output from the Orinoco River in Venezuela between June and December.

3.9. Final thoughts

This study showed the relationship between abundances of clumped isotopes in CO_2 extracted by the acid digestion of a shallow water coral and the growth temperature of the coral in the island of Tobago. The coral reflects higher clumped signals that result in an offset as large as 8°C between expected and measured Δ_{47} values. Thus, clumped

signals of the shallow water coral exhibit straightforward temperature sensitivity and can be used as important proxy in paleotemperature research.

Combining unconventional (clumped) and conventional (stable) isotopes in the skeleton of a modern coral allow us to remove the influence of temperature to calculate the oxygen isotopic composition of water and SSS. As a result of these findings, past fluviatile input into oceans can be calibrated using recent organisms.

The oxygen isotopic composition of the modern organism skeleton is impacted by changes in SST stronger than effect of outflow of Orinoco River that has significantly influence on δ^{18}Ow.

CHAPTER 4

CLUMPED SIGNALS OF CALCRETE COMPLEXES IN THE BAHAMAS

4.1. Summary

The $\delta^{18}O$ values of calcretes are valuable proxies for the reconstruction of paleoclimate and paleoenvironmental conditions recording both temperature and the $\delta^{18}O$ values of rainfall. In the Bahamas calcretes form under different rainfall regimes and therefore samples were taken from a relatively wet area (New Providence) and a drier area (Hog Cay) in order to investigate understanding the role of rainfall in interpreting calcrete formation. These samples were analyzed using the clumped isotope method which allows the determination of formation temperature as well as the $\delta^{18}O$ of the precipitating water.

The formation temperatures are higher or equal than the mean annual summer temperature (MAST) in Hog Cay, while formation temperature values are consistent with mean annual temperature (MAT) under the subtropical conditions of New Providence. The amount of rainfall between Hog Cay and New Providence is a prevailing factor formation temperatures in calcrete formation where the difference between MAT and MAST is restricted by approximately 3°C few degrees. The $\delta^{18}O$ of calcrete complex is influenced by small temperature effect and mostly $\delta^{18}O$ of the water directly related to rainfall and intensive evaporation demonstrated by co-varying of the traditional isotopes.

4.2. Background

Calcretes or caliches belong to a special group of soil carbonates consisting predominantly of calcium carbonate (Cerling, 1984), and form in a variety of configurations from powdery to nodular to indurated within regions of weathering. The calcium carbonate has precipitated and cemented into pre-existing soil profiles or weathered materials in vadose and phreatic zones where ground-waters become supersaturated with respect to calcium carbonate (Goudie, 1973; Wright and Tucker, 1991).

As calcretes have been observed in regions where the annual rainfall is less than 300 mm year (Goudie, 1973), rainfall has been implicated as one of the most influential climatic factors in their formation (Rossinsky and Swart, 1993). However, calcretes have also been observed in southern-west Australia where the annual runoff is about 800 mm/year (Semeniuk and Searle, 1985). For this reason, evaporation is also thought to exert a significant influence on calcrete formation (Salomons et al., 1978). The relationship between rainfall and evaporation is therefore considered to be more important than the actual amount of rainfall (Rossinsky and Swart, 1993).

Over the last four decades, many authors have examined the $\delta^{18}O$ and $\delta^{13}C$ of calcretes in order to understand climate conditions (Magaritz et al., 1981; Talma and Netterberg, 1983; Cerling, 1984; Cerling and Hay, 1986; Amundson et al., 1988; Quade et al., 1989 (a,b); Rossinsky et al., 1993). As a result of these studies, it has been suggested that the $\delta^{13}C$ of calcretes is influenced by the atmospheric concentration of

CO_2 and the $\delta^{13}C$ of the soil CO_2 which is in turn controlled by the proportion of C_3 and C_4 plants (Cerling., 1984; Quade et al., 1989). On the other hand, the $\delta^{18}O$ of calcretes is predominantly influenced by temperature and the $\delta^{18}O$ value of the precipitating water which is in turn controlled by the initial $\delta^{18}O$ of the meteoric water and evaporation which results in $\delta^{18}O$ enrichment of waters (rainfall, groundwater) (Salomons et al., 1978; Rossinsky and Swart, 1993).

Although numerous studies have been conducted on $\delta^{13}C$ in soil carbonates (Cerling and Hay, 1984; Quade et al., 1989; Cerling, 1991; Achyuthan et al., 2007), the $\delta^{18}O$ of carbonates in modern soil formations have received less attention and because of this there are complications when interpreting the $\delta^{18}O$ of calcretes. Specifically lacking is knowledge of the isotopic composition of rainfall and the impact of evaporation (Rossinsky and Swart, 1993). Calcretes form in equilibrium with the precipitating fluid which is not the same as rainfall because of enrichment in $\delta^{18}O$ due to the effect of evaporation (Cerling and Quade, 1993; Quade et al., 2007).

The $\delta^{18}O$ of calcretes depends not only on the $\delta^{18}O_w$ but also the formation temperature. Hence both $\delta^{18}O_w$ and temperature are needed to solve equations of the traditional oxygen paleothermometry. In this respect, calcrete mineralization temperature estimates can be determined using a suitable traditional paleotemperature equation where $\delta^{18}O_w$ is well constrained. However, the $\delta^{18}O$ of ancient meteoric water in the geological record can be imprecisely assumed from present day rainfall composition.

The temperature can be determined using carbonate clumped isotope geothermometry which is based on enrichment of multiple substituted isotopologues relative to stochastic isotopic distribution in CO_2 extracted by the phosphoric acid reaction with carbonate. Reported as Δ_{47} can be used to determine accurately the carbonate formation temperature without knowledge of the oxygen isotopic composition of the precipitating fluid (Ghosh et al., 2006; Eiler, 2007; Huntington 2011). Once the temperature has been determined, values can be applied to solve calcite-water oxygen isotope paleotemperature equations (Kim and O'Neill, 1997, 2007) to unravel $\delta^{18}O$ values of co-existing water.

Over the last decade this approach has served as a potential tool to successfully overcome certain limitations in reconstructing past temperatures and oxygen isotopic composition of water (Ghosh et al., 2006, 2007; Eiler, 2007; Affek et al., 2008a; Affek et al., 2008b; Tripati et al., 2010; Eagle et al., 2011; Huntington et al., 2011; Thiagarajan et al., 2011). Although there has been some limited application of the clumped isotope method to soil carbonates (Ghosh et al., 2006b; Breecker et al., 2009; Passey et al., 2012; Leier et al., 2013; Quade et al., 2013; Peters et al., 2013; Eagle 2013; Hough et al., 2014), there has been no work to date on young calcretes whose diagenetic history is reasonably well constrained.

4.3. Recent studies

Passey et al. (2010) analyzed fossil paleosol carbonates collected from Turkana Basin using the clumped isotope technique to reveal the temperature history of Northern Kenya. While conditions in the Pliocene and Pleistocene are believed to have been cooler

and more vegetated than at present, Passey et al. (2010) suggested that the paleoclimate of Northern Kenya was similar to, or warmer than, the present. They also discussed the influence of shading, solar heating and seasonality on the paleosol carbonates during their precipitation. Therefore, effect of solar heating or conversely, shading is considered as significant factors to interpret the temperature data obtained from clumped isotope measurements and seasonality of paleosol carbonate accumulation is crucial parameter in temperate climates.

Peters et al. (2013) measured modern soil carbonate samples collected from the Southern Central Andes, Argentina using clumped isotope thermometry in order to understand the effects of environmental parameters on soil carbonate accumulation. The formation temperatures were found to be in disequilibrium with mean annual or summer air temperatures. In addition, Peters et al. (2013) proposed that variations in rainfall govern the timing of carbonate precipitation. They do not find any statistically significant variations in clumped isotopic composition of their samples with depth or average annual air temperature. Although mean formation temperatures T (Δ_{47}) of soil carbonate samples collected above 2 km elevation show summer soil temperatures, the temperatures below 2 km reflected an average annual soil temperature. Summer month rainfall below 2 km postpones soil dewatering and the formation of carbonate until the fall season. The seasonal changes significantly affect carbonate precipitation. The oxygen isotopic composition of soil fluid reflects similar values with respect to that of recent meteoric waters.

Leier et al. (2013) investigated the paleo-elevation scenario of the Eastern Cordillera of Central Bolivia by analyzing paleosol carbonate samples collected from

Oligocene-Miocene strata. They suggested that paleo-elevations were from 0 to 1.5 km in the Oligocene-Early Miocene while paleo-elevations were approximately 2.5 km in the mid-Miocene. Samples showed significant variations in conventional ($\delta^{18}O$) and unconventional (Δ_{47}) isotopes depending on surface uplift.

Quade et al. (2013) used clumped isotope signals of recent soil and buried paleosol carbonates sampled from India, Pakistan, Tibet, Nevada and Arizona to determine relative surface and burial formation temperatures. The surface formation temperatures, which were 10 to 15°C higher than mean annual air temperature, are directly impacted by solar radiation, soil depth and shading. Although they pointed out that clumped signals in paleosol carbonates reliably document realistic temperature values down between 2.5 km to 4 km (burial depth) or 90-120^{o}C, the temperature values in paleosol carbonates is reset deeper than 4 km. The formation temperature values ≥ 40°C derived from paleo-soil carbonates demonstrate warmer climate regions with respect to the present as a consequence of resetting during diagenetic alteration.

Hough et al. (2014) correlated clumped signals (Δ_{47}) and conventional isotopes ($\delta^{18}O$) of recent soil carbonates with seasonal changes in soil moisture and temperature recorded from nearby climate stations in semi-arid to arid climate settings of Western Nebraska and Wyoming to unravel seasonality in soil carbonate precipitation.

Although temperature estimates for the formation of the soil carbonates are higher 3-5^{o}C than the mean annual summer temperature, they are higher 15-16^{o}C than the average annual air temperature. As a result, the study demonstrated that soil carbonate accumulations occur in the warmest months and that their formation temperature is

affected by solar radiation. In addition, the $\delta^{18}O$ of soil water estimates obtained from clumped signatures, in conjunction with traditional isotopes, is similar to the oxygen isotopic composition of mean summer rainfall. As a result of these findings, soil carbonates are believed to form during the first warm days of the year due to soil dewatering and after storm events in mid to late summer.

The clumped signals and $\delta^{18}O_w$ values of recent soil carbonates are inversely correlated with sample elevations which were reconstructed by combining of Δ_{47} and $\delta^{18}O_w$. However, $\delta^{18}O_w$ and rainfall showed a complex interaction between topographic, climate and environmental factors. Therefore, a combination of clumped and stable isotopes was determined to be a suitable proxy for paleo-elevation and paleoclimate studies.

4.4. Objectives of the study

The $\delta^{18}O$ of calcretes is a strong proxy for the reconstruction of paleoclimate and paleoenvironmental conditions and records the $\delta^{18}O$ values of rainfall which is in turn affected by several climate, topographic and environmental factors. Understanding the role of rainfall is crucial in interpreting calcrete formations and can be better understood by analyzing calcrete samples formed under different rainfall regimes in similar latitudes.

Climatically, the Bahamian islands vary from subtropical in the north to semi-arid in the south (Sealey, 1990; Carew et al., 1997). For this reason, Hog Cay, Exumas located in the southern Bahamas and New Providence Island in the northern Bahamas were determined suitable sites for further study.

Modern calcrete samples from two field sites were collected in order to characterize the prevailing conditions. Although the islands formed during the last interglacial highstand (5e) (Jackson, K pers. comm), calcrete formation would be expected to occur in shallow marine deposits during times of lowstands and subaerial exposure (Harrison, 1977; Esteban and Klappa, 1983; Hopley, 1986).

Accumulation temperatures of soil carbonates were considered to reflect mean annual air temperature of the regions in which they formed (Quade et al., 1989; Cerling and Quade, 1993; Mack and Cole, 2005; Dworkin et al., 2005). However, this assumption has been invalidated by recent soil carbonate studies using clumped isotope geothermometry (Breecker et al., 2009; Passey et al., 2010; Quade et al., 2013; Eagle 2013; Peters et al., 2013; Hough et al., 2014). The studies have demonstrated that soil carbonates reflects environmental conditions of the summer season and disagree with average annual conditions. The first aim of this study is to calculate the formation temperatures of the calcretes by applying the clumped isotope technique to test the suggestion of the recent publications in two different field sites.

The oxygen isotopic composition of the fluid will be calculated based on the paleotemperature equations of Kim and O'Neill (1997) and Kim et al. (2007), in conjunction with the measured temperature estimates obtained from clumped isotope analyses. The second goal is to reveal if there is any correlation between calculated $\delta^{18}O$ of precipitating fluid and $\delta^{18}O$ of calcrete and the formation temperatures.

4.5. Study areas

New Providence Island, located at the leeward, northwest corner of eastern GBB is known as Yellow bank (Figure 4.1) after one of its most striking features, the distinctively colored eolianites (Ball, 1967). Layers of eolianites, formed during the last three Pleistocene highstands, are exposed on the foreshore and beach and occur subtidally (Hearty and Kindler, 1997; Garrett and Gould, 1984).

The climate of New Providence is sub-tropical with fairly high mean temperatures and moderate rainfall. The mean annual temperature in New Providence, Bahamas is 24.5°C (Figure 4.2). The annual average rainfall in Nassau, New Providence is reportedly 1359.2 mm per year, or 113.3 mm per month (http://www.bahamas.climatemps.com).

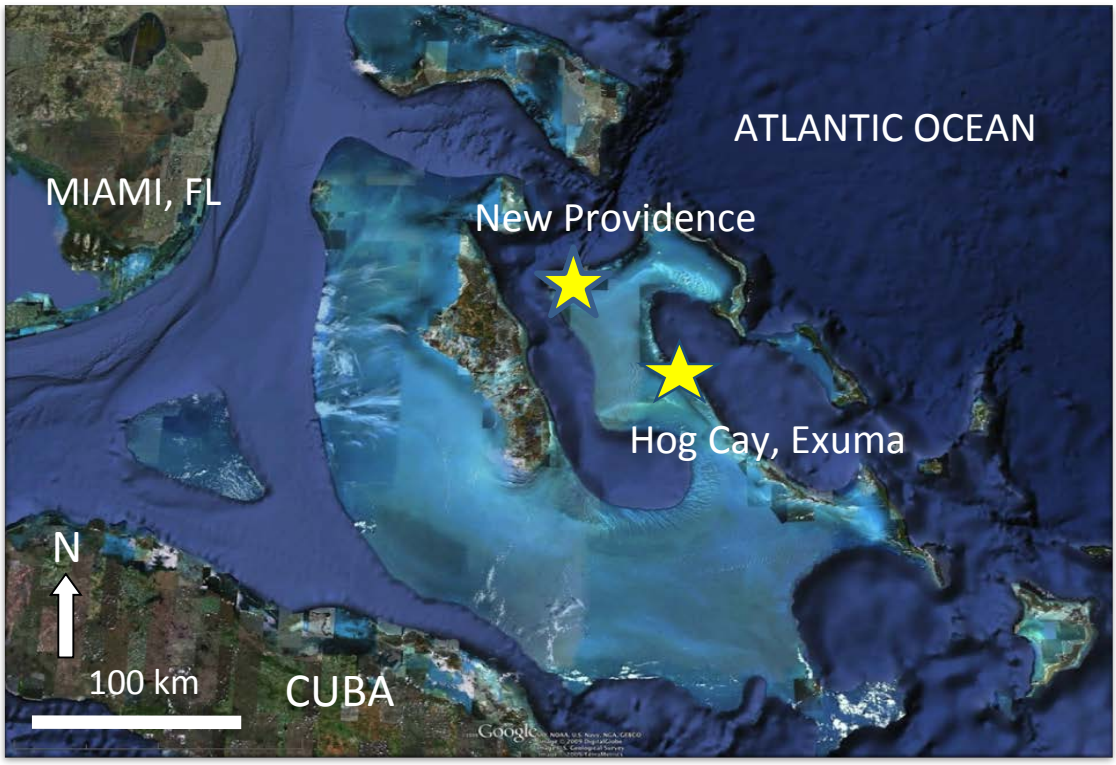

Figure 4.1: *Map of locations of collected samples from the Bahama Islands.*

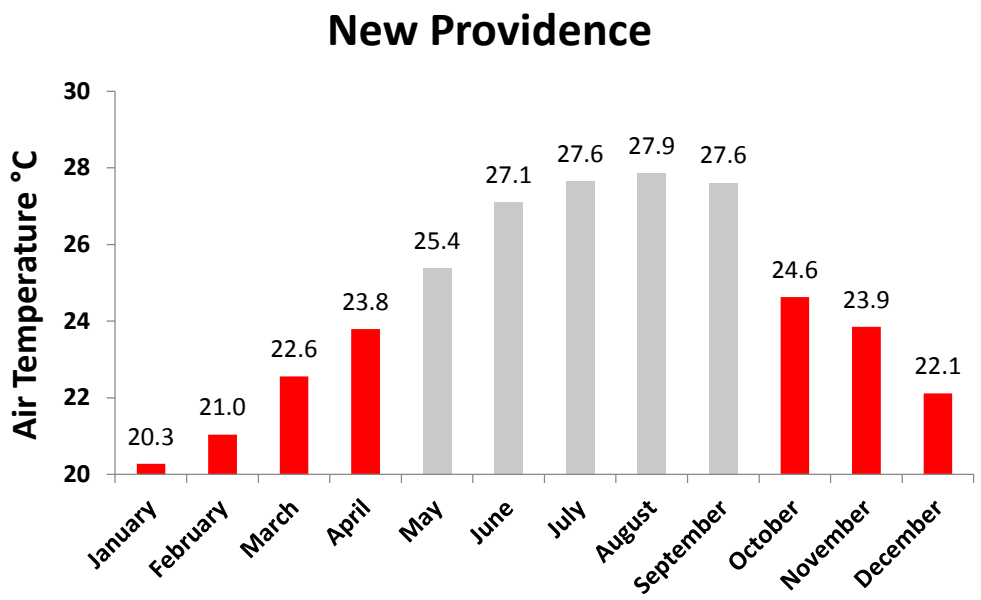

Figure 4.2: *Mean temperature data are shown from 1953-1955 for Oakes Airport in New Providence exhibiting seasonal patterns of air temperature (British Caribbean Meteorological Service, Bahama Division) Gray columns mark summer months and red columns reflect winter months.*

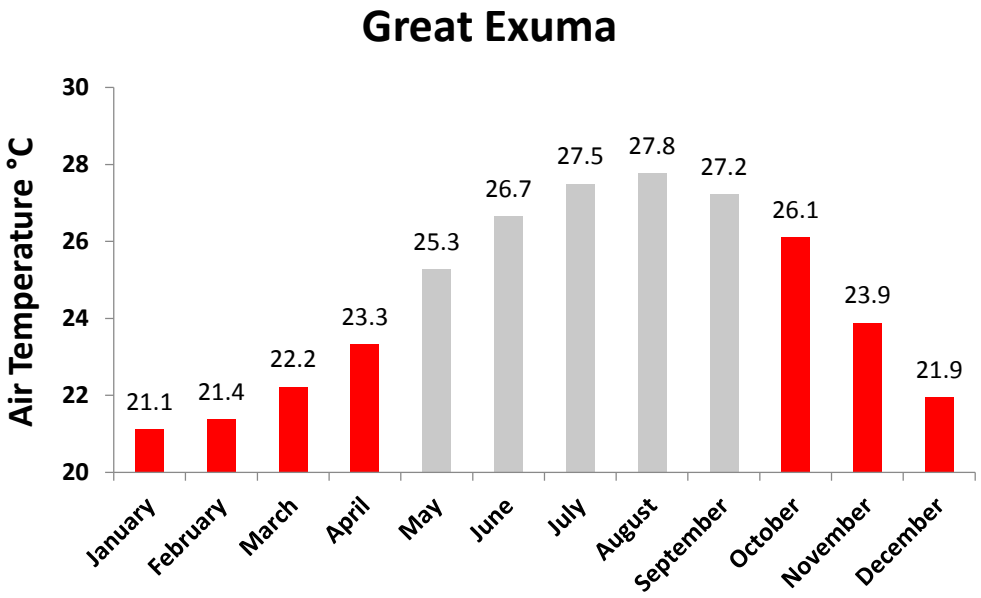

Figure 4.3: *The distribution of mean annual temperatures in Great Exuma reflects similar climatic conditions to Hog Cay, Exumas. Gray columns marks warm months and red columns reflect cold months.*

The Exuma Cays, a group of approximately 50 small islands and hundreds of little cays along the bank edge in the Central Bahamas, lie NW-SE from Sail Rocks at the northern end of Exuma Sound southwards to Great Exuma (Andres et al., 2009). To the west of the Exumas lies the GBB and to the east Exuma Sound. Lying somewhat in the lee of Cat Island located further east the Exuma Cays are partially sheltered from the persistent winds and resulting waves.

Most of the islands along the eastern edge of the GBB are fragments of a dune ridge, and reach at least 20 m in height. Sediments are composed of shallow water carbonates such as ooids, skeletal and coated grains (Ginsburg et al., 1958). Nearly all cays contain extensive sand flats and are dry at low tide.

The climate of Hog Cay is identified as one of low precipitation and high annual temperature. The cays can be expected to be drier than larger islands at the same latitude. Rainfall is estimated to average less than 60 cm per year in the Exuma Cays. Rainfall is mainly from regional weather including tropical disturbances and winter cold fronts (General Management Plan, the Bahamas National Trust).

4.6. Methodology

4.6.1. Materials

One calcrete outcrop sample (Figure 4.4a) was collected from New Province, Bahamas. Six subsamples were cut from this outcrop sample. Also, one short penetrative calcrete core (Figure 4.4b) (length: 60 cm) was drilled on Hog Cay with thirteen subsamples taken at equal intervals. In total, 19 calcretes were prepared for clumped

isotopes measurements and XRD analyses. As the calcrete forms at the surface and influences the host rock over variable distance, I have referred to these samples as calcrete complexes. A calcrete complex therefore refers to the calcrete laminated surface and the host rock immediately below the surface.

Figure 4.4a: *The outcrop sample from New Providence, Bahamas (Right side).*

Figure 4.4b: *The short calcrete core from New Providence, Bahamas (Left side).*

4.6.2. Preparation

The samples were collected by cutting the core with a diamond saw and then rinsed with deionized water. The samples were dried in the oven at 40°C for at least 24 hours and then finely ground using a mortar and pestle. Approximately 8±0.3 mg of the

sample was weighed out into two small copper sample boats for a single clumped isotope measurement.

4.6.3. XRD analyses

The mineralogy of the samples was determined using XRD (Swart and Melim, 2000). The samples are presumed to be wholly comprised of aragonite, HMC or LMC. In this procedure, regions of the suitable peaks are analyzed using a scan between 23 and 32 2θ (CuKα radiation).

4.6.4. Stable isotope analysis

In order to acquire high resolution $\delta^{18}O$ data of the core, 36 subsamples were taken from top to bottom. Moreover, 12 subsamples were retrieved from the outcrop sample. The 48 powdered specimens were measured using a Kiel III attached to a Finnigan Delta Plus. Data obtained was corrected for isobaric interferences using the procedures outlined in Craig (1957) modified for a triple collector mass spectrometer. Oxygen isotope values of carbonate samples ($\delta^{18}O_C$) are reported with respect to Vienna Pee-Dee Belemnite (V-PDB) according to standard notation. Average standard deviation based on replicate analyses of internal standards is less than 1%.

4.6.5. Clumped isotope analysis

The samples were digested at 90°C (Swart et al., 1991) with CO_2 extracted using the gas purification line in the Stable Isotope Laboratory at the University of Miami, RSMAS. The CO_2 was measured on a Thermo Finnigan MAT 253 mass spectrometer

which is configured to analyze from mass 44 through mass 49 (Eiler and Schauble, 2004). The clumped signals (Δ_{47}) were calculated using the equation described by various authors (Affek et al., 2008; Huntington et al., 2009). The calculated Δ_{47} values were modified to the reference framework of Dennis et al. (2011) and then were adapted using an experimentally measured acid fractionation factor of 0.092 ‰ for acid digestion at 90°C (Henkes et al., 2013). Finally, the clumped signals were converted to formation temperature values using recent calibration equations (Dennis et al., 2011; Henkes et al., 2013; Wacker et al., 2014; Fernandez et al., 2014; Tang et al., 2014). A series of in-house and inter-laboratory carbonate Δ_{47} standards have been analyzed along with the samples.

4.6.6. Determining of oxygen composition of the fluid

Clumped isotope paleothermometry is based on the carbonate mineral alone and thus can provide the temperature of recrystallization of a carbonate without advance knowledge of the $\delta^{18}O$ from which it grew (Ghosh et al., 2007). Temperature estimates derived from clumped isotope analyses can be combined with the oxygen isotopic composition of the carbonate mineral to calculate theoretical $\delta^{18}O$ values of soil water using the carbonate-water oxygen isotope paleothermometry equation of Kim and O'Neill (1997).

$$\mathbf{1000\ In\alpha_{calcite\text{-}water} = 18.03\ (10^3\ T\ (K^{-1})) - 32.42} \qquad \mathbf{(19)}$$

Based on the XRD data, the majority of samples are composed of 100% LMC, however, some of samples contain both aragonite and low-Mg due to diagenetic effects (Table 4.1).

$$1000\ \ln\alpha_{aragonite\text{-}water} = 17.88\ (\pm 0.13)\ (10^3\ T\ (K^{-1})) - 31.14\ (\pm 0.46) \quad (20)$$

For this reason, another paleotemperature equation for aragonite-water oxygen fractionation is needed to calculate the oxygen isotopic composition of precipitating water. Obtained water values have therefore been recalculated using the paleotemperature equations of Kim and O'Neill (1997) and Kim et al. (2007) according to the percentage of aragonite and LMC contained within the sample.

4.7. Results

4.7.1. Clumped isotopes

No	Sample ID	Depth	Mean Δ 47	Dennis Temp.	Fernandez Temp.	Wacker Temp.	Tang Temp.	Henkes Temp.	Aragonite	Low-Mg	18Ow-aragonite	18Ow-LowMg	18Ow-calculated	n
Unit		cm	‰	°C	°C	°C	°C	°C	%	%	‰	‰	‰	
1	CC 01	0	0.684	30.64	32.01	19.65	26.42	30.00	63	37	0.25	1.11	0.68	1
2	CC 02	5	0.741	18.83	12.95	-0.02	8.42	8.32	0	100	-2.42	-1.77	-1.77	1
3	CC 03	10	0.698	27.73	27.18	14.64	21.87	24.45	0	100	-0.60	0.02	0.02	1
4	CC 04	15	0.722	22.78	19.18	6.37	14.32	15.33	0	100	-1.58	-0.95	-0.95	1
5	CC 05	20	0.726	21.97	17.89	5.04	13.09	13.88	0	100	-2.18	-1.60	-1.60	1
6	CC 06	25	0.692	28.96	29.21	16.74	23.78	26.77	0	100	-0.81	-0.24	-0.24	1
7	CC 07	30	0.675	32.76	35.58	23.36	29.78	34.13	0	100	0.16	0.76	0.76	1
8	CC 08	35	0.688	29.82	30.63	18.21	25.12	28.41	0	100	-0.23	0.34	0.34	1
9	CC 09	40	0.709	25.42	23.41	10.74	18.32	20.14	0	100	-1.16	-0.53	-0.53	1
10	CC 10	45	0.675	32.78	35.62	23.41	29.82	34.18	0	100	0.45	1.11	1.11	1
11	CC 11	50	0.707	25.78	24.00	11.35	18.87	20.81	91	9	2.08	3.77	1.54	1
12	CC 12	55	0.706	25.92	24.22	11.57	19.08	21.06	71	29	0.95	2.47	0.96	1
13	CC 13	60	0.717	23.81	20.82	8.06	15.86	17.19	62	38	0.62	2.19	0.90	1
14	HC 01	0.0	0.708	25.65	23.78	11.12	18.66	20.56	39	61	-0.91	0.27	-0.31	1
15	HC 02	0.6	0.728	21.54	17.21	4.35	12.45	13.11	45	55	-1.53	-0.48	-1.12	1
16	HC 03	1.2	0.706	26.05	24.44	11.79	19.28	21.30	31	69	-0.76	0.14	-0.23	1
17	HC 04	1.8	0.677	32.19	34.62	22.36	28.87	33.01	21	79	0.04	0.88	0.67	1
18	HC 05	2.4	0.748	17.61	11.07	-1.95	6.63	6.22	0	100	-3.04	-2.12	-2.12	1
19	HC 06	3.0	0.741	18.90	13.07	0.10	8.53	8.45	22	78	-2.24	-1.07	-1.37	1

Table 4.1: *Summary of clumped isotope data together with mineralogy and oxygen composition of water. n denotes number of analyses of samples.*

Temperature estimates, XRD results, and theoretically calculated oxygen isotopic composition of the fluid from clumped isotope measurements and XRD analyses are presented in Table 4.1. Values of Δ_{47} of the core samples range from 0.684‰ to 0.741‰. The range of Δ_{47} values indicates the formation temperatures of 18.8°C to 32.7°C using the equation of Dennis et al. (2011). In contrast, the clumped signals of outcrop samples from New Providence range from 0.677‰ to 0.748‰ resulting in temperature estimates between 17.61°C and 32.19°C.

4.7.2. XRD

On the basis of X-Ray mineralogy, the penetrative calcrete core is composed of 100% LMC from the top to a depth of 50 cm, not including the thin blackish crust at the top of the core. However, the core between 50 cm and 60 cm is made up of aragonite and LMC, as is the outcrop sample (Table 4.1).

4.7.3. Stable isotopes

Stable isotope measurements are summarized in Table 4.2. The calcrete complex collected from Hog Cay, Exumas have $\delta^{18}O_C$ between -4.26±0.03‰ and -0.63±0.02‰ with the majority of samples falling between -3.00‰ and -1.50‰. However, the calcrete complex from New Providence has $\delta^{18}O_C$ values between -3.53±0.04‰ and -2.41±0.02‰ with the majority having values of approximately -3.50‰ – 2.00‰. Both the oxygen isotopic composition of the outcrop and the core samples become slightly heavier downward.

The $\delta^{13}C$ values of the short core show a wide compositional range from -9.56±0.01‰ to 3.43±0.03‰. Although the carbon values are almost constant downward, excluding the top sample, the values vary significantly below 45 cm. On the other hand, the $\delta^{13}C$ of the outcrop samples change between -5.25±0.06‰ and 2.51±0.03‰ and are highly variable from top to bottom.

No	Sample ID	stdv-13C	stdv-18O	13Carbon (‰)	18Oxygen (‰)	No	Sample ID	stdv-13C	stdv-18O	13Carbon (‰)	18Oxgen (‰)
1	CC 01.a	0.02	0.04	-4.53	-2.55	25	CC 09.a	0.02	0.04	-8.65	-1.43
2	CC 01.b	0.02	0.04	-2.38	-2.18	26	CC 09.b	0.03	0.02	-6.85	-2.10
3	CC 01.c	0.02	0.03	-9.33	-4.26	27	CC 09.c	0.04	0.07	-9.02	-2.69
4	CC 02.a	0.01	0.02	-9.13	-2.76	28	CC 10.a	0.02	0.03	-7.93	-2.48
5	CC 02.b	0.02	0.03	-8.92	-2.77	29	CC 10.b	0.02	0.02	0.32	-0.63
6	CC 02.c	0.02	0.02	-8.66	-2.53	30	CC 10.c	0.03	0.04	-2.26	-1.31
7	CC 03.a	0.02	0.03	-8.48	-2.72	31	CC 11.a	0.03	0.04	3.43	0.10
8	CC 03.b	0.01	0.02	-9.07	-3.03	32	CC 11.b	0.01	0.03	2.40	-1.30
9	CC 03.c	0.02	0.03	-9.10	-2.95	33	CC 11.c	0.02	0.03	2.98	-1.02
10	CC 04.a	0.02	0.03	-8.65	-2.85	34	CC 12.a	0.02	0.03	3.19	-0.72
11	CC 04.b	0.02	0.03	-9.02	-3.07	35	CC 12.b	0.02	0.04	2.64	-0.83
12	CC 04.c	0.02	0.03	-9.52	-3.51	36	CC 12.c	0.02	0.06	2.19	-1.58
13	CC 05.a	0.01	0.03	-9.56	-3.50	37	HC 01.a	0.02	0.04	-1.92	-1.89
14	CC 05.b	0.01	0.02	-9.22	-3.21	38	HC 01.b	0.01	0.03	-3.84	-3.21
15	CC 05.c	0.02	0.03	-9.32	-3.24	39	HC 02.a	0.02	0.04	-2.90	-2.70
16	CC 06.a	0.03	0.02	-8.89	-2.66	40	HC 02.b	0.03	0.02	-0.52	-3.40
17	CC 06.b	0.01	0.03	-9.00	-2.68	41	HC 03.a	0.02	0.03	-4.75	-3.13
18	CC 06.c	0.03	0.02	-9.02	-3.13	42	HC 03.b	0.02	0.04	-5.23	-3.53
19	CC 07.a	0.01	0.02	-8.55	-2.17	43	HC 04.a	0.06	0.08	-5.25	-3.61
20	CC 07.b	0.03	0.04	-9.35	-2.62	44	HC 04.b	0.01	0.04	-5.01	-3.52
21	CC 07.c	0.02	0.03	-9.25	-2.60	45	HC 05.a	0.01	0.03	-3.47	-2.81
22	CC 08.a	0.02	0.02	-8.29	-2.25	46	HC 05.b	0.01	0.03	-1.77	-3.06
23	CC 08.b	0.01	0.03	-8.93	-2.68	47	HC 06.a	0.03	0.03	2.51	-2.71
24	CC 08.c	0.02	0.04	-8.10	-2.53	48	HC 06.b	0.01	0.02	0.83	-2.41

Table 4.2: *Summary of stable isotope analyses of the samples collected from calcrete complexes.*

4.8. Discussion

4.8.1. Building history of the calcrete formations

Original marine sediments form in average SST (25°C) with range of $\delta^{18}O_w$ from 0‰ to 1‰ on GBB (Swart et al., 2009). When the sediments are exposed by meteoric diagenesis during the lowstand times, $\delta^{18}O_w$ become lighter and is equilibrium with $\delta^{18}O$ of the fresh water (-2‰). After dewatering processes resulted from solar radiation, calcrete begin to precipitate in weathered zones.

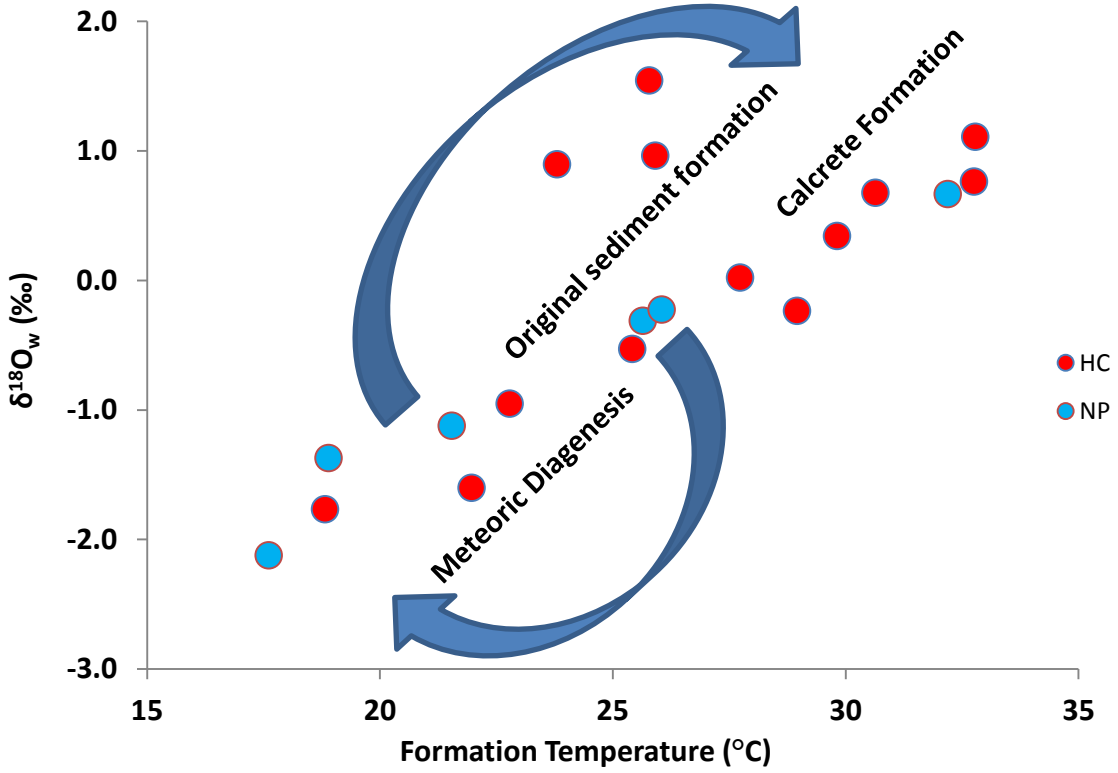

Figure 4.5: *The calculated oxygen isotopic composition of water is directly associated with temperature of mineralization of both outcrop and core samples.*

Based on Figure 4.1, the three bottom samples of the core were considered to be diagenetically unaltered limestone. In addition to, few samples of the core have been

modified by meteoric diagenesis and then have been transformed to calcrete. The rest of the subsamples are good examples of calcrete formation. On the other hand, most of the outcrop subsamples reflected diagenetically altered sediments and a transition between fresh water diagenesis and calcrete formation. For these reasons, the unaltered samples will be ignored for next interpretations.

4.8.2. Relationship between the formation temperature and air temperature

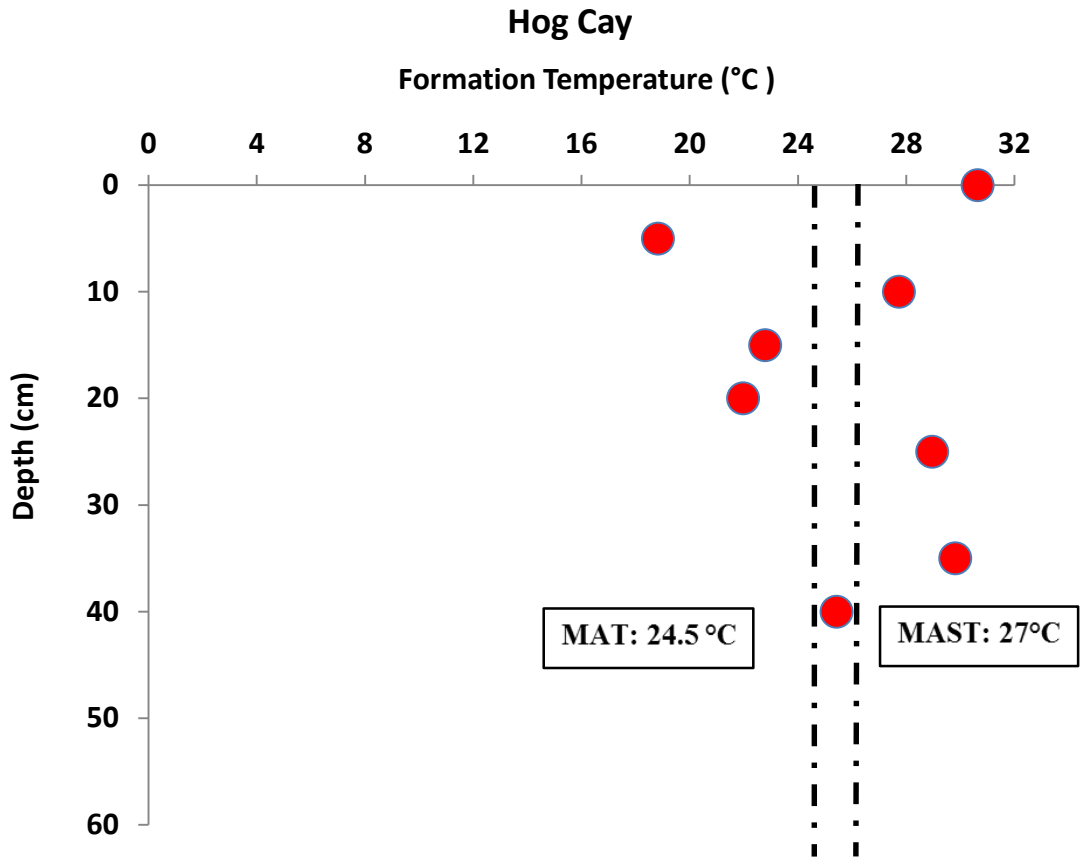

Figure 4.6: *Plot of formation temperature estimates from the short core versus depth. MAT and MAST refer to mean annual air temperature and mean annual summer temperature respectively.*

This study records temperature values measured using the clumped isotope (Eiler, 2007, 2011). Formation temperatures in the calcrete complex exceed the mean annual air

temperature (MAST) by approximately 5°C demonstrate that accumulation occurs in Hog Cay during warmest months of years (June through September) (Figure 4.5). This observation is consistent with assumption of recent studies in semi-arid to arid climate regions using clumped isotope method (Breecker et al., 2009; Passey et al., 2010; Quade et al., 2007, 2013).

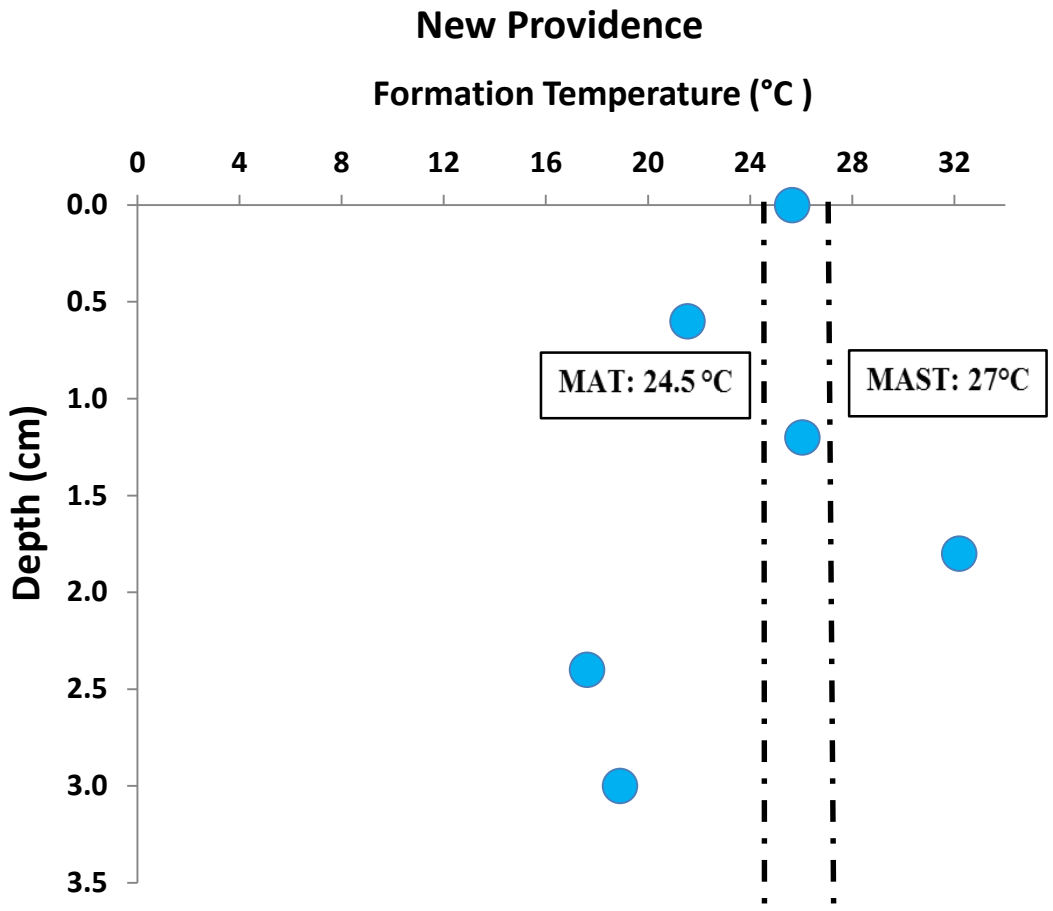

Figure 4.7*: Clumped isotope temperature values of the outcrop sample from New Providence plotted against depth, displaying mean annual temperature (MAT) and mean annual summer temperature (MAST).*

The majority of the temperature estimates which equal or higher than mean temperature values in the hottest month (August) suggest this complex may not form

every year and probably only accumulate after extremely warm events (Passey et al., 2010; Peters et al., 2012).

The high formation temperature values of this study in Hog Cay can be mostly explained by the heating effects of radiative solar energy (Breshears et al., 1998; Coops et al., 2000; Bartlett et al., 2006). In addition, sparse vegetation (negligible shading effect) (See in 4.7.2), limited precipitation and flat landscapes (Kelly Jackson pers. comm.) can be considered important in encouraging calcrete formation in this area.

On the other hand, as with the upper samples from the core, the outcrop sample from New Providence and the temperature values it suggests are highly variable and tend to be closer to MAT (Figure 4.6). Using clumped isotope geothermometry, the formation temperatures of soil carbonates agree with MAT where the carbonates precipitated under wetter conditions in Bolivia (Ghosh et al., 2006b) and Argentina (Peters et al., 2012).

In this study, the average formation temperature of the outcrop sample is about 24.5^{o}C, consistent with MAT in New Providence that has wetter conditions than those seen on Hog Cay, Exumas. The timing of dewatering, therefore, may be more critical than the formation temperature where calcretes form under moderate rainfall regions (Hough et al., 2014).

4.8.3. Stable isotope signatures of Bahamian calcretes

The $\delta^{18}O$ and $\delta^{13}C$ values of this study are within the range of measurements reported for pedogenic carbonates (Figure 4.7). Although the $\delta^{18}O$ content is almost

constant (approximately -3‰) at the two sites, bottom samples from the core are significantly enriched in $\delta^{18}O$ (below 45 cm).

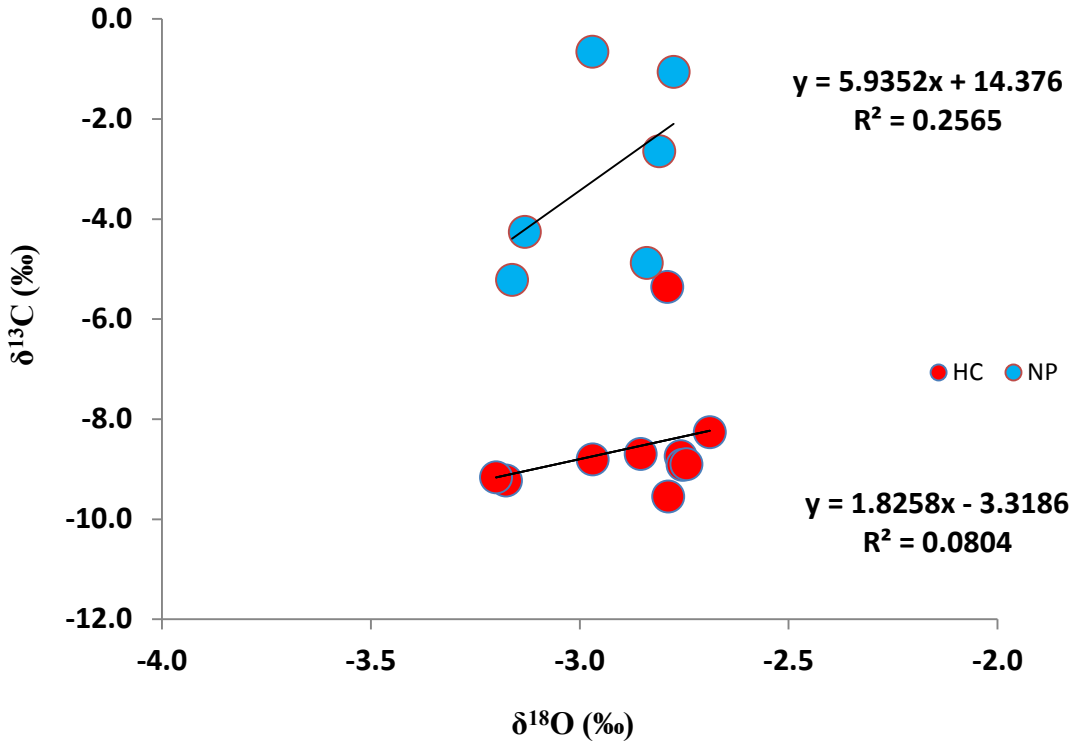

Figure 4.8: *Positive relationship between oxygen and carbon isotopic composition of young calcrete samples collected from New Providence and Hog Cay. Blue and red circles show core calcretes (HC) and hand sample calcrete (NP).*

In terms of $\delta^{13}C$ content, the core values are highly depleted and vary insignificantly with increasing depth from the top to 50 cm. However, the carbon isotopic composition of the outcrop sample collected from New Providence changes by as much as 6‰.

The $\delta^{13}C$ of calcretes is influenced by the atmospheric concentration of CO_2 which is about -8‰ at present compared to -6.5‰ prior to the industrial revolution (Marino and McElroy, 1991) and plants utilizing the C_3 and C_4 have different carbon

isotope values averaging -26‰ and -12‰ respectively (Cerling, 1984, 1991; Quade et al., 1989, Mack et al., 1991; Cerling and Quade, 1993). Therefore, the highly negative (mean -9‰) $\delta^{13}C$ values of the subsamples obtained from the short core can be explained by the effects of atmospheric CO_2 and C_4 vegetation. On the other hand, both the high carbon and oxygen values determined for the outcrop sample can be considered a consequence of the high evaporation expected at the calcrete forming surface in semi-arid and low vegetation regions (Talma and Netterberg, 1983).

Overall, there is a positive correlation between the $\delta^{18}O$ and $\delta^{13}C$ of the samples (Figure 4.7). Although such a relationship has been observed (Cerling, 1984; Cerling and Quade, 1993; Achyuthan et al., 2007) where evaporation is a major process for calcrete formation (Salomons et al., 1978), there is no positive correlation on a world-wide basis. Therefore, the significant co-variation can be thought of as indicating arid or semi-arid climate settings (Andrews et al., 1997).

4.8.4. Correlation between temperature and $\delta^{18}O$ of fluid versus $\delta^{18}O$ of calcretes

The $\delta^{18}O$ composition of carbonates depends both on temperature and the $\delta^{18}O$ of the water. Figure 4.8 shows that the $\delta^{18}O$ of the calcrete samples is almost constant (-2.9‰). However, the formation temperatures vary significantly between 17.6°C and 33.1°C. Therefore, the oxygen isotopic composition of the Bahamian calcrete complex is controlled by only a small temperature effect and mostly by the $\delta^{18}O$ of the precipitating fluid.

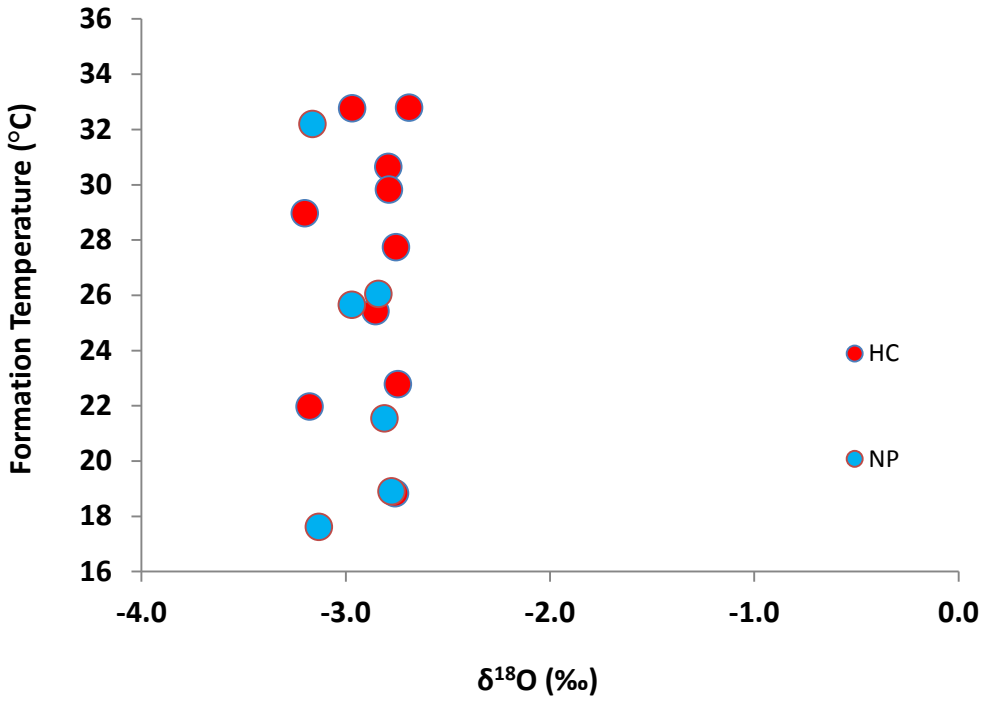

Figure 4.9: *The $\delta^{18}O$ of the samples is influenced by a small temperature effect. The formation temperature estimates were determined based on the equation of Dennis et al. (2011). T (Δ_{47}) and $\delta^{18}O_C$ refer to the formation temperature obtained from clumped isotopes and oxygen isotopic composition of the calcretes derived from stable isotope analyses.*

Although the $\delta^{18}O$ of the outcrop sample collected from New Providence changes insignificantly, the variability of the $\delta^{18}O$ of the water is about 3.5‰. However, there is a positive relationship between the $\delta^{18}O$ of the short core drilled from Hog Cay, Exumas and the calculated $\delta^{18}O$ of the water (Figure 4.9) with both of them co-varying throughout the core.

A strong correlation was observed between the formation temperature and the $\delta^{18}O$ of the water (Figure 4.10) which becomes heavier with increasing temperature. The

oxygen isotopic composition of the water is influenced by a number of parameters, however, temperature can be considered as a leading component.

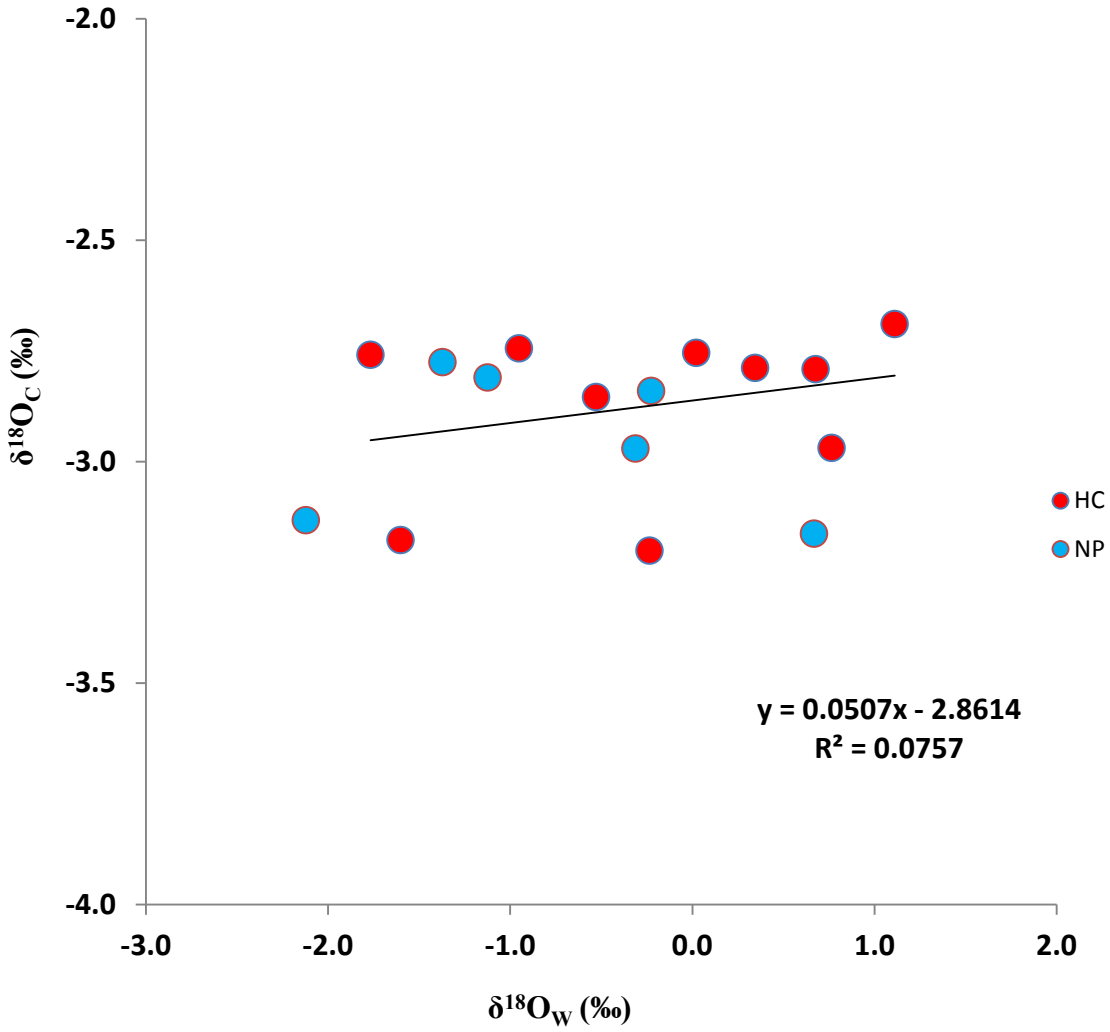

Figure 4.10: *Correlation between calculated oxygen isotopic composition of the fluid and measured oxygen isotopic composition of the calcrete complex samples. They are well correlated in Hog Cay, Exumas and New Providence. The oxygen isotopic composition of calcretes and water denote* $\delta^{18}Oc$ *and* $\delta^{18}O_W$ *respectively*

4.9. Conclusions

This work recorded the clumped signatures of young calcrete complexes and calibrated the clumped isotope paleothermometry of calcretes in the different climatic settings of Hog Cay and New Providence, Bahama Islands. In the sub-arid conditions of Hog Cay the formation temperatures of calcretes are higher than the MAT and the MAST by approximately 8ºC and 5ºC respectively. This tends to suggest that calcrete complex forms in semi-arid regions during the summer months by solar radiation. On the other hand, the clumped isotope temperatures of the calcretes are highly variable and the average formation temperature value is consistent with MAT under the subtropical conditions of New Providence. As a result of these observations, the amount of rainfall between Hog Cay (less than 1000mm) and New Providence (nearly 1350mm) has influence on formation temperatures in calcrete accumulation where the difference between MAT and MAST is limited to a few degrees.

Although there is a poor relationship within stable isotopes of globally collected pedogenic carbonates, a co-variation was observed between the oxygen and carbon isotopic compositions of the calcretes formed under semi-arid and subtropical settings in this study due to a strong evaporative effect.

The carbon signals of the core sample are highly depleted and reflect negative values between CO_2 concentration and the proportion of C_4 vegetation. However, $\delta^{13}C$ values of the outcrop sample precipitated in New Providence are in equilibrium with the atmospheric concentration of CO_2 due to an absence of vegetation.

The $\delta^{18}O$ of calcretes which are in equilibrium with precipitating water are driven by the small effect of formation temperature and the strong influence of $\delta^{18}O$ of the water.

REFERENCES

Achyuthan, H., Quade, J., Placzek, C., and Roe, L. J., (2007) Stable isotopic composition of pedogenic carbonates from the eastern margin of the Thar Desert, Rajasthan, India. Quaternary International 162–163, 50–60.

Affek, H.P., (2012) Clumped isotope paleothermometry: Principles, applications, and challenges. in Linda C. Ivany and Brian Huber (eds.), Reconstructing Earth's Deep-Time Climate – The State of the Art in 2012. Paleontological Society Papers, v. 18. 101-114.

Affek H. P., Bar-Matthews M., Ayalon A., Matthews A. and Eiler J. M. (2008) Glacial/interglacial temperature variations in Soreq cave speleothems as recorded by clumped isotope' thermometry. Geochim. Cosmochim. Acta 72, 5351–5360.

Allan, J.R. and Matthews, R.K. (1977) Carbon and oxygen isotopes as diagenetic and stratigraphic tools - Surface and subsurface data, Barbados, West-Indies. Geology, 5, 16-20.

Allan, J.R. and Matthews, R.K. (1982) Isotope signatures associated with early meteoric diagenesis. Sedimentology, 29, 797-817.

Allison, N., et al., (2005), Strontium in coral aragonite: 3. Sr coordination and geochemistry in relation to skeletal structure, Geochim. Cosmochim. Acta, 69, 3801 – 3811.

Allison, N., Finch, A. A., Sutton, S. R., and Newville, M., (2001) : Strontium heterogeneity and speciationin coral aragonite: implications for the strontium paleothermometer, Geochim. Cosmochim.Ac., 65, 2669–2676.

Amundson, R.G., Chadwick, O.A., Sowers, J.M., and Doner, H.E., 1988, Relationship between climate and vegetation and the stable carbon isotope chemistry of soils in the eastern Mojave Desert, Nevada, Quaternary Research, 29, 245-254, 1988.

Anderson, T.F., Arthur, M.R., (1983) : Stable isotopes of oxygen and carbon and their application to sedimentologic and paleoenvironmental problems, p. 1–1 to 1–151, Stable Isotopes in Sedimentary Geology.

Andres, M.S., Reid, R.P., Bowlin, E., Gaspar, A.P. and Eisenhauer, A. (2009): Microbes versus metazoans as dominant reef builders: insights from modern marine environments in the Exuma Cays, Bahamas. Perspectives in Sedimentary Geology: A Tribute to the Career of Robert Nathan Ginsburg, IAS Special Publication(41,p.149-165).

Andrews, J.E., Riding, R., Dennis, P.F., (1997): The stable isotope record of environmental and climatic signals in modern terrestrial microbial carbonates from Europe. Palaeogeography, Palaeoclimatology, Palaeoecology 129, 171–189.

Bak, R.P.M., (1977): Coral reefs and their zonation in the Netherlands Antilles. Studies in Geology 4, 3–16.

Ball, M.M., (1967) Carbonate sand bodies of Florida and the Bahamas, Jour. Sed. Petrology, 37, 556-591.

Bartlett, M. G., Chapman, D. S., and Harris, R. N., (2006): A decade of ground-air temperature tracking at Emigrant Pass Observatory, Utah, J. Climate, 19, 3722–3731.

Bathurst, R.G.C. (1975): Carbonate Sediments and their Diagenesis. Developments in Sedimentology, Vol. 12. Elsevier, Amsterdam, 439 pp.

Beck, J. W., Edwards, R. L., Ito, E., Taylor, F., W., Recy, J., Rougerie, F., Joannot, P., and Henin, C., (1992): Sea-surface temperature from coral skeletal strontium/calcium ratios, Science, 10 257, 644–647.

Bemis, B.E., Spero, H.J., Bijma, J., Lea, W., (1998). Reevaluation of the oxygen isotopic composition of planktonic foraminifera: Experimental results and revised paleotemperature equations. Paleoceanography, 13(2):150–160.

Berner, R.A., (1966): Chemical diagenesis and some modern carbonate sediments: Am. Jour. Sci. v.264, p. 1-36.

Bigeleisen J, Mayer MG (1947): Calculation of equilibrium constants for isotopic exchange reactions. J Chem. Phys 15:261-267.

Black, M., (1933): The precipitation of calcium carbonate on the Great Bahama Bank. Geol. Mag., 70, 455–466.

Breecker, D.O., Sharp, Z.D., McFadden, L.D., (2009): Seasonal bias in the formation and stable isotopic composition of pedogenic carbonate in modern soils from central New Mexico, USA. Geol. Soc. Am. Bull. 121, 630–640.

Breshears, D.D., Nyhan, J.W., Heil, C.E., Wilcox, B.P., (1998). Effects of woody plants on microclimate in a semi-arid woodland: soil temperature and evaporation in canopy and intercanopy patches. Int. J. Plant Sci. 159, 1010–1017.

Bristow, T.F., Bonifacie, M., Derkowski, A., Eiler, J.M., and Grotzinger, J.P., (2011): A hydrothermal origin for isotopically anomalous cap dolostone cements from south China. Nature, 474, 68.

Budd, A.F., Johnson, K.G., (1999): Origination preceding extinction during late Cenozoic turnover of Caribbean reefs. Paleobiology 25, 188–200.

Came R., Eiler J. M., Veizer J., Azmy K., Brand U., and Weidman C., (2007): Coupling of surface temperatures and atmospheric CO_2 concentrations during the Paleozoic era. Nature 449, 198–201.

Carew, J.L., and Mylroie, J.E., (1997): Geology of the Bahamas. In: Geology and Hydrogeology of Carbonate Islands pp. 91–139. Elsevier Science, New York.

Cerling, T.E., (1984): The stable isotopic composition of modern soil carbonate and its relationship to climate, Eanh Planer. Sci. Lett., 71, 229-240.

Cerling, T.E., (1986): An isotopic study of paleosol carbonates from Olduvai Gorge, Quaternary Research, 25, 63-78.

Cerling T. E., (1991): Carbon dioxide in the atmosphere: evidence from Mesozoic and Cenozoic paleosols. Am. J. Sci. 291, 371–400.

Cloud, P.E., (1962): Environment of Calcium Carbonate Deposition west of Andros Island, Bahamas. U.S. Geological Survey. Prof. Pap., 350:438 pp.

Cohen, A.L., G.D. Lane, S.R. Hart., and P.S. Lobel., (2001): Kinetic control of skeletal Sr/Ca in a symbiotic coral: implications for the palaeotemperature proxy, Paleoceanography, 16, 20-26.

Correge, T., Gagan, M.K., Beck JW., Burr, GS., Cabioch, G., Le Cornec, F., (2004): Interdecadal variation in the extent of South Pacific tropical waters during the Younger Dryas event. Nature 428:927–929.

Coops, N.C., R.H. Waring., and J.B. Moncrieff., (2000): Estimating mean monthly incident solar radiation on horizontal and inclined slopes from mean monthly temperatures extremes. International Journal of Biometeorology 44:204-211.

Craig, H., Isotopic standards for carbon and oxygen and correction factors for mass-spectrometricanalysisof carbondioxide, Geochim Cosmochim. Acra, 12, 133-149, 1957.

Craig, H., Gordon, L.I., (1965): Deuterium and ^{18}O variations in the ocean and the marine atmosphere. Stable Isotopes in Oceanographic Studies and Paleotemperatures, Cons. Naz. di Rech., Spoleto, Italy, 121 pp.

Daeron M., Guo W., Eiler J. M., Genty D., Blamart D., Boch R.,Drysdale R., Maire R., Wainer K. and Zanchetta G. (2011): ^{13}C-^{18}O clumping in speleothems: observations from natural caves and precipitation experiments. Geochim. Cosmochim. Acta 75, 3303–3317.

Dana, J.D., (1846). Zoophytes, United States Exploring Expedition during the Years 1838-1842 under the Command of Charles Wilkes, pp. 121–708.

Delaygue, G., Jouzel, J., Dutay, J.C., (2000): ^{18}O-salinity relationship simulated by an oceanic general circulation model. Earth and Planetary Science Letters 178, 113-123.

Dennis, K.J. and Schrag, D.P. (2010) Clumped isotope thermometry of carbonatites as an indicator of diagenetic alteration. Geochimica et Cosmochimica Acta, 74, 4110-4122

Dennis, K. J., Affek H. P., Passey B. H., Schrag D. P. and Eiler J. M. (2011): Defining the absolute reference frame for 'clumped' isotope studies of CO2. Geochim. Cosmochim. Acta 75, 7117–7131.

Dennis, K. J., Cochran J. K., Landman N. H., and Schrag D. P. (2013): The climate of the late Cretaceous: new insights from the application of the carbonate clumped isotope thermometer to Western Interior Seaway macrofossil. Earth Planet. Sci. Lett. 362, 51–65.

De Villiers, S., Nelson, B. K., and Chivas, A. R., (1995): Biological controls on coral Sr/Ca and $\delta^{18}O$ reconstructions of sea surface temperatures, Science, 269, 1247–1249.

Dunham, R.J., (1962): Classification of carbonate rocks according to depositional texture. In: Classification of Carbonate Rocks pp. 108–121. American Association Petroleum Geologists, Tulsa, OK.

Dworkin, S.I., Nordt, L., and Atchley, S., (2005): Determining terrestrial paleotemperatures using the oxygen isotopic composition of pedogenic carbonate: Earth and Planetary Science Letters, v. 237, p. 56–68, doi:10.1016/j.epsl.2005.06.054.

Eagle R. A., Schauble E. A., Tripati A. K., Tutken T., Hulbert R.C., and Eiler J. M. (2010): Body temperatures of modern and extinct vertebrate from ^{13}C–^{18}O bond abundances in bioapatit. PNAS 107, 10377–10382.

Eagle R. A., Eiler J. M., Tripati A. K., Ries J. B., Freitas P. S., Hiebenthal C., Wanamaker, Jr., A. D., Taviani M., Elliot M., Marenssi S., Nakamura K., Ramirez P. and Roy K. (2013): The influence of temperature and seawater carbonate saturation state on ^{13}C–^{18}O bond.

Eiler, J.M. (2007): "Clumped-isotope" geochemistry–the study of naturally-occurring, multiply-substituted isotopologues. Earth Planet. Sci. Lett. 262, 309–327.

Eiler, J.M. (2011): Paleoclimate reconstruction using carbonate clumped isotope thermometry. Quaternary Science Reviews, 30, 3575-3588.

Eiler, J. M., and Schauble E., (2004): $^{18}O^{13}C^{16}O$ in Earth's atmosphere. Geochim. Cosmochim. Acta 68(23), 4767–4777.

Emery K.O, Tracey Jr, Ladd HS (1954): Geology of Bimini and nearby atolls. I. Geology. US Geology Survey Prof Pap 260-A:1-264.

Enfield D.B (1996) Relationships of Inter-American rainfall to Tropical Atlantic and Pacific SST variability. Geophys. Res. Lett. 23: 3305-3308

Enfield, D.B., Mestas-Nuñez, A.M., Mayer D.M., Cid-Serrano, L., (1999) How ubiquitous is the dipole relationship in tropical Atlantic sea surface temperatures? J. Geophys. Res. 104: 7841-7848.

Enos, P., (1974): Reefs, platforms and basins of Middle Cretaceous in northeast Mexico Am. Assoc. Pet. Geol. Bull., 58: 800--809.

Epstein, S., Buchsbaum, R., Lowenstam, H.A., and Urey, H.C., (1953): Revised carbonate-water isotopic temperature scale. Bull. Geol. Soc. Am., 64, 1315–1326.

Epstein S., Buchsbaum, R., Lowenstam H., and Urey, H., (1951): Carbonate–water paleotemperature scale. Bull. Geol. Soc. Am. 62, 417–425.

Epstein, S., T, Mayeda., (1953): Variation of $\delta^{18}O$ content of waters from natural sources. Geo-chimica et Cosmochimica Acta, 4(5):213–224.

Erez, J., B. Luz., (1983): Experimental paleotemperatures equation for planktonic foraminifera. Geochimica et Cosmochimica Acta, 47(6):1025–1031

Esteban, M., and Klappa, C.F., (1983): Subaerial exposure environment In: P.A. Scholle, D.G. Bebout and C.H. Moore. (Editors), Carbonate Depositional Environments. American Association of Petroleum Geologists, Tulsa, Oklahoma, pp. 1-54.

Eugster, H.P. and Hardie, L.A., (1975): Sedimentation in an Ancient Playa-Lake Complex: The Wilkins Peak Member 1279 of the Green River Formation of Wyoming. Geological Society of America Bulletin.

Fairbanks, R. G., Dodge D., (1979): Annual periodicity of the $^{18}O/^{16}O$ and $^{13}C/^{12}C$ ratios in the coral Montastrea Annularis, Geochim. Cosmochim Acta 43, 1009-1020.

Fernandez, A., Tang, J., and Rosenheim, B.E., (2014): Siderite 'clumped' isotope thermometry: a new paleoclimate proxy for humid continental environments. Geochimica et Cosmochimica Acta.

Ferry, J.M., Passey, B.H., Vasconcelos, C. and Eiler, J.M. (2011): Formation of dolomite at 40-80 °C in the Latemar carbonate buildup, Dolomites, Italy, from clumped isotope thermometry. Geology, 39, 571-574.

Freile, D., (1992): Carbonate facies and flux: western Great Bahama Bank. PhD dissertation, Boston University, Boston.

Froelich, P.N, Jr., Atwood, D.K., Giese GS (1978): Influence of the Amazon River discharge on surface salinity and dissolved silicate concentration in the Caribbean Sea. Deep-Sea Res. II 25: 735-744.

Frost, C. D., and Snoke, A, W., (1989): Tobago, West Indies, a fragment of a Mesozoic oceanic island arc : petrochemical evidence. Journal of the Geological Society, London, 146, 953-964.

Fugilister, F. C., (1947): Average monthly sea surface temperatures of the western North Atlantic Ocean: Mass. Inst. Technology and Woods Hole Oceanog. lust., Papers in Phys. Oceanography and Meteorology, v. 10, no. 2, p. 1-25, pls. 1-16.

Garrett, P., and Gould, S.J., (1984): Geology of New Providence Island, Bahamas, Geol. Soc. America Bull., 95, 209-220.

Gebelein, C.D., (1974): Guidebook for modern Bahamian platform environments. Geol. Soc. Am. Ann. Mtg Field Guide, 93 pp. Geological Society of America, Boulder, Colorado, USA.

Gentry., D.K, Sosdian., S, Grossmann, E.L, Y. Rosenthal, Y, Hicks, D., Lear, C.H, (2008): Stable isotope and Sr/Ca profiles from the marine gastropod Conusermineus: Testing a multiproxy approach for inferring paleotemperature and paleosalinity. Palaios, 23(3–4):195–209.

Ghosh, P., Adkins J., Affek H., Balta, B., Guo, W. F., Schauble E. A., Schrag D., and Eiler J. M. (2006a): ^{13}C-^{18}O bonds in carbonate minerals: a new kind of paleothermometer. Geochim. Cosmochim. Acta 70(6), 1439–1456.

Ghosh, P., Bhattacharya, S.K., Jani, R.A., (1995): Palaeoclimate and palaeovegetation in Central India during the Upper Cretaceous based on stable isotope composition of the palaeosol carbonates. Palaeogeography, Palaeoclimatology, Palaeoecology 114, 285–296.

Ghosh P., Garzione C. M. and Eiler J. M. (2006b): Rapid uplift of the altiplano revealed through ^{13}C–^{18}O bonds in paleosol carbonates. Science 27, 511–515.

Ghosh, P., Eiler, J., Campana, S.E., Feeney, R.F., (2007): Calibration of the carbonate 'clumped isotope' paleothermometer for otoliths. Geochimica et Cosmochimica Acta 71.

Ginsburg, R.N., (1956): Environmental relationships of grain size and constituent particles in some South Florida carbonate sediments. AAPG Bull., 40, 2384–2427.

Ginsburg, R.N., (2005): Disobedient sediments can feedback on their transportation, deposition and geomorphology. Sed. Geol., 175, 9–18.

Ginsburg, R.N., Harris, P.M, Eberli, G.P, Swart P.K., (1991): The growth potential of a bypass margin, Great Bahama Bank. J Sedim Petrol 61:976-987.

Ginsburg, R.N., Lloyd, R.M., McCallum, J.S., Stockman, K.W. and Moody, R.A., (1958): Surface sediments of Great Bahama Bank, Shell Development Company, Houston, Texas, USA.

Giry, C., Felis, T., Scheffers, S., Fensterer, C., (2010): Assessing the potential of Southern Caribbean corals for reconstructions of Holocene temperature variability. IOP Conference Series: Earth and Environmental Science 9.

Gonfiantini, R., (1986): Environmental Isotopes in Lake Studies. In: Handbook of Environmental Isotope Geochemistry 2, pp. 113-168. Elsevier, Amsterdam.

Goudie, A, S., (1973): Duricrusts in Tropical and Subtropical Landscapes. Clarendon Press, Oxford.

Grauel, A.L., Schmid, T.W., Hu, B., Bergami, G., Capotondi, L., Zhou, L., Bernasconi, S.M., (2013): Calibration and application of the 'clumped isotope' thermometer to foraminifera for high-resolution climate reconstructions Geochim. Cosmochim. Acta, 108, pp. 125.

Gross, M.G., (1964): Variations in the $^{18}O/^{16}O$ and $^{13}C/^{12}C$ ratios of diagenetically altered limestones in the Bermuda islands. Journal of Geology, 72, 172-193.

Gross, M.G., and Tracey, J.I., (1966): Oxygen And Carbon Isotopic Composition Of Limestones And Dolomites Bikini and Eniwetok Atolls. Science, 151, 1082-1084.

Grossman, E.L., (2012): Applying Oxygen Isotope Paleothermometry in Deep Time, Reconstructing Earth's Deep-Time Climate–The State of the Art. Paleontological Society Papers, v. 18. Paleontological Society, p. 39-67.

Grosmann, E. L., Ku, T.L., (1986): Oxygen and carbon isotope fractionation in biogenic aragonite – temperature effects. Chemical Geology, 59(1): 59–74.

Guo, W., Mosenfelder, III., J. and Eiler, J., (2009): Isotopic fractionations associated with phosphoric acid digestion of carbonate minerals: insights from first-principles theoretical modeling and clumped isotope measurements. Geochimica et Cosmochimica Acta 73, 7203–7225.

Guzmán, H.M., Tudhope, A.W., (1998): Seasonal variation in skeletal extension rate and stable isotopic ($^{13}C/^{12}C$ and $^{18}O/^{16}O$) composition in response to several environmental variables in the Caribbean reef coral *Siderastrea siderea*. Mar. Ecol. Prog. Ser. 166: 109.

Harrison, R.S., (1977): Caliche profiles: indicators of near surface subaerial diagenesis, Barbados, West Indies. Bulletin of Canadian Petroleum Geologists 25, 123–173.

Hearty, P.J., and Kindler, P., (1997): The stratigraphy and surficial geology of New Providence and surrounding islands, Bahamas: Journal of Coastal Research, v. 13, n. 3, p. 798-812.

Helmle, K.P., Dodge, R.E., Ketcham, R.A., 2000. Skeletal architecture and density banding in Diploria Strigosa by X-ray computed tomography. Proceedings 9th International Coral Reef Symposium, Bali, Indonesia 1, pp. 365–371.

Hellweger, F.L., Gordon, A.L., (2002): Tracing Amazon River water into the Caribbean Sea. J. Mar. Res. 60: 537-549

Henkes, G.A., Passey, B.H., Wanamaker Jr., A.D., Grossman, E.L., Ambrose Jr., W. G., Carrol, M. L., (2013): Carbonate clumped isotope compositions of modern marine mollusk and brachiopod shells. Geochim. Cosmochim. Acta 106, 307–325.

Herbert, T.D., Schuffert, J.D., Andreasen, D., Heusser, L., Lyle, M., Mix, A., Ravelo, A, Husseini, S.I., Matthews, R.K., (1972): Distribution of high-magnesium calcite in lime muds of the Great Bahama Bank; diagenetic implications. J. Sed. Petrol., 42(1), 179–182.

Hetzinger, S., Pfeiffer, M., Dullo, W.C., Ruprecht, E., Garbe-Schönberg, D., (2006): Sr/Ca and $\delta^{18}O$ in a fast-growing Diploria strigosa coral: evaluation of a new climate archive for the tropical Atlantic. Geochemistry, Geophysics, Geosystems.

Hetzinger, S., Pfeiffer, M., Dullo., W.C., Keenlyside, N., Latif, M., Zinke, J., (2008): Caribbean coral tracks Atlantic Multidecadal Oscillation and past hurricane activity Geology 36,11-14

Hetzinger, S., Pfeiffer, M., Dullo, W.-C., Garbe-Schönberg, D., Halfar, J., (2010): Rapid 20th century warming in the Caribbean and impact of remote forcing on climate in the northern tropical Atlantic as recorded in a Guadeloupe coral. Palaeogeography, Palaeoclimatology, Palaeoecology 296, 111–124.

Hill, P. S., Tripati and Schauble, E. A., (2014): Theoretical constraints on the effects of pH, salinity, and temperature on clumped isotope signatures of dissolved inorganic carbon species and precipitating carbonate minerals. Geochim. Cosmochim. Acta 125, 610–652.

Hopley, D., (1986): Beachrock as a sea-level indicator, in Van de Plassche, O. Sea-Level Research: A Manual for the Collection and Evaluation of Data. Norwick: Geo Gooks.p. 157-173.

Hough, B.G, Fan, M, Passey, B.H., (2014): Calibration of the clumped isotope geothermometer in soil carbonate in Wyoming and Nebraska: Implications for paleoelevation and paleoclimate reconstruction. Earth and Planetary Science Letters 391, 120-130.

Hudson, J.D., Anderson, T.F., (1989): Ocean temperatures and isotopic compositions through time. Transactions of the Royal Society of Edinburgh: Earth Science, 80:183–192.

Huntington, K.W., Budd, D.A., Wernicke, B.P., and Eiler, J.M., (2011): Use of clumped-isotope thermometry to constrain the crystallization temperature of diagenetic calcite. Journal of Sedimentary Research, 81, 656-669.

Huntington, K.W., Eiler, J.M., Affek, H.P., Guo, W., Bonifacie, M., Yeung, L.Y., Thiagarajan, N., Passey, B., Tripati, A., Daeron, M. and Came, R. (2009): Methods and limitations of 'clumped' CO_2 isotope (Δ_{47}) analysis by gas-source isotope ratio mass spectrometry. Journal of Mass Spectrometry, 44, 1318-1329.

Husseini, S.I. and Matthews, R.K. (1972): Distribution of high-magnesium calcite in lime muds of the Great Bahama Bank; diagenetic implications. J. Sed. Petrol., 42(1), 179-182.

Illing, L.V., (1954): Bahamian calcareous sands. Am. Assoc. Pet. Geol. Bull., 38:95.

Jackson, T. A., and Donovan, S. K., (1994): Tobago: Caribbean Geology: An Introduction, pp. 193-207. University of the West Indies Publishers Association.

Jackson, T.A., Duke, M.J., M., Smith, T.E., and Huang, C.H., (1988): The geochemistry of the metavolcanics in the Parlatuvier Formation, Tobago: evidence of an island arc origin: in L. Barker (ed.), Transactions of the 11th Caribbean Geological Conference, Dover Beach, Barbados, p. 21.1-21.8.

Juillet-Leclerc, A., Reynaud S., (2010): Light effects on the isotopic fractionation of skeletal oxygen and carbon in the cultured zooxanthellate coral, Acropora: implications for coral-growthrates. Biogeosciences 7:893–906.

Kenny, J., (2000): View from the Ridge; Exploring the natural history of Trinidad and Tobago. Prospect Press. Pg.18.

Kim, S.T., O'Neill, J.R., (1997): Equilibrium and non-equilibrium oxygen isotope effects in synthetic carbonates. Geochimica et Cosmochimica Acta, 61:3461–3475.

Kim S.T., O'Neil J. R., Hillaire-Marcel, C., and Mucci, A., (2007): Oxygen isotope fractionation between synthetic aragonite and water: influence of temperature and Mg^{2+} concentration. Geochim. Cosmochim. Acta 71, 4704–4715.

Kinsman, D. J. J., and H. D. Holland (1969): The co-precipitation of Sr^{2+} with aragonite between 16 and 96C, Geochim. Cosmochim. Acta, 33,1 – 17.

Kluge, T., and Affek, H. P., (2012): Quantifying kinetic fractionation in Bunker Cave speleothems using Δ_{47}. Quatern. Sci. Rev. 49, 82–94.

Knutson, D.W., Buddemeier, R.W., Smith, S.V., (1972): Coral chronometers: seasonal growth bands in reef corals. Science 177:270-272.

Kornicker, S.L., (1963): The Bahama banks: A "living" fossil-environment. Journal of Geological Education Vol. 11, No. 1, pp. 17-25.

Kuhnert, H., Crueger, T., Pätzold, J., (2005): NAO signature in a Bermuda coral Sr/Ca record. Geochemistry, Geophysics, Geosystems.

Leder, J. J., Swart, P. K., Szmant, A. M., and Dodge R. E. (1996): The origin of variations in the isotopic record of scleractinian corals: I. Oxygen. Geochim. Cosmochim. Acta 60, 2857-2870.

Leier, A., McQuarrie, N., Garzione, C.N., and Eiler, J., (2013): Oxygen isotope evidence for multiple pulses of rapid surface uplift in the Central Andes, Bolivia: Earth and Planetary Science Letters, v. 371, p. 49–58,.2013 .04 .025.

Le Grande, A.N., Schmidt, G.A., (2006): Global gridded data set of the oxygen isotopic composition in seawater. Geophysical Research Letters, 33(12), L12604,

Levitus S, Burgett R, Boyer TP (1994) World Ocean Atlas 1994 Volume 3: Salinity. U.S. Department of Commerce, Washington, D.C. (99).

Lewis, W. M., Jr., and J. F. Saunders (1989): Concentration and transport of dissolved and suspended substances in the Orinoco River, Biogeochemistry, 7, 203-240.

Linsley, B.K., Wellington, G.M., D.P. Schrag, (2000): Decadal sea surface temperature variability in the sub-tropical South Pacific from 1726 to 1997 Science, 290: 1145-1148.

Lowenstam, H. and Epstein, S. (1957): On the origin of sedimentary aragonite needles of the Great Bahama Bank. Journal of Geology, 65, 364-375.

Loyd, S.J., Corsetti, F.A., Eiler, J.M. and Tripati, A.K. (2012) Determining the diagenetic conditions of concretion formation: Assessing temperatures and pore water using clumped isotopes. Journal of Sedimentary Research, 82, 1006-1016.

Mack, G.H., Cole, D.R., (2005): Geochemical model of $\delta^{18}O$ of pedogenic calcite versus latitude and its application to Cretaceous palaeoclimate. Sedimentary Geology 174, 122–155.

Mack, G.H., Cole, D.R., Giordano, T.H., Schaal, W.C., Barcelos, J.H., (1991): Paleoclimatic controls on stable oxygen and carbon isotopes in caliche of the Abo Formation Permian, south- Ž .central New Mexico, U.S.A. J. Sediment. Petrol. 61, 458–472.

Magaritz, A. Kaufman., and Yaalon, D.H., Calcium carbonate nodules in soils (1981): $^{18}0/^{16}0$ and $^{13}C/^{12}C$ and ^{14}C contents, Geoderma 25, 157-172.

Marino, B.D., and McElroy, M.B., (1991): Isotopic composition of atmospheric CO_2 inferred from carbon in C_4 plant cellulose: Nature, v. 349, p. 127–131, National Oceanic and Atmospheric Administration.

McCrea, J. M., (1950): On the isotopic chemistry of carbonates and a paleotemperature scale. J. Chem. Phys. 18, 849–857.

Miller, A., Thompson, J.C., Peterson, R.E. and Haragan, D.R. (1983): Elements of meteorology. 4th ed. Columbus, U.S.A.

Milliman, J.D., (1974): Marine Carbonates. Springer Verlag, Berlin, Heidelberg, New York, 375.

Milliman, J.D., Freile, D., Steinen, R., and Wilber, R.J., (1993): Great Bahama Bank aragonitic muds: mostly inorganically precipitated, mostly exported. J. Sed. Petrol, 63(4), 589–595.

Morse, J. W., Thurmond, W., Brown, E., and Ostlund, H. G., 1984, The carbonate chemistry of GBB waters: After 18 years another look: Journal of Geophysical Res, v. 89, p. 3604–3614.

Moses, C.S., Swart, P.K., (2006): Stable isotope and growth records in corals from the island of Tobago: not simply a record of the Orinoco. Proc 10th International Coral Reef Symp 1:580–587.

Mullins, H.T., (1986): Carbonate depositional environments, modern and ancient. Periplatform carbonates, Quarterly, 81, 1–63. Colorado School of Mines Press, Golden (Colorado), USA.

Müller-Karger, F.E., McClain, C.R., Fisher T.R., Esaias W.E., Varela, R., (1989): Pigment distribution in the Caribbean Sea: Observations from space. Prog. Oceanography. 23: 23-64.

Neumann, A.C., and Land, L.S., (1975): Lime mud deposition and calcareous algae in the Bight of Abaco, Bahamas: a budget. J. Sed. Petr., 45, 763–786.

Newell, N.D., Imbrie, J., Purdy, E.G., Thurber, D.L., (1959): Organism communities and bottom facies, Great Bahama Bank. Bull. Am. Museum Natural History, 117, 177–228.

Newell, N.D., Rigby, J.K., (1957): Geological studies on the Great Bahama Bank. In: L.J. LeBlanc and J.G. Breeding (Editors), Regional Aspects of Carbonate Deposition. SEPM Spec. Publ., 5: 15-72.

Passey, B.H., Henkes, G.A., (2012): Carbonate clumped isotope bond reordering and geospeedometry. Earth Planet. Sci. Lett. 351–352, 223–236.

Passey B. H., Levin N. E., Cerling T. E., Brown F. H. and Eiler J. M. (2010): High-temperature environments of human evolution in East Africa based on bond ordering in paleosol carbonates. Proc. Natl. Acad. Sci. 107, 11245–11249.

Pearson, P.N., (2012): The Marine Stable Isotope Record, Reconstructing Earth's Deep-Time Climate-The State of the Art in 2012. Paleontological Society.

Peters, N.A., Huntington, K., Hoke, G.D., (2013): Hot or not? Impact of seasonally variable soil carbonate formation on paleotermperature and O-isotope records from clumped isotope thermometry. Earth Planet. Sci. Lett. 361, 208–218.

Pezzi, L.P., Cavalcanti, I.F.A., (2001): The relative importance of ENSO and tropical Atlantic sea surface temperature anomalies for seasonal precipitation over South America: A numerical study. Clim. Dyn. 17: 205-212.

Purdy, E., (1963a): Recent calcium carbonate facies of the Great Bahama Bank.1. Petrography and reaction groups. J. Geol., 71, 334–335.

Purdy, E., (1963b): Recent calcium carbonate facies of the Great Bahama Bank. 2. Sedimentary facies. J. Geol., 71, 472–497.

Reijmer, J.J., Swart, P.K., Bauch, T., Otto, R., Reuning, L., Roth, S. and Zechel, S., (2009): A re-evaluation of facies variations on Great Bahama Bank 1: new facies maps of Western Great Bahama Bank. In: Perspectives in Sedimentary Geology: A Tribute to the Career of Robert Nathan Ginsburg (Eds P.K. Swart, G.P. Eberli and J.A. McKenzie) Blackwell, Oxford. Spec. Publ. Int. Assoc. Sedimentol., 41, 29–46.

Risk M.J, Van Wissen, F.A., Beltran, J.C., (1992): Sclerochronology of Tobago corals: A record of the Orinoco? 7th International Coral Reef Symposium 1: 156-161.

Rosenfeld, J.K, (1979): Interstitial water and sediment chemistry of two cores from Florida Bay: Jou. Sed. Pet., v. 49, p. 989-994.

Rossinsky, V.J., and Swart, P.K., (1993): Climatic control on the isotopic composition of calcretes in the British West Indies; Continental Isotopic Indicators of Climate (Ed P.K. Swart, McKenzie, J., Lohmann, K.C., and Savin S), 78 pp. 67-76. AGU, Washington.

Rozanski, K., Araguas-Araguas, L. and Gonfiantini, R. (1993): Isotopic patterns in modern global precipitation: In: Climate Change in Continental Isotopic Records, P.K. Swart, K.C. Lohmann, J. McKenzie, and S. Savin, editors, Geophysical Monograph 78, American Geophysical Union, 1-36.

Saenger, C., Affek, P.H., Felis, T., Thiagarajan, N., Lough, J.M., Holcomb, M., (2012): Carbonate clumped isotope variability in shallow water corals: Temperature dependence and growth-related vital effects Geochimica et Cosmochimica Acta, Vol. 99, pp. 224-242.

Salomons, W., Goudie, A., and Mook, W.G., (1978): Isotopic composition of calcrete deposits from Europe, Africa and India, Earth Surface Processes, 3, 43-57.

Salomons, W., and Mook, W.G., (1976): Isotope chemistry of carbonate precipitation and dissolution in soils, Soil Sci. 122, 15-24.

Schmidt, G.A., (1999): Forward modeling of carbonate proxy data from planktonic foraminifera using oxygen isotope tracers in a global ocean model. Paleoceanography 14, 482-497.

Sealey, N.E., (1990): The Bahamas Today. MacMillan Education Ltd., London, 120 pp.

Semeniuk, V., Searle, D.J., (1985): Distribution of calcrete in Holocene coastal sands in relationship to climate, Southeastern Australia, Jour. Sed. Petrology, 55, 86-95.

Shackleton, N. J., (1974): Attainment of isotopic equilibrium between ocean water and the benthnic foraminifera genus Uvigerina: isotopic changes in the ocean during the last glacial. Centre National de la Recherche Scientifique Colloq. Internationau, 219: 203–209.

Shinn, E.A., Steinen, R.P., Lidz, B.H., and Swart, P.K., (1989): Whitings, a sedimentologic dilemma. J. Sedimentary Petrol., 59, 147–161.

Smith, B. N., and Epstein, S., (1971): Two categories of $^{13}C/^{12}C$ ratios for higher plants. Plant Physiol. 47, 380-384.

Smith, C.L., (1940a): The Great Bahama Bank. 2. Calcium carbonate precipitation. J. Marine Res., 3, 147–189.

Smith, C.L., (1940b): The Great Bahama Bank. 1. General hydrographic and chemical factors J. Marine Res., 3, 1–31.

Smith, N.P., (1995): On long-term net flow over Great Bahama Bank. J. Phys. Oceanogr., 25, 679.

Smith, S.V., Buddemeier, R.W., Redalie, R.C., Houck, J.E., (1979): Strontium-calcium thermometry in coral skeletons, Science, 204, 404-406.

Swart, P.K., (1981): The strontium, magnesium and sodium composition of recent scleractinian coral skeletons as standards for palaeoenvironmental analyses. Palaeo. Palaeo.34, 115-136.

Swart P.K., (1983) Carbon and oxygen Isotope fractionation in scleractlnian corals: a review Earth-Science Rev., 19:51-80

Swart, P.K., Burns, S.J. and Leder, J.J., (1991): Fractionation of the stable isotopes of oxygen and carbon in carbon dioxide during the reaction of calcite with phosphoric acid as a function of temperature and technique. Chem. Geol., 86, 89–96.

Swart, P.K., Dodge, R.E., Hudson, H.J., (1996): A 240-year stable oxygen and carbon isotopic record in a coral from south Florida: Implications for the prediction of precipitation in southern Florida. Palaios 11: 362-375.

Swart, P.K., and Melim, L.A., (2000): The origin of dolomites in Tertiary sediments from the margin of Great Bahama Bank. Sedimentary Res., 70, 738–748.

Swart, P.K., and Price, R., (2002): Origin of salinity variations in Florida Bay. Limnology and Oceanography, 47:1234–1241.

Swart, P.K., Reijmer, J.J. and Otto, R. (2009): A reevaluation of facies on Great Bahama Bank II: Variations in the $\delta^{13}C$, $\delta^{18}O$ and mineralogy of surface sediments. In: Perspectives in Carbonate Geology: A Tribute to the Career of Robert Nathan Ginsburg, IAS Special Publication (Eds P.K. Swart, G.P. Eberli and J.A. McKenzie), 41, pp. 47-60. Wiley-Blackwell, Oxford.

Quade J., Cerling, T. E., and Bowman J. R., (1989): Systematic variation in the carbon and oxygen isotopic composition of Holocene soil carbonate along elevation transects in the southern Great Basin, USA. Geol. Soc. Am. Bull. 101, 464–475.

Quade, J., Garzione, C., and Eiler, J., (2007): Paleosol carbonate in paleoelevation reconstruction. In Paleoelevation: Geochemical and Thermodynamic Approaches (ed. M. Kohn). Rev. Mineral. Geochem. Mineral. Soc. Am. Bull. 66, 53–87.

Talma, A.S., and Netterberg, F., (1983): Stable isotope abundances in calcretes, in Residual Deposits: Surface Related Weathering Processes edited by Wilson, R.C.L., Oxford, Blackwell Scientific Publications.

Tang, J., Dietzel, M., Fernandez, A., Tripati, A.K, Rosenheim, B.E., (2014): Evaluation of kinetic effects on clumped isotopes fractionation Δ_{47} (during inorganic calcite precipitation Geochim. (Cosmochim Acta 134,1208136).

Thiagarajan N., Adkins J. and Eiler J. (2011): Carbonate clumped isotope thermometry of deep-sea corals and implications for vital effects. Geochim. Cosmochim. Acta 75, 4416–4425.

Traverse, A., and Ginsburg, R.N., (1966): Palynology of the surface sediments of Great Bahama Bank, as related to water movement and sedimentation. Marine Geol., 4, 417–459.

Tripati, A. K., Eagle, R. A., Thiagarajan N., Gagnon, A. C., Bauch H., Halloran, P. R., and Eiler, J. M., (2010): ^{13}C–^{18}O isotope signatures and 'clumped isotope' thermometry in foraminifera and coccoliths. Geochim. Cosmochim. Acta 74, 5697–5717.

Urey, H.C., (1947): The thermodynamic properties of isotopic substances. Journal of the Chemical Society of London: 562–581.

Urey, H. C., Lowenstam, H. A., Epstein, S., and McKinney, C. R., (1951): Measurement of paleotemperatures and temperatures of the Upper Cretaceous of England, Denmark, and the Southeastern United-States. Geological Society of America Bulletin 62, 399.

Van De Velde, J.H., Bowen, G.J., Passey, B.H. and Bowen, B.B. (2013): Climatic and diagenetic signals in the stable isotope geochemistry of dolomitic paleosols spanning the Paleocene-Eocene boundary. Geochimica et Cosmochimica Acta, 109, 254-267.

Wacker, U., Fiebig, J., and Scho¨ne, B. R., (2013): Clumped isotope analysis of carbonates comparison of two different acid digestion techniques. Rapid Commun. Mass Spectrom. 27, 1631–1642.

Wang, H., and Fu, R., (2002): Cross-equatorial flow and seasonal cycle of precipitation over South America. J. Climate, 15, 1591–1608.

Wang, Z. G., Schauble, E. A., and Eiler, J. M., (2004): Equilibrium thermodynamics of multiply substituted isotopologues of molecular gases. Geochimica et Cosmochimica Acta 68, 4779-4797.

Watanabe, T., Winter, A., and Oba, T (2001): Seasonal changes in sea surface temperature and salinity during the Little Ice Age in the Caribbean Sea deduced from Mg/Ca and 18O/16O ratios in corals, Mar. Geol., 173, 21–35.

Weber, J.N., and Woodhead, P.J.M., (1972): Temperature dependence of oxygen-18 concentration in reef coral carbonates. Journal of geophysical Research Vol.77 No.3.

Weber, J. N., (1973): Incorporation of strontium into reef coral skeletal carbonate, Geochim. Cosmochim. Acta, 37(9), 2173 – 2190.

Well, S.M., R.W., Buddemeier, S.V. Smith., and P.M., Kroopnick, (1981): The stable isotopic composition of coral skeletons: control by environmental variables, Geochimica et Cosmochimica Acta, 45, 1147-1153.

Wellington, G.M., Dunbar, R.B., (1995): Regional variation in the stable isotopic signature of ENS0 events in reef corals in the eastern Pacific. Coral Reefs 14: 5-25.

Woodley, J.D., Chornesky, E.A., Clifford, P.A., Jackson, J.B.C., Kaufman, L.S., Knowlton, N., Lang, J.C., Pearson, M.P., Porter, J.W., Rooney, M.C., Rylaarsdam, K.W., Tunnicliffe, V.J., Wahle, C.M., Wulff, J.L., Curtis, A.S.G., Dallmeyer, M.D., Jupp, B.P., Koehl, M.A.R., Neigel, J., Sides, E.M., (1981): Hurricane Allen's impact on Jamaican coral reefs. Science 214, 749–755.

Wright, V,P. and Tucker, M,E., (1991); Calcretes: An introduction. In: Calcretes, V.P. Wright and M.E. Tucker (Eds). Blackwell, Oxford, p. 1-22.

Zaarur, G. Olack and Affek, H.P., (2011): Paleo-environmental implication of clumped isotopes in land snail shells Geochim. Cosmochim. Acta, 75(pp. 6859)

Zaarur S., Affek H. P. and Brandon M. T. (2013): A revised calibration of the clumped isotope thermometer. Earth Planet. Sci. Lett. 382, 47–57.

Zeebe, R.E., 1999. An explanation of the effect of seawater carbonate concentration on foraminiferal oxygen isotopes. Geochimica et Cosmochimica Acta, 63(13–14):2001–2007.

APPENDIX 1. Clumped isotopes data of the GBB project

Run ID	C01888	C01935	C01911	Average	C01974	C02189	C02192	Average	C02240	C02339	C01526	Average	C01565	C02209	C02213	Average	C01566	C02196	C02200	Average
Sample	GBB 903.8	GBB 903.8	GBB 903.08	GBB 903.8	GBB 903.11	GBB 903.11	GBB 903.11	GBB 903.11	GBB 902.2	GBB 902.02	Bahama 902	GBB 902.2	Bahama 902	GBB 902.9	GBB 902.9	GBB 902.9	Bahama 902	GBB 902.16	GBB 902.16	GBB 902.16
Date	09/12/13	09/27/13	09/19/13		10/10/13	12/27/13	12/28/13		01/12/14	02/18/14	04/12/13		04/29/13	01/03/14	01/04/14		04/29/13	12/30/13	12/31/13	
Block	11	20	20	17	20	10	10	13.3333333	10	10	11	10.3333333	10	10	10	10	10	10	10	10
CC	6	6	6	6	6	6	6	6	6	6	6	6	6	6	6	6	6	6	6	6
	0	0	0	0	0	0	0	0	0	0	0	0	0	0	0	0	0	0	0	0
δ13C	4.46916878	4.50125873	4.67309033	4.54783928	4.4418356	4.46357316	4.49285989	4.46608957	4.35292115	4.39497571	4.4751638	4.40768689	4.29501251	4.45831045	4.45511764	4.40281353	4.36026275	4.25006795	4.33415363	4.3148281
sd	0.00568176	0.00685067	0.00656759	0.00636667	0.0067165	0.00651502	0.0047896	0.00600707	0.00747693	0.00589701	0.00691317	0.00676237	0.00529414	0.00784986	0.0072647	0.0068029	0.00592053	0.00678678	0.00637039	0.0063592
se	0.00069414	0.00062279	0.00059705	0.00063799	0.000610	0.00083416	0.00061325	0.000686	0.00095732	0.00075503	0.00084458	0.00085231	0.00067785	0.00100507	0.00093015	0.00087102	0.00075805	0.00086896	0.00081564	0.0008142
δ18O	8.19396768	8.25049605	8.44635509	8.29693961	8.1497264	8.28750492	8.24267193	8.22663442	8.18696639	8.07237469	8.07318988	8.11084365	8.07917819	8.30710097	8.4505063	8.27892849	7.73773409	7.76097825	7.88991924	7.7959679
Carbonat	0.23972252	0.29625089	0.49210994	0.34269445	0.1954812	0.33325977	0.28842677	0.27238926	0.23272124	0.11812954	0.11894472	0.1565985	0.12493303	0.35285581	0.49626115	0.32468333	-0.2165111	-0.1932669	-0.0650539	-0.1582773
sd	0.00974039	0.01056104	0.01112322	0.01047489	0.0111453	0.00912428	0.01050683	0.01025881	0.00981536	0.01049458	0.01011436	0.01014144	0.00899864	0.01221809	0.01015236	0.01045636	0.00993953	0.01024392	0.00958652	0.0099233
se	0.00118998	0.00096009	0.00105112	0.00105376	0.0010132	0.00116824	0.00134526	0.00117557	0.00125673	0.00134369	0.00123567	0.00127787	0.00115216	0.00156437	0.00129988	0.00133388	0.00127263	0.00131116	0.00122743	0.0012706
δ45CO2	7.33968516	7.37161791	7.53923717	7.41684675	7.3126091	7.33737861	7.36348012	7.33782264	7.23024608	7.26614254	7.34150743	7.27929868	7.17243868	7.33305229	7.33457607	7.28002235	7.22297039	7.12017242	7.20321892	7.1821206
sd	0.00568176	0.00685067	0.00656759	0.00636667	0.0067165	0.00651502	0.0047896	0.00600707	0.00747693	0.00589701	0.00691317	0.00676237	0.00529414	0.00784986	0.0072647	0.0068029	0.00592053	0.00678678	0.00637039	0.0063592
se	0.00069414	0.00062279	0.00059705	0.00063799	0.000610	0.00083416	0.00061325	0.000686	0.00095732	0.00075503	0.00084458	0.00085231	0.00067785	0.00100507	0.00093015	0.00087102	0.00075805	0.00086896	0.00081564	0.0008142
δ46CO2	14.1371015	14.1939713	14.391139	14.2407373	14.092588	14.2310818	14.1860917	14.1699206	14.1298249	14.0147635	14.0157491	14.0534458	14.0213926	14.2507622	14.3948579	14.2223375	13.6784242	13.7015527	13.8305634	13.736847
sd	0.00974039	0.01056104	0.01112322	0.01047489	0.0111453	0.00912428	0.01050683	0.01025881	0.00981536	0.01049458	0.01011436	0.01014144	0.00899864	0.01221809	0.01015236	0.01045636	0.00993953	0.01024392	0.00958652	0.0099233
se	0.00118998	0.00096009	0.00110112	0.00105376	0.0010132	0.00116824	0.00134526	0.00117557	0.00125673	0.00134369	0.00123567	0.00127787	0.00115216	0.00156437	0.00129988	0.00133388	0.00127263	0.00131116	0.00122743	0.0012706
δ47CO2	22.0042852	22.1047358	22.4717131	22.193578	21.920490	22.0898638	22.0556294	22.0219946	21.8188385	21.748906	21.7961445	21.787963	21.6409595	22.1063026	22.2314594	21.992907	21.3441177	21.312862	21.4895137	21.382164
sd	0.09631192	0.09443788	0.098339	0.09636293	0.0966802	0.10418244	0.09873116	0.09986463	0.09285654	0.09777668	0.08539634	0.09200985	0.09703275	0.10492362	0.1099658	0.10397406	0.09774062	0.09254446	0.09266135	0.0943155
se	0.01176637	0.00858526	0.00893991	0.00976385	0.0087891	0.01333919	0.01264123	0.01158985	0.01188906	0.01251902	0.01043282	0.01161364	0.01242377	0.01343409	0.01407968	0.01331251	0.0125144	0.0118491	0.01186407	0.0120759
δ48CO2	39.7712802	39.7846378	40.88811	40.1480093	38.983158	39.3062988	39.2954577	39.1949717	38.5771176	38.2983792	38.7528026	38.5427665	39.5375919	42.4556167	42.8062027	41.5998038	37.8307639	37.6685772	37.9379016	37.812414
sd	0.54768547	0.64422347	0.67393456	0.62194783	0.6626021	0.67315731	0.60072178	0.64549375	0.51800466	0.50833105	0.60104209	0.54245927	0.59084423	0.70912912	0.65246137	0.65081158	0.58745532	0.60302625	0.59589547	0.595459
se	0.06691043	0.05856577	0.06126678	0.06224766	0.0602365	0.08618896	0.07691454	0.0744669	0.0663237	0.06508512	0.07342898	0.06827927	0.07564985	0.09079468	0.08353912	0.08332788	0.07521595	0.0772096	0.0762966	0.0762407
δ49CO2	-4.5196679	-14.506691	-17.624871	-12.217077	-9.946624	-4.0116632	-15.293098	-9.7504617	-12.250737	-2.6662962	-34.060475	-16.325836	-19.932949	-13.873352	-14.801595	-16.202632	-17.565233	-9.1369442	-9.9025157	-12.201564
sd	6.74915353	8.88512502	6.42334414	7.35254089	8.2293642	8.31519359	6.11948441	7.55468076	6.61339946	1.91600649	13.19682	7.24207531	8.10763841	7.23958956	6.44823391	7.26515396	11.3996811	6.80795354	6.42775014	8.2117949
se	0.82454034	0.80773864	0.58394038	0.73873978	0.7481240	1.06465144	0.78351969	0.86543172	0.84675903	0.24531949	1.61224816	0.90144223	1.03807673	0.92693446	0.82561175	0.93020765	1.45957959	0.87166913	0.82298907	1.0514126
Δ47CO2	0.40583526	0.41623601	0.41234641	0.41146923	0.3947596	0.40066979	0.38415291	0.39319411	0.34336268	0.34993779	0.31810584	0.33713543	0.33370453	0.40207064	0.38304834	0.37294117	0.32454148	0.37666097	0.33930992	0.3468375
sd	0.09631192	0.09443788	0.098339	0.09636293	0.0966802	0.10418244	0.09873116	0.09986463	0.09285654	0.09777668	0.08539634	0.09200985	0.09703275	0.10492362	0.1099658	0.10397406	0.09774062	0.09254446	0.09266135	0.0943155
se	0.01176637	0.00858526	0.00893991	0.00976385	0.0087891	0.01333919	0.01264123	0.01158985	0.01188906	0.01251902	0.01043282	0.01161364	0.01242377	0.01343409	0.01407968	0.01331251	0.0125144	0.0118491	0.01186407	0.0120759
Δ48CO2	10.9844503	10.8840603	11.5635113	11.1440073	10.306836	10.3450754	10.4241774	10.3586964	9.8378396	9.7959416	10.2359274	9.95656954	10.9879171	13.367307	13.4201337	12.5917859	10.0110755	9.8071544	9.8121983	9.8768099
sd	0.54768547	0.64422347	0.67393456	0.62194783	0.6626021	0.67315731	0.60072178	0.64549375	0.51800466	0.50833105	0.60104209	0.54245927	0.59084423	0.70912912	0.65246137	0.65081158	0.58745532	0.60302625	0.59589547	0.595459
se	0.06691043	0.05856577	0.06126678	0.06224766	0.0602365	0.08618896	0.07691454	0.0744669	0.0663237	0.06508512	0.07342898	0.06827927	0.07564985	0.09079468	0.08353912	0.08332788	0.07521595	0.0772096	0.0762966	0.0762407
Δ49CO2	-0.0391505	-0.0489272	-0.0524668	-0.0468482	-0.044278	-0.0388332	-0.0496634	-0.0442585	-0.0464891	-0.0370583	-0.0674158	-0.0503311	-0.0536481	-0.0483821	-0.0495452	-0.0505252	-0.0507806	-0.0425763	-0.0436395	-0.0456655
sd	6.74915353	8.88512502	6.42334414	7.35254089	8.2293642	8.31519359	6.11948441	7.55468076	6.61339946	1.91600649	13.19682	7.24207531	8.10763841	7.23958956	6.44823391	7.26515396	11.3996811	6.80795354	6.42775014	8.2117949
se	0.82454034	0.80773864	0.58394038	0.73873978	0.7481240	1.06465144	0.78351969	0.86543172	0.84675903	0.24531949	1.61224816	0.90144223	1.03807673	0.92693446	0.82561175	0.93020765	1.45957959	0.87166913	0.82298907	1.0514126

Run ID	C01786	C01788	C01886	Average	C02006	C02033	C02188	Average	C02204	C02207	C02290	Average	C02005	C02025	C02191	Average	C02210	C02214	C02302	Average
Sample	GBB 903.2	GBB 903.6	GBB 903.6	GBB 903.6	GBB 90318	GBB 903.18	GBB 903.18	GBB 903.18	GBB 902.13	GBB 902.13	GBB 902.13	GBB 902.13	GBB 90319	GBB 903.19	GBB 903.19	GBB 903.19	GBB 903.21	GBB 903.21	GBB 903.21	GBB 903.21
Date	07/26/13	07/26/13	09/10/13		10/25/13	11/06/13	12/27/13		01/01/14	01/02/14	02/06/14		10/25/13	11/01/13	12/28/13		01/03/14	01/04/14	02/09/14	
Block	11	20	20	17	10	20	8	12.6666667	10	10	10	10	10	14	10	11.3333333	10	10	10	10
CC	6	6	6	6	6	6	6	6	6	6	6	6	6	6	6	6	6	6	6	6
	0	0	0	0	0	0	0	0	0	0	0	0	0	0	0	0	0	0	0	0
δ13C	4.96341778	4.57185704	4.63046409	4.72191297	4.34161694	4.34810115	4.38158255	4.35710022	4.54570021	4.56626579	4.5727128	4.5615596	4.39340721	4.43024792	4.42276116	4.4154721	4.48821178	4.49131193	4.3375769	4.43903354
sd	0.00655541	0.00631311	0.00648921	0.00645258	0.00722064	0.00676901	0.00790465	0.0072981	0.00610049	0.00689773	0.00750738	0.0068352	0.00628176	0.00530884	0.0058892	0.0058266	0.0068564	0.00581981	0.00826411	0.00698011
se	0.00080087	0.00057392	0.00058993	0.00065491	0.00092451	0.00061536	0.00112924	0.0008897	0.00078109	0.00088316	0.00096122	0.00087516	0.0008043	0.00057583	0.00075403	0.00071139	0.00087787	0.00074515	0.00105811	0.00089371
δ18O	8.03442591	8.16715367	8.29243382	8.16467113	8.02949076	8.0266789	8.08880224	8.04832397	8.29709432	8.16557449	8.21012852	8.22426578	8.09751631	7.95977707	7.98344208	8.01357849	8.11507641	8.09235047	8.09401342	8.1004801
Carbonate	0.08018075	0.21290852	0.33818867	0.21042598	0.0752456	0.07243374	0.13455708	0.09407881	0.34284916	0.21132933	0.25588337	0.27002062	0.14327115	0.00553191	0.02919692	0.05933333	0.16083126	0.13810532	0.13976827	0.14623495
sd	0.01236053	0.0092923	0.01053426	0.01072903	0.0127357	0.01134192	0.01122199	0.01176654	0.01012659	0.01138039	0.01280537	0.01143745	0.00867247	0.01041567	0.00932599	0.00947138	0.01029783	0.00956342	0.01485107	0.01157077
se	0.00151008	0.00084475	0.00095766	0.00110416	0.00163064	0.00103108	0.00160314	0.00142162	0.00129658	0.00145711	0.00163956	0.00146442	0.0011104	0.00112974	0.00119407	0.00114474	0.0013185	0.00122447	0.00190148	0.00148149
δ45CO2	7.79901411	7.43531804	7.49433325	7.5762218	7.2146574	7.22066081	7.25407752	7.22979858	7.414842	7.43001508	7.43747777	7.42744495	7.26546206	7.29572949	7.28944208	7.28354454	7.35508785	7.35728359	7.21289725	7.3084229
sd	0.00655541	0.00631311	0.00648921	0.00645258	0.00722064	0.00676901	0.00790465	0.0072981	0.00610049	0.00689773	0.00750738	0.0068352	0.00628176	0.00530884	0.0058892	0.0058266	0.0068564	0.00581981	0.00826411	0.00698011
se	0.00080087	0.00057392	0.00058993	0.00065491	0.00092451	0.00061536	0.00112924	0.0008897	0.00078109	0.00088316	0.00096122	0.00087516	0.0008043	0.00057583	0.00075403	0.00071139	0.00087787	0.00074515	0.00105811	0.00089371
δ46CO2	13.9778101	14.1103703	14.2363811	14.1081872	13.9715603	13.9687483	14.0312431	13.9905172	14.2408883	14.1087718	14.1535558	14.1677386	14.040024	13.9016917	13.9254562	13.955724	14.0578663	14.0350363	14.0363882	14.0430969
sd	0.01236053	0.0092923	0.01053426	0.01072903	0.0127357	0.01134192	0.01122199	0.01176654	0.01012659	0.01138039	0.01280537	0.01143745	0.00867247	0.01041567	0.00932599	0.00947138	0.01029783	0.00956342	0.01485107	0.01157077
se	0.00151008	0.00084475	0.00095766	0.00110416	0.00163064	0.00103108	0.00160314	0.00142162	0.00129658	0.00145711	0.00163956	0.00146442	0.0011104	0.00112974	0.00119407	0.00114474	0.0013185	0.00122447	0.00190148	0.00148149
δ47CO2	22.3320319	22.0429702	22.2490236	22.2080086	21.6726259	21.6895866	21.7817229	21.7146451	22.1685103	22.0611668	22.0156968	22.0817913	21.8102952	21.717415	21.7153107	21.7476736	21.9201986	21.8866951	21.6878966	21.8315967
sd	0.08257454	0.09758287	0.09053897	0.09023213	0.09089821	0.1058435	0.10735207	0.10136459	0.09840551	0.09577308	0.08595758	0.09337872	0.09107753	0.10241754	0.07857483	0.09068997	0.09351915	0.10313092	0.08620394	0.09428467
se	0.01008809	0.00887117	0.00823082	0.00906336	0.01163832	0.00962214	0.01533601	0.01219882	0.01259953	0.01226249	0.01100574	0.01195592	0.01166128	0.01110874	0.01006048	0.0109435	0.0119739	0.01320456	0.01103728	0.01207192
δ48CO2	38.7717407	39.3417058	39.5832553	39.2322339	38.6599906	39.241013	38.4602122	38.7870719	41.445708	38.9371669	38.5718714	39.6515821	38.6340544	38.6506438	38.3067641	38.5304875	42.1291176	39.7461596	38.5104036	40.1285603
sd	0.52701346	0.6258183	0.62194498	0.59159224	0.67887954	0.58235285	0.59594843	0.61906027	0.62309562	0.56391933	0.59329985	0.59343827	0.5435643	0.54886716	0.68731504	0.59324883	0.50081138	0.54363226	0.51287185	0.51910516
se	0.06438494	0.05689257	0.05654045	0.05927266	0.08692162	0.05294117	0.08513549	0.07499943	0.07977922	0.07220247	0.07596426	0.07598198	0.06959628	0.059533	0.08800167	0.07237698	0.06412233	0.06960498	0.06566651	0.06646461
δ49CO2	-14.918903	-21.697625	-5.5549696	-14.057166	-7.0039846	-14.879024	-3.7465109	-8.5431733	-14.260323	-11.348787	-0.040749	-8.5499531	-3.7234866	-18.187723	-9.7029715	-10.53806	-15.950459	-14.079943	-2.4312053	-10.820536
sd	10.0495537	7.20608573	8.81167183	8.68910377	9.39425177	7.05882653	7.22936551	7.89414794	7.82847147	8.3685046	2.30214495	6.16637367	8.79791482	8.95060133	6.96984223	8.23945279	7.40738104	7.31348437	2.45736108	5.7260755
se	1.2277484	0.6550987	0.80106108	0.89463606	1.20281069	0.6417115	1.0327665	0.95909623	1.00233306	1.07147722	0.29475946	0.78952325	1.12645756	0.97082902	0.89239685	0.99656115	0.94841796	0.93639572	0.31463285	0.73314884
Δ47CO2	0.41141712	0.37180972	0.39068621	0.39130435	0.36991527	0.38311031	0.3784044	0.37714333	0.38885007	0.39659956	0.30095566	0.3621351	0.38619593	0.39868547	0.37996881	0.3882834	0.38473595	0.37187072	0.32368728	0.36009799
sd	0.08257454	0.09758287	0.09053897	0.09023213	0.09089821	0.1058435	0.10735207	0.10136459	0.09840551	0.09577308	0.08595758	0.09337872	0.09107753	0.10241754	0.07857483	0.09068997	0.09351915	0.10313092	0.08620394	0.09428467
se	0.01008809	0.00887117	0.00823082	0.00906336	0.01163832	0.00962214	0.01533601	0.01219882	0.01259953	0.01226249	0.01100574	0.01195592	0.01166128	0.01110874	0.01006048	0.0109435	0.0119739	0.01320456	0.01103728	0.01207192
Δ48CO2	10.3299506	10.6200463	10.6037549	10.5179173	10.2337083	10.8044358	9.92050551	10.3195499	12.4052909	10.2298712	9.7854812	10.8068811	10.0720767	10.3638536	9.9819932	10.1393078	13.4353644	11.1635475	9.95906804	11.5193266
sd	0.52701346	0.6258183	0.62194498	0.59159224	0.67887954	0.58235285	0.59594843	0.61906027	0.62309562	0.56391933	0.59329985	0.59343827	0.5435643	0.54886716	0.68731504	0.59324883	0.50081138	0.54363226	0.51287185	0.51910516
se	0.06438494	0.05689257	0.05654045	0.05927266	0.08692162	0.05294117	0.08513549	0.07499943	0.07977922	0.07220247	0.07596426	0.07598198	0.06959628	0.059533	0.08800167	0.07237698	0.06412233	0.06960498	0.06566651	0.06646461
Δ49CO2	-0.0493548	-0.0557772	-0.0404914	-0.0485411	-0.0411139	-0.0487192	-0.0381198	-0.042651	-0.0488194	-0.0457806	-0.0349579	-0.043186	-0.0381255	-0.051866	-0.04371	-0.0445672	-0.050053	-0.0482074	-0.0368176	-0.045026
sd	10.0495537	7.20608573	8.81167183	8.68910377	9.39425177	7.05882653	7.22936551	7.89414794	7.82847147	8.3685046	2.30214495	6.16637367	8.79791482	8.95060133	6.96984223	8.23945279	7.40738104	7.31348437	2.45736108	5.7260755
se	1.2277484	0.6550987	0.80106108	0.89463606	1.20281069	0.6417115	1.0327665	0.95909623	1.00233306	1.07147722	0.29475946	0.78952325	1.12645756	0.97082902	0.89239685	0.99656115	0.94841796	0.93639572	0.31463285	0.73314884

Run ID	C02232	C02235	C02297	Average	C01863	C01866	Average	C01865	C02241	Average	C02007	C02032	C02185	Average	C02211	C02215	C02234	Average	C02233	C02224	C02295	Average
Sample	GBB 903.47	GBB 903.47	GBB 903.47	GBB 903.47	GBB 903.20	GBB 903.20	GBB 903.20	GBB 903.14	GBB 903.14	GBB 903.14	GBB 90315	GBB 903.15	GBB 903.15	GBB 903.15	GBB 903.28	GBB 903.28	GBB 903.28	GBB 903.28	GBB 903.36	GBB 903.36	GBB 903.36	GBB 903.36
Date	01/10/14	01/11/14	02/08/14		08/26/13	08/27/13		08/27/13	01/12/14		10/25/13	11/05/13	12/26/13		01/03/14	01/04/14	01/10/14		01/10/14	01/06/14	02/07/14	
Block	10	20	10	13.3333333	20	20	20	10	10	10	10	10	10	10	10	10	10	10	10	10	10	10
CC	6	6	6	6	6	6	6	6	6	6	6	6	6	6	6	6	6	6	6	6	6	6
	0	0	0	0	0	0	0	0	0	0	0	0	0	0	0	0	0	0	0	0	0	0
δ13C	4.38845223	4.36364081	4.31019986	4.35409763	4.37721244	4.47349221	4.42535232	4.44441286	4.36951973	4.40696629	4.40772665	4.32977934	4.46948381	4.40232993	4.53939732	4.53042815	4.50951089	4.52644546	4.48741102	4.45528483	4.40540614	4.44936733
sd	0.00697643	0.00557536	0.00642436	0.00632538	0.0066636	0.00612479	0.00639419	0.00557663	0.00909571	0.00733617	0.00598551	0.00592373	0.00546069	0.00578998	0.00542204	0.00639337	0.00681083	0.00620875	0.00513999	0.00637379	0.0057619	0.00575856
se	0.00089324	0.00050685	0.00082256	0.00074088	0.00060578	0.0005568	0.00058129	0.00071401	0.00116459	0.0009393	0.00076637	0.00075846	0.00069917	0.00074133	0.00069422	0.00081859	0.00087204	0.00079495	0.00065811	0.00081608	0.00073774	0.00073731
δ18O	7.97775009	8.15955759	8.10067273	8.0793268	7.95338678	8.06250488	8.00794583	8.03385811	8.07263989	8.053249	8.08007617	7.94061531	8.06625326	8.02898158	8.09658911	8.1125892	8.08181477	8.09699769	8.08063205	8.06101413	8.11484742	8.08549787
Carbonate	0.02350493	0.20531244	0.14642757	0.12508165	-0.0008584	0.10825973	0.05370068	0.07961295	0.11839473	0.09900384	0.12583102	-0.0136298	0.11200811	0.07473643	0.14234395	0.15834405	0.12756961	0.14275254	0.12638689	0.10676898	0.16060226	0.13125271
sd	0.0101448	0.01297052	0.0128347	0.01198334	0.00905519	0.00934192	0.00919855	0.00863408	0.01184995	0.01024202	0.00985185	0.01078059	0.01033861	0.01032368	0.00861967	0.01133793	0.00911631	0.0096913	0.01067563	0.00915484	0.01012905	0.00998651
se	0.00129891	0.00117914	0.00164331	0.00137379	0.0008232	0.00084927	0.00083623	0.00110548	0.00151723	0.00131136	0.0012614	0.00138031	0.00132372	0.00132181	0.00110364	0.00145167	0.00116722	0.00124084	0.00136687	0.00117216	0.00129689	0.00127864
δ45CO2	7.2570282	7.23945286	7.18738578	7.22795561	7.24569941	7.33959983	7.29264962	7.31137511	7.24223423	7.27680467	7.27836541	7.20073161	7.33595207	7.27168303	7.40259501	7.39467297	7.37404969	7.39043922	7.35324887	7.3224464	7.27728218	7.31765915
sd	0.00697643	0.00557536	0.00642436	0.00632538	0.0066636	0.00612479	0.00639419	0.00557663	0.00909571	0.00733617	0.00598551	0.00592373	0.00546069	0.00578998	0.00542204	0.00639337	0.00681083	0.00620875	0.00513999	0.00637379	0.0057619	0.00575856
se	0.00089324	0.00050685	0.00082256	0.00074088	0.00060578	0.0005568	0.00058129	0.00071401	0.00116459	0.0009393	0.00076637	0.00075846	0.00069917	0.00074133	0.00069422	0.00081859	0.00087204	0.00079495	0.00065811	0.00081608	0.00073774	0.00073731
δ46CO2	13.9196654	14.1023051	14.0430231	14.0216645	13.8951603	14.0050087	13.9500845	13.9761623	14.0149771	13.9955697	14.0225289	13.8822283	14.0087669	13.9711747	14.0393954	14.0554546	14.0244872	14.039779	14.0232528	14.0034729	14.0574643	14.0280633
sd	0.0101448	0.01297052	0.0128347	0.01198334	0.00905519	0.00934192	0.00919855	0.00863408	0.01184995	0.01024202	0.00985185	0.01078059	0.01033861	0.01032368	0.00861967	0.01133793	0.00911631	0.0096913	0.01067563	0.00915484	0.01012905	0.00998651
se	0.00129891	0.00117914	0.00164331	0.00137379	0.0008232	0.00084927	0.00083623	0.00110548	0.00151723	0.00131136	0.0012614	0.00138031	0.00132372	0.00132181	0.00110364	0.00145167	0.00116722	0.00124084	0.00136687	0.00117216	0.00129689	0.00127864
δ47CO2	21.6507867	21.8594374	21.6954948	21.7352396	21.649745	21.8520958	21.7509204	21.8080806	21.7800918	21.7940862	21.8199156	21.5879934	21.8325502	21.7468197	21.9363852	21.9368993	21.8658628	21.9130491	21.8813805	21.810622	21.7545101	21.8155042
sd	0.0920868	0.10561191	0.09015671	0.09595181	0.10795272	0.0987186	0.10333566	0.10004412	0.10363878	0.10184145	0.09927691	0.08653262	0.09457763	0.09346239	0.11032054	0.10407408	0.09737579	0.10392347	0.09116635	0.08478929	0.09278842	0.08958135
se	0.01179051	0.00960108	0.01154338	0.01097832	0.00981388	0.00897442	0.00939415	0.01280934	0.01326959	0.01303946	0.01271111	0.01107937	0.01210942	0.01196663	0.0141251	0.01332532	0.01246769	0.01330604	0.01167265	0.01085616	0.01188034	0.01146972
δ48CO2	38.0090284	47.5692821	38.4734383	41.3505829	39.0976744	38.8318695	38.9647719	38.6499778	38.4327044	38.5413411	38.5898651	39.0571605	38.6049575	38.7506611	40.4401006	39.3888171	40.6533031	40.1607402	38.4248024	38.2530155	37.3343408	38.0040529
sd	0.5536786	1.03298115	0.55900811	0.71511904	0.57770959	0.64628127	0.61199543	0.63360111	0.58415273	0.60887692	0.56763718	0.57301275	0.58839998	0.57634997	0.4989118	0.5448676	0.54515978	0.52964645	0.71326271	0.61733622	0.45195196	0.59418363
se	0.07085149	0.09390738	0.07157365	0.07877751	0.05251905	0.05875284	0.05563595	0.08112431	0.07479309	0.0779587	0.07267849	0.07336676	0.0753369	0.07379405	0.06387911	0.06976317	0.06980056	0.06781428	0.09132393	0.0790418	0.05786652	0.07607742
δ49CO2	-8.1255029	-22.271928	-1.851999	-10.74981	-16.902478	-4.1133856	-10.507932	-3.3066125	-17.183467	-10.24504	-3.3987151	-44.928774	-10.456747	-19.594745	-14.199449	-10.74716	-17.690327	-14.212312	-20.251291	-16.715952	25.6172515	-3.7833302
sd	7.86275564	7.01912868	1.98242769	5.62143734	5.93948849	6.1039998	6.02174414	6.58504774	7.49352592	7.03928683	8.31048574	7.00764314	7.22651209	7.51488032	6.90075771	8.22036677	7.1304854	7.41720329	6.34372415	7.61533623	2.14907923	5.36937987
se	1.0067227	0.63810261	0.25382386	0.63288305	0.5399535	0.55490907	0.54743129	0.84312897	0.95944768	0.90128832	1.06404866	0.89723676	0.92526006	0.96218183	0.88355149	1.05251011	0.9129651	0.94967557	0.81223065	0.97504389	0.2751614	0.68747865
Δ47CO2	0.35558904	0.40041984	0.35079024	0.36893304	0.3899729	0.38526791	0.38762041	0.39908625	0.40473123	0.40190874	0.39940651	0.3880925	0.36621436	0.38457113	0.36991278	0.36292077	0.34456932	0.35913429	0.38224468	0.36371062	0.30254241	0.34949924
sd	0.0920868	0.10561191	0.09015671	0.09595181	0.10795272	0.0987186	0.10333566	0.10004412	0.10363878	0.10184145	0.09927691	0.08653262	0.09457763	0.09346239	0.11032054	0.10407408	0.09737579	0.10392347	0.09116635	0.08478929	0.09278842	0.08958135
se	0.01179051	0.00960108	0.01154338	0.01097832	0.00981388	0.00897442	0.00939415	0.01280934	0.01326959	0.01303946	0.01271111	0.01107937	0.01210942	0.01196663	0.0141251	0.01332532	0.01246769	0.01330604	0.01167265	0.01085616	0.01188034	0.01146972
Δ48CO2	9.70391287	18.6364584	9.90990303	12.7500915	10.8117322	10.3342264	10.5729793	10.2148006	9.92615363	10.0704771	10.0639557	10.7981057	10.1060514	10.3227043	11.8297132	10.7753228	12.066811	11.5572823	9.9019851	9.77431035	8.77340504	9.4832335
sd	0.55336786	1.03298115	0.55900811	0.71511904	0.57770959	0.64628127	0.61199543	0.63360111	0.58415273	0.60887692	0.56763718	0.57301275	0.58839998	0.57634997	0.4989118	0.54486776	0.54515978	0.52964645	0.71326271	0.61733622	0.45195196	0.59418363
se	0.07085149	0.09390738	0.07157365	0.07877751	0.05251905	0.05875284	0.05563595	0.08112431	0.07479309	0.0779587	0.07267849	0.07336676	0.0753369	0.07379405	0.06387911	0.06976317	0.06980056	0.06781428	0.09132393	0.0790418	0.05786652	0.07607742
Δ49CO2	-0.0421432	-0.0561217	-0.0362448	-0.0448366	-0.0505626	-0.0385118	-0.0445372	-0.0376503	-0.0510513	-0.0443508	-0.0377924	-0.0775624	-0.0446394	-0.0533314	-0.0483763	-0.0450655	-0.0516901	-0.0483773	-0.0541394	-0.0506591	-0.0098438	-0.0382141
sd	7.86275564	7.01912868	1.98242769	5.62143734	5.93948849	6.1039998	6.02174414	6.58504774	7.49352592	7.03928683	8.31048574	7.00764314	7.22651209	7.51488032	6.90075771	8.22036677	7.1304854	7.41720329	6.34372415	7.61533623	2.14907923	5.36937987
se	1.0067227	0.63810261	0.25382386	0.63288305	0.5399535	0.55490907	0.54743129	0.84312897	0.95944768	0.90128832	1.06404866	0.89723676	0.92526006	0.96218183	0.88355149	1.05251011	0.9129651	0.94967557	0.81223065	0.97504389	0.2751614	0.68747865

Run ID	C01890	C01934	Average	C02218	C02222	C02303	Average	C02197	C02201	C01527	Average	C01973	C02031	C02186	Average	C01753	C01933	C02365	C02366	Average	C02190	C02193	C01972	Average
Sample	GBB 903.3	GBB 903.3	GBB 903.3	GBB 902.27	GBB 902.27	GBB 902.27	GBB 902.27	GBB 902.05	GBB 902.05	Bahama 902	GBB 902.5	GBB 903.5	GBB 903.5	GBB 903.05	GBB 903.5	GBB.903.3	GBB 903.2	GBB 903.2	GBB 903.2	GBB 903.2	GBB 903.04	GBB 903.04	GBB 903.4	GBB 903.4
Date	09/12/13	09/27/13		01/05/14	01/06/14	02/09/14		12/30/13	12/31/13	04/12/13		10/10/13	11/05/13	12/26/13		07/15/13	09/27/13	02/25/14	02/25/14		12/27/13	12/28/13	10/10/13	
Block	20	10	11.5	10	10	10	10	10	10	20	13.3333333	10	10	10	10	20	10	10	10	15	10	10	10	10
CC	6	6	6	6	6	6	6	6	6	6	6	6	6	6	6	6	6	6	6	6	6	6	6	6
	0	0	0	0	0	0	0	0	0	0	0	0	0	0	0	0	0	0	0	0	0	0	0	0
δ13C	4.85507076	4.80042012	3.31385961	4.80119525	4.80712409	4.79622553	4.80151496	5.09480193	4.96444525	4.8061862	4.95514446	4.85380414	4.92963661	5.00382279	4.92908785	4.80045673	4.99154408	4.9674089	5.02674608	0.03606235	4.99603379	5.02745496	5.06629846	5.02992907
sd	0.00609787	0.0061376	0.00639661	0.00556628	0.00690826	0.00522089	0.00589848	0.00620784	0.00639611	0.00648325	0.0063624	0.00651607	0.00617777	0.006738	0.00647728	0.00589809	0.00632552	0.00551925	0.00424118	0.00581965	0.00675614	0.0064976	0.0059717	0.00640848
se	0.00055435	0.00078584	0.00081668	0.00071269	0.00088451	0.00066847	0.00075522	0.00079483	0.00081894	0.00058939	0.00073439	0.0008343	0.00079098	0.00086271	0.00082933	0.00053619	0.0008099	0.00070667	0.00054303	0.0006286	0.00086504	0.00083193	0.0007646	0.00082052
δ18O	8.28770248	8.32147589	7.33125011	7.9270183	7.96340864	7.96077495	7.95040063	8.66288113	8.59408193	8.45335182	8.57010496	8.3679985	8.54942183	8.43231505	8.44991179	8.17699801	8.24621466	8.23601769	8.36936927	4.73693187	8.33790001	8.45389178	8.28818036	8.35999072
Carbonate	0.33345732	0.36723073	-0.622995	-0.0272269	0.00916348	0.0065298	-0.0038445	0.70863597	0.63983678	0.49910667	0.6158598	0.41375334	0.59517667	0.47806989	0.49566664	0.22275285	0.29196951	0.28177253	0.41512411	-3.2173133	0.38365486	0.49964663	0.3339352	0.40574556
sd	0.01048397	0.00925467	0.01072694	0.00987671	0.00877176	0.01322172	0.0106234	0.00988822	0.01114361	0.0095653	0.01019904	0.00989823	0.00990065	0.00982298	0.00987395	0.01034001	0.01037828	0.01088968	0.00882991	0.01029112	0.01020713	0.01205943	0.01161493	0.01129383
se	0.00095309	0.00118494	0.00137139	0.00126458	0.00112311	0.00169287	0.00136019	0.00126606	0.00142679	0.00086957	0.00118747	0.00126734	0.00126765	0.0012577	0.00126423	0.00094	0.0013288	0.00139428	0.00113055	0.0011218	0.00130689	0.00154405	0.00148714	0.00144603
δ45CO2	7.70520888	7.65492829	6.2270077	7.64321235	7.64993082	7.63960819	7.64425045	7.94227761	7.81763359	7.66450553	7.80813891	7.70655174	7.7835212	7.84952762	7.77986685	7.65040504	7.83212101	7.80912359	7.86907924	3.06513439	7.83923144	7.87241136	7.90367887	7.87177389
sd	0.00609787	0.0061376	0.00639661	0.00556628	0.00690826	0.00522089	0.00589848	0.00620784	0.00639611	0.00648325	0.0063624	0.00651607	0.00617777	0.006738	0.00647728	0.00589809	0.00632552	0.00551925	0.00424118	0.00581965	0.00675614	0.0064976	0.0059717	0.00640848
se	0.00055435	0.00078584	0.00081668	0.00071269	0.00088451	0.00066847	0.00075522	0.00079483	0.00081894	0.00058939	0.00073439	0.0008343	0.00079098	0.00086271	0.00082933	0.00053619	0.0008099	0.00070667	0.00054303	0.0006286	0.00086504	0.00083193	0.0007646	0.00082052
δ46CO2	14.232093	14.2659171	13.2677944	13.8695436	13.9061232	13.9034541	13.8930403	14.6095931	14.5401889	14.3984461	14.516076	14.3127767	14.4952394	14.3777173	14.3952445	14.120737	14.1906868	14.1803901	14.3145131	10.6541191	14.2828272	14.399448	14.2330117	14.3050956
sd	0.01048397	0.00925467	0.01072694	0.00987671	0.00877176	0.01322172	0.0106234	0.00988822	0.01114361	0.0095653	0.01019904	0.00989823	0.00990065	0.00982298	0.00987395	0.01034001	0.01037828	0.01088968	0.00882991	0.01029112	0.01020713	0.01205943	0.01161493	0.01129383
se	0.00095309	0.00118494	0.00137139	0.00126458	0.00112311	0.00169287	0.00136019	0.00126606	0.00142679	0.00086957	0.00118747	0.00126734	0.00126765	0.0012577	0.00126423	0.00094	0.0013288	0.00139428	0.00113055	0.0011218	0.00130689	0.00154405	0.00148714	0.00144603
δ47CO2	22.5020753	22.4635922	19.7549991	22.0601783	22.0849628	22.0369715	22.0607042	23.1245228	22.9159336	22.5646439	22.8683667	22.5679751	22.8448683	22.7846757	22.7325064	22.3170919	22.5916013	22.5236579	22.7304499	13.7708759	22.654267	22.8225942	22.7083393	22.7284002
sd	0.08438288	0.08579337	0.0863708	0.08020287	0.10093303	0.10397408	0.09503666	0.08618433	0.09161092	0.10326798	0.09368774	0.09868856	0.10122907	0.11061224	0.10350995	0.11772871	0.07563055	0.07884445	0.09185099	0.09106389	0.09288514	0.09307646	0.09676567	0.09424242
se	0.00767117	0.01098471	0.01099436	0.01026893	0.01292315	0.01331252	0.0121682	0.01103477	0.01172958	0.009388	0.01071745	0.01263578	0.01296105	0.01416245	0.01325309	0.01070261	0.0096835	0.010095	0.01176031	0.00980279	0.01189272	0.01191722	0.01238957	0.01206651
δ48CO2	40.574281	39.7079259	37.3515617	38.3458231	38.043109	38.2177551	38.2022291	41.2520087	40.3381764	40.4545008	40.681562	39.5520945	40.348359	39.7360704	39.8788413	39.9114408	39.5255885	39.0993469	39.6637882	31.4749219	39.244549	39.6794617	39.0828751	39.3356286
sd	0.60161491	0.57320423	0.58027881	0.5953273	0.50674706	0.75350823	0.61852753	0.64528773	0.53692787	0.60423231	0.59548264	0.58819624	0.56919593	0.61770142	0.59169786	0.56358367	0.62040225	0.58912273	0.56545326	0.58380315	0.56664338	0.62474797	0.43693421	0.54277519
se	0.05469226	0.07339128	0.07347368	0.07622385	0.06488231	0.09647684	0.07919434	0.08262063	0.06874657	0.05493021	0.0687658	0.07531081	0.07287807	0.07908856	0.07575915	0.05123488	0.07943437	0.07542944	0.07239887	0.06405652	0.07255125	0.07999078	0.05594369	0.06949524
δ49CO2	-10.175061	-13.249053	-12.460379	-55.964853	-39.916063	-2.3637268	-32.748214	-76.776934	-76.225009	-23.603284	-58.868409	-17.193732	-8.0051086	-14.133056	-13.110632	-18.016331	-10.89622	-1.8234945	-1.9507089	-9.7560844	-11.455583	-15.437067	-11.008853	-12.633834
sd	5.12612018	8.39673629	8.50325172	8.13984716	6.24488061	2.05002214	5.47824997	7.00249391	6.7976918	7.8000917	7.20009247	9.0220865	7.00072853	6.03791572	7.35357692	6.9076842	10.2838026	2.00718666	1.97791237	7.08987457	6.65209564	6.83437115	10.6275311	8.0379993
se	0.46601093	1.07509192	1.12088274	1.04220063	0.79957503	0.26247844	0.70141803	0.89657747	0.87035525	0.70909925	0.82534399	1.15515981	0.89635144	0.77307589	0.94152905	0.62797129	1.31670599	0.25699392	0.25324573	0.73282951	0.85171357	0.87505156	1.36071593	1.02916035
Δ47CO2	0.42672323	0.40765275	0.18382445	0.40993333	0.39177535	0.35795574	0.38655481	0.42642922	0.4173292	0.36800221	0.40392021	0.41145324	0.4263679	0.4141121	0.41731108	0.40995747	0.42471341	0.39176683	0.40246102	0.02099743	0.38924364	0.40668953	0.4246095	0.40684756
sd	0.08438288	0.08579337	0.0863708	0.08020287	0.10093303	0.10397408	0.09503666	0.08618433	0.09161092	0.10326798	0.09368856	0.10122907	0.11061224	0.10350995	0.11772871	0.07563055	0.07884445	0.09185099	0.09106389	0.09288514	0.09307646	0.09676567	0.09424242
se	0.00767117	0.01098471	0.01099436	0.01026893	0.01292315	0.01331252	0.0121682	0.01103477	0.01172958	0.009388	0.01071745	0.01263578	0.01296105	0.01416245	0.01325309	0.01070261	0.0096835	0.010095	0.01176031	0.00980279	0.01189272	0.01191722	0.01238957	0.01206651
Δ48CO2	11.5757103	10.6660865	10.360715	10.1313938	9.76404092	9.93924643	9.94489371	11.4814588	10.7320265	11.1275521	11.1136791	10.4212421	10.8314876	10.4706701	10.5744666	11.1533658	10.6387613	10.2448771	10.5263473	9.7811522	10.1819704	10.3723646	10.1240386	10.2261245
sd	0.60161491	0.57320423	0.58027881	0.5953273	0.50674706	0.75350823	0.61852753	0.64528773	0.53692787	0.60423231	0.59548264	0.58819624	0.56919593	0.61770142	0.59169786	0.56358367	0.62040225	0.58912273	0.56545326	0.58380315	0.56664338	0.62474797	0.43693421	0.54277519
se	0.05469226	0.07339128	0.07347368	0.07622385	0.06488231	0.09647684	0.07919434	0.08262063	0.06874657	0.05493021	0.0687658	0.07531081	0.07287807	0.07908856	0.07575915	0.05123488	0.07943437	0.07542944	0.07239887	0.06405652	0.07255125	0.07999078	0.05594369	0.06949524
Δ49CO2	-0.0451537	-0.048131	-0.0440769	-0.0886246	-0.0732034	-0.0369376	-0.0662552	-0.1102766	-0.1095078	-0.058371	-0.0927184	-0.0520741	-0.043628	-0.0493853	-0.0483624	-0.0524583	-0.0459004	-0.0371062	-0.0375403	-0.0330918	-0.0466176	-0.0507056	-0.0461594	-0.0478275
sd	5.12612018	8.39673629	8.50325172	8.13984716	6.24488061	2.05002214	5.47824997	7.00249391	6.7976918	7.8000917	7.20009247	9.0220865	7.00072853	6.03791572	7.35357692	6.9076842	10.2838026	2.00718666	1.97791237	7.08987457	6.65209564	6.83437115	10.6275311	8.0379993
se	0.46601093	1.07509192	1.12088274	1.04220063	0.79957503	0.26247844	0.70141803	0.89657747	0.87035525	0.70909925	0.82534399	1.15515981	0.89635144	0.77307589	0.94152905	0.62797129	1.31670599	0.25699392	0.25324573	0.73282951	0.85171357	0.87505156	1.36071593	1.02916035

Run ID	C02203	C02206	C01586	Average	C02217	C02221	C02288	Average	C02195	C02199	C01585	Average	C02219	C02223	C02287	Average
Sample	GBB 902.46	GBB 902.46	GBB 902.46	GBB 902.46	GBB 902.52	GBB 902.52	GBB 902.52	GBB 902.52	GBB 902.39	GBB 902.39	GBB 902.39	GBB 902.39	GBB 902.41	GBB 902.41	GBB 902.41	GBB 902.41
Date	01/01/14	01/02/14	05/06/13		01/05/14	01/06/14	02/06/14		12/30/13	12/31/13	05/06/13		01/05/14	01/06/14	02/06/14	
Block	10	10	20	13.3333333	10	10	10	10	10	10	13	11	10	10	10	10
CC	6	6	6	6	6	6	6	6	6	6	6	6	6	6	6	6
	0	0	0	0	0	0	0	0	0	0	0	0	0	0	0	0
δ13C	4.86724107	4.89623608	4.72026189	4.82791301	4.33330402	4.35202383	4.30614308	4.33049031	3.40472068	3.37385994	3.37735089	3.3853105	3.67390302	3.6469421	3.61584168	3.64556227
sd	0.00627017	0.00622797	0.00739054	0.00662956	0.00608077	0.00656999	0.00580194	0.0061509	0.00537319	0.00613797	0.00544756	0.00565291	0.00666061	0.0055979	0.00671147	0.00632332
se	0.00080281	0.00079741	0.00067187	0.00075736	0.00077856	0.0008412	0.00074286	0.00078754	0.00068797	0.00078589	0.0006129	0.00069558	0.0008528	0.00071674	0.00085932	0.00080962
δ18O	7.87189439	7.85529607	7.82582395	7.8510048	7.77264757	7.78408852	7.77509206	7.77727605	7.69465202	7.59699871	7.44401506	7.57855526	7.80669629	7.77728772	7.80390088	7.79596163
Carbonate	-0.0823508	-0.0989491	-0.1284212	-0.1032404	-0.1815976	-0.1701566	-0.1791531	-0.1769691	-0.2595931	-0.3572464	-0.5102301	-0.3756899	-0.1475489	-0.1769574	-0.1503443	-0.1582835
sd	0.00971113	0.01137658	0.01159864	0.01089545	0.01168295	0.01005572	0.01200453	0.01124773	0.00933316	0.01089606	0.01097019	0.0103998	0.01108737	0.01119273	0.00918556	0.01048855
se	0.00124338	0.00145662	0.00105442	0.00125148	0.00149585	0.0012875	0.00153702	0.00144012	0.00119499	0.0013951	0.00123424	0.00127478	0.00141959	0.00143308	0.00117609	0.00134292
δ45CO2	7.70352521	7.73024321	7.56398015	7.66591619	7.19874348	7.21669231	7.17330207	7.19624595	6.32384983	6.29177375	6.29022589	6.30194982	6.5802903	6.55403176	6.52565168	6.55332458
sd	0.00627017	0.00622797	0.00739054	0.00662956	0.00608077	0.00656999	0.00580194	0.0061509	0.00537319	0.00613797	0.00544756	0.00565291	0.00666061	0.0055979	0.00671147	0.00632332
se	0.00080281	0.00079741	0.00067187	0.00075736	0.00077856	0.0008412	0.00074286	0.00078754	0.00068797	0.00078589	0.0006129	0.00069558	0.0008528	0.00071674	0.00085932	0.00080962
δ46CO2	13.8142888	13.79767	13.7676894	13.793216	13.7134514	13.7249868	13.7158514	13.7180966	13.6331497	13.5349578	13.3812379	13.5164485	13.7462972	13.7166897	13.7433677	13.7354515
sd	0.00971113	0.01137658	0.01159864	0.01089545	0.01168295	0.01005572	0.01200453	0.01124773	0.00933316	0.01089606	0.01097019	0.0103998	0.01108737	0.01119273	0.00918556	0.01048855
se	0.00124338	0.00145662	0.00105442	0.00125148	0.00149585	0.0012875	0.00153702	0.00144012	0.00119499	0.0013951	0.00123424	0.00127478	0.00141959	0.00143308	0.00117609	0.00134292
δ47CO2	22.0322418	22.0717629	21.8125598	21.9721882	21.3842762	21.4040125	21.3213144	21.3698677	20.4064948	20.2603002	20.038975	20.2352567	20.7752123	20.6872519	20.6552308	20.7058983
sd	0.0963609	0.10640501	0.11941516	0.10739369	0.10388824	0.09806151	0.08601978	0.09598984	0.097297	0.11992327	0.08770437	0.10164155	0.10861113	0.09753999	0.09118105	0.09911073
se	0.01233775	0.01362377	0.01085592	0.01227248	0.01330153	0.01255549	0.0110137	0.01229024	0.0124576	0.0153546	0.00986751	0.01255991	0.01390623	0.01248872	0.01167454	0.01268983
δ48CO2	37.9573974	38.047124	38.8305441	38.2783552	37.4673939	37.4874084	37.4345688	37.4631237	38.3615905	37.0267546	37.2357583	37.5413678	37.5234023	37.1747494	37.50281	37.4003206
sd	0.59945457	0.51060957	0.62753739	0.57920051	0.52601354	0.66594368	0.55028691	0.58074804	0.70976081	0.56615543	0.68485408	0.6535901	0.50856725	0.62516398	0.58506709	0.57293277
se	0.07675229	0.06537686	0.05704885	0.06639267	0.06734913	0.08526535	0.07045702	0.07435717	0.09087556	0.07248877	0.0770521	0.08013881	0.06511536	0.08004405	0.07491016	0.07335652
δ49CO2	-8.9493303	-27.900302	-22.906654	-19.918762	-3.4721085	-9.8886216	-0.4321399	-4.5976233	-8.2866049	-8.2630539	-31.737664	-16.095774	-12.322383	-14.00089	-0.4816287	-8.9349674
sd	5.85589244	6.31702639	8.57616736	6.91636207	9.17060345	7.6890172	2.14540325	6.33500797	5.13693889	6.82949305	8.71398592	6.89347262	8.98761868	7.47537628	2.25192089	6.23830528
se	0.7497702	0.80881235	0.77965158	0.77941138	1.17417545	0.98447777	0.27469074	0.81111465	0.65771763	0.87442698	0.98040001	0.83751487	1.15074665	0.95712386	0.28832892	0.79873314
Δ47CO2	0.37458219	0.40208441	0.34757092	0.37474584	0.35462774	0.34437819	0.31666691	0.33855761	0.37036125	0.35532087	0.28929888	0.338327	0.3591573	0.32861631	0.30037368	0.32938243
sd	0.0963609	0.10640501	0.11941516	0.10739369	0.10388824	0.09806151	0.08601978	0.09598984	0.097297	0.11992327	0.08770437	0.10164155	0.10861113	0.09753999	0.09118105	0.09911073
se	0.01233775	0.01362377	0.01085592	0.01227248	0.01330153	0.01255549	0.0110137	0.01229024	0.0124576	0.0153546	0.00986751	0.01255991	0.01390623	0.01248872	0.01167454	0.01268983
Δ48CO2	9.86359332	9.98400352	10.8060262	10.2178744	9.58767246	9.58417218	9.55094892	9.57426452	10.6179385	9.5143443	10.0241554	10.0521461	9.57674562	9.29643801	9.56254232	9.47857532
sd	0.59945457	0.51060957	0.62753739	0.57920051	0.52601354	0.66594368	0.55028691	0.58074804	0.70976081	0.56615543	0.68485408	0.6535901	0.50856725	0.62516398	0.58506709	0.57293277
se	0.07675229	0.06537686	0.05704885	0.06639267	0.06734913	0.08526535	0.07045702	0.07435717	0.09087556	0.07248877	0.0770521	0.08013881	0.06511536	0.08004405	0.07491016	0.07335652
Δ49CO2	-0.0431938	-0.0614861	-0.0564446	-0.0537082	-0.0372048	-0.0434436	-0.0342463	-0.0382982	-0.0408211	-0.0405829	-0.0630113	-0.0481385	-0.0451931	-0.0467345	-0.0336851	-0.0418709
sd	5.85589244	6.31702639	8.57616736	6.91636207	9.17060345	7.6890172	2.14540325	6.33500797	5.13693889	6.82949305	8.71398592	6.89347262	8.98761868	7.47537628	2.25192089	6.23830528
se	0.7497702	0.80881235	0.77965158	0.77941138	1.17417545	0.98447777	0.27469074	0.81111465	0.65771763	0.87442698	0.98040001	0.83751487	1.15074665	0.95712386	0.28832892	0.79873314

APPENDIX 2.Clumped isotope data of the Tobago project

Run ID	C02472	C02719	Average	C02373	C02480	Average	C02374	C02717	C02734	Average	C02380	C02710	C02718	Average	C02381	C02535	C02735	Average	C02387	C02736
Sample	TC 01.01	TC 01.01	TC 01.01	TC 01.02	TC 01.02	TC 01.02	TC 01.03	TC 01.03	TC 01.03	TC 01.03	TC 01.04	TC 01.04	TC 01.04	TC 01.04	TC 01.05	TC 01.05	TC 01.05	TC 01.05	TC 02.01	TC 02.01
Date	03/15/14	05/27/14		02/26/14	03/16/14		02/26/14	05/27/14	05/30/14		02/27/14	05/26/14	05/27/14		02/27/14	03/24/14	05/30/14		02/28/14	05/30/14
Block	20	10	15	10	10	10	10	10	10	10	10	10	10	10	10	10	10	10	10	5
CC	6	6	6	6	6	6	6	6	6	6	6	6	6	6	6	6	6	6	6	6
	0	0	0	0	0	0	0	0	0	0	0	0	0	0	0	0	0	0	0	0
δ13C	-0.70835	-0.72113	-0.71474	-0.80684	-0.86406	-0.83545	-0.82635	-0.6221	-0.69478	-0.71441	-1.25409	-1.32324	-1.3565	-1.31128	-0.86426	-0.89157	-0.79378	-0.84987	-0.93171	-0.83835
sd	0.006607	0.005936	0.006272	0.005865	0.006048	0.005957	0.005242	0.004876	0.005396	0.005171	0.004724	0.004117	0.00498	0.004607	0.005793	0.00579	0.005691	0.005758	0.005999	0.004999
se	0.000601	0.00076	0.00068	0.000751	0.000774	0.000763	0.000671	0.000624	0.000691	0.00066	0.000605	0.000527	0.000638	0.00059	0.000742	0.000741	0.000729	0.000737	0.000768	0.000898
δ18O	3.911513	4.09061	4.001062	4.105938	4.017952	4.061945	4.124072	4.241282	4.130081	4.165145	3.773272	3.784213	3.816079	3.791188	3.975941	4.001376	4.099694	4.02567	3.992717	3.921349
Carbonate	-4.04273	-3.86363	-3.95318	-3.84831	-3.93629	-3.8923	-3.83017	-3.71296	-3.82416	-3.7891	-4.18097	-4.17003	-4.13817	-4.16306	-3.9783	-3.95287	-3.85455	-3.92858	-3.96153	-4.0329
sd	0.009396	0.009656	0.009526	0.009436	0.009841	0.009638	0.009525	0.00927	0.00896	0.009252	0.008905	0.010374	0.008629	0.009303	0.011338	0.011857	0.009465	0.010887	0.009586	0.010204
se	0.000854	0.001236	0.001045	0.001208	0.00126	0.001234	0.00122	0.001187	0.001147	0.001185	0.00114	0.001328	0.001105	0.001191	0.001452	0.001518	0.001212	0.001394	0.001227	0.001833
δ45CO2	2.340005	2.33366	2.336832	2.253621	2.197077	2.225349	2.235866	2.431464	2.359664	2.342331	1.822896	1.758276	1.728037	1.769736	2.195563	2.170706	2.265689	2.210653	2.132724	2.218179
sd	0.006607	0.005936	0.006272	0.005865	0.006048	0.005957	0.005242	0.004876	0.005396	0.005171	0.004724	0.004117	0.00498	0.004607	0.005793	0.00579	0.005691	0.005758	0.005999	0.004999
se	0.000601	0.00076	0.00068	0.000751	0.000774	0.000763	0.000671	0.000624	0.000691	0.00066	0.000605	0.000527	0.000638	0.00059	0.000742	0.000741	0.000729	0.000737	0.000768	0.000898
δ46CO2	9.823102	10.00304	9.913072	10.01827	9.929735	9.974001	10.03645	10.15465	10.04276	10.07795	9.683058	9.69391	9.725861	9.700943	9.887519	9.913022	10.01202	9.93752	9.904237	9.832716
sd	0.009396	0.009656	0.009526	0.009436	0.009841	0.009638	0.009525	0.00927	0.00896	0.009252	0.008905	0.010374	0.008629	0.009303	0.011338	0.011857	0.009465	0.010887	0.009586	0.010204
se	0.000854	0.001236	0.001045	0.001208	0.00126	0.001234	0.00122	0.001187	0.001147	0.001185	0.00114	0.001328	0.001105	0.001191	0.001452	0.001518	0.001212	0.001394	0.001227	0.001833
δ47CO2	12.18964	12.28048	12.23506	12.30826	12.15146	12.22986	12.30733	12.55271	12.3707	12.41025	11.49888	11.33413	11.35662	11.39654	12.10464	12.11704	12.23711	12.15293	12.07687	12.00487
sd	0.094244	0.084277	0.089261	0.080101	0.076232	0.078166	0.086453	0.093531	0.081923	0.087302	0.088316	0.078924	0.084336	0.083859	0.086063	0.084664	0.083836	0.084854	0.075191	0.0824
se	0.008568	0.010791	0.009679	0.010256	0.00976	0.010008	0.011069	0.011975	0.010489	0.011178	0.011308	0.010105	0.010798	0.010737	0.011019	0.01084	0.010734	0.010864	0.009627	0.014799
δ48CO2	26.93474	25.21841	26.07657	27.86018	27.56478	27.71248	27.46099	25.55196	25.30803	26.10699	26.52371	24.32762	24.45991	25.10375	27.20711	27.66485	25.22267	26.69821	27.25131	24.86557
sd	0.607582	0.479583	0.543582	0.617063	0.567319	0.592191	0.585505	0.405057	0.542709	0.51109	0.6138	0.57515	0.426051	0.538334	0.632764	0.522178	0.524792	0.559911	0.530307	0.535892
se	0.055235	0.061404	0.058319	0.079007	0.072638	0.075822	0.074966	0.051862	0.069487	0.065438	0.078589	0.07364	0.05455	0.068927	0.081017	0.066858	0.067193	0.071689	0.067899	0.096249
δ49CO2	-0.41617	-0.90297	-0.65957	-9.54377	-2.03713	-5.79045	-1.1344	-0.95722	-10.7068	-4.26612	-1.2792	2.607651	-1.49593	-0.05583	-1.32003	-0.1865	-1.24171	-0.91608	-0.57983	-0.96207
sd	2.353969	1.821839	2.087904	1.90619	1.773531	1.839861	1.855541	1.656642	2.735549	2.082577	2.209147	1.659578	1.719626	1.862783	1.97038	1.911266	1.919662	1.933769	2.073628	1.860698
se	0.213997	0.233263	0.22363	0.244063	0.227077	0.23557	0.237578	0.212111	0.350251	0.266647	0.282852	0.212487	0.220176	0.238505	0.252281	0.244713	0.245787	0.247594	0.265501	0.334191
Δ47CO2	0.081291	0.002101	0.041696	0.096996	0.086555	0.091776	0.09661	0.022634	0.025768	0.048337	0.066989	-0.04001	-0.01782	0.003052	0.083017	0.095961	0.020384	0.066454	0.103894	0.014608
sd	0.094244	0.084277	0.089261	0.080101	0.076232	0.078166	0.086453	0.093531	0.081923	0.087302	0.088316	0.078924	0.084336	0.083859	0.086063	0.084664	0.083836	0.084854	0.075191	0.0824
se	0.008568	0.010791	0.009679	0.010256	0.00976	0.010008	0.011069	0.011975	0.010489	0.011178	0.011308	0.010105	0.010798	0.010737	0.011019	0.01084	0.010734	0.010864	0.009627	0.014799
Δ48CO2	7.052775	5.01148	6.032127	7.570798	7.457839	7.514319	7.143235	5.036705	5.020291	5.73341	6.92897	4.753202	4.819361	5.500511	7.191373	7.589301	4.997787	6.59282	7.201364	5.004528
sd	0.607582	0.479583	0.543582	0.617063	0.567319	0.592191	0.585505	0.405057	0.542709	0.51109	0.6138	0.57515	0.426051	0.538334	0.632764	0.522178	0.524792	0.559911	0.530307	0.535892
se	0.055235	0.061404	0.058319	0.079007	0.072638	0.075822	0.074966	0.051862	0.069487	0.065438	0.078589	0.07364	0.05455	0.068927	0.081017	0.066858	0.067193	0.071689	0.067899	0.096249
Δ49CO2	-0.0219	-0.02271	-0.02231	-0.03111	-0.02354	-0.02733	-0.0229	-0.02315	-0.0324	-0.02615	-0.02194	-0.01809	-0.02214	-0.02072	-0.02276	-0.02167	-0.02299	-0.02247	-0.022	-0.02233
sd	2.353969	1.821839	2.087904	1.90619	1.773531	1.839861	1.855541	1.656642	2.735549	2.082577	2.209147	1.659578	1.719626	1.862783	1.97038	1.911266	1.919662	1.933769	2.073628	1.860698
se	0.213997	0.233263	0.22363	0.244063	0.227077	0.23557	0.237578	0.212111	0.350251	0.266647	0.282852	0.212487	0.220176	0.238505	0.252281	0.244713	0.245787	0.247594	0.265501	0.334191

Run ID	C02577	Average	C02388	C02578	Average	C02397	C02579	Average	C02435	C02580	C02668	Average	C02400	C02441	C02582	Average	C02401	C02442	C02709	Average
Sample	TC 02.01	TC 02.01	TC 02.02	TC 02.02	TC 02.02	TC 02.03	TC 02.03	TC 02.03	TC 02.04	TC 02.04	TC 02.04	TC 02.04	TC 02.05	TC 02.05	TC 02.05	TC 02.05	TC 03.01	TC 03.01	TC 03.01	TC 03.01
Date	03/30/14		02/28/14	03/30/14		03/03/14	03/30/14		03/09/14	03/30/14	05/18/14		03/03/14	03/11/14	03/31/14		03/03/14	03/11/14	05/26/14	
Block	10	8.333333	10	10	10	10	10	10	10	10	10	10	10	10	10	10	10	10	8	9.333333
CC	6	6	6	6	6	6	6	6	6	6	6	6	6	6	6	6	6	6	6	6
	0	0	0	0	0	0	0	0	0	0	0	0	0	0	0	0	0	0	0	0
δ13C	-0.75653	-0.84219	-1.02522	-0.90803	-0.96662	-0.77788	-0.87018	-0.82403	-1.06587	-1.0341	-0.96653	-1.02217	-1.08739	-1.11527	-1.14082	-1.11449	-1.0155	-1.03598	-1.00917	-1.02022
sd	0.004955	0.005317	0.005086	0.004673	0.00488	0.004923	0.004743	0.004833	0.005243	0.004701	0.004696	0.00488	0.006388	0.006048	0.005006	0.005814	0.006185	0.005245	0.006098	0.005843
se	0.000634	0.000767	0.000651	0.000598	0.000625	0.00063	0.000607	0.000619	0.000671	0.000602	0.000601	0.000625	0.000818	0.000774	0.000641	0.000744	0.000792	0.000672	0.000871	0.000778
δ18O	4.047788	3.987285	3.943261	3.986668	3.964965	4.02489	4.012535	4.018712	3.907118	3.932776	3.951588	3.930494	3.935623	3.926284	3.913141	3.925016	3.976001	4.023958	4.037751	4.01257
Carbonate	-3.90646	-3.96696	-4.01098	-3.96758	-3.98928	-3.92936	-3.94171	-3.93553	-4.04713	-4.02147	-4.00266	-4.02375	-4.01862	-4.02796	-4.0411	-4.02923	-3.97824	-3.93029	-3.91649	-3.94168
sd	0.009223	0.009671	0.008443	0.009614	0.009029	0.010137	0.007849	0.008993	0.009908	0.010584	0.010424	0.010305	0.007722	0.009904	0.009034	0.008886	0.008897	0.010742	0.007193	0.008944
se	0.001181	0.001414	0.001081	0.001231	0.001156	0.001298	0.001005	0.001151	0.001269	0.001355	0.001335	0.001319	0.000989	0.001268	0.001157	0.001138	0.001139	0.001375	0.001028	0.001181
δ45CO2	2.29905	2.216651	2.043304	2.154778	2.099041	2.27827	2.19116	2.234715	2.003964	2.034624	2.098708	2.045766	1.98465	1.958163	1.93374	1.958851	2.053471	2.035744	2.061366	2.050194
sd	0.004955	0.005317	0.005086	0.004673	0.00488	0.004923	0.004743	0.004833	0.005243	0.004701	0.004696	0.00488	0.006388	0.006048	0.005006	0.005814	0.006185	0.005245	0.006098	0.005843
se	0.000634	0.000767	0.000651	0.000598	0.000625	0.00063	0.000607	0.000619	0.000671	0.000602	0.000601	0.000625	0.000818	0.000774	0.000641	0.000744	0.000792	0.000672	0.000871	0.000778
δ46CO2	9.959939	9.898964	9.854348	9.898209	9.876278	9.936885	9.924279	9.930582	9.817945	9.843794	9.862836	9.841525	9.846544	9.837102	9.823842	9.835829	9.887266	9.935415	9.94933	9.924004
sd	0.009223	0.009671	0.008443	0.009614	0.009029	0.010137	0.007849	0.008993	0.009908	0.010584	0.010424	0.010305	0.007722	0.009904	0.009034	0.008886	0.008897	0.010742	0.007193	0.008944
se	0.001181	0.001414	0.001081	0.001231	0.001156	0.001298	0.001005	0.001151	0.001269	0.001355	0.001335	0.001319	0.000989	0.001268	0.001157	0.001138	0.001139	0.001375	0.001028	0.001181
δ47CO2	12.29944	12.12706	11.9021	12.0779	11.99	12.26235	12.14647	12.20441	11.82872	11.9034	11.88185	11.87132	11.83333	11.79468	11.7742	11.80074	11.94318	11.99699	11.96348	11.96788
sd	0.077801	0.078464	0.085639	0.093809	0.089724	0.076312	0.076215	0.076264	0.097333	0.095992	0.092386	0.095237	0.08176	0.091053	0.089224	0.087346	0.092666	0.100506	0.108484	0.100552
se	0.009961	0.011463	0.010965	0.012011	0.011488	0.009771	0.009758	0.009765	0.012462	0.012291	0.011829	0.012194	0.010468	0.011658	0.011424	0.011183	0.011865	0.012868	0.015498	0.01341
δ48CO2	27.91853	26.67847	26.88355	27.68316	27.28336	27.46497	27.50109	27.48303	27.631	27.35994	24.38496	26.45864	27.06865	28.12798	27.31061	27.50241	27.25128	28.19451	25.11186	26.85255
sd	0.547002	0.537734	0.546708	0.530744	0.538726	0.573108	0.619136	0.596122	0.543981	0.594747	0.530852	0.556527	0.484621	0.607955	0.644434	0.579003	0.640861	0.614006	0.529524	0.594797
se	0.070036	0.078061	0.069999	0.067955	0.068977	0.073379	0.079272	0.076326	0.06965	0.07615	0.067969	0.071256	0.062049	0.077841	0.082511	0.074134	0.082054	0.078615	0.075646	0.078772
δ49CO2	-4.58567	-2.04252	-1.32591	-6.1555	-3.7407	-1.29829	-1.76396	-1.53112	-1.39208	-3.34754	5.379483	0.213289	-1.34663	-1.28304	-1.31011	-1.31326	-1.55886	-1.94424	-1.42096	-1.64135
sd	1.781819	1.905381	1.938669	1.841242	1.889955	2.073372	1.722306	1.897839	1.589109	2.060812	1.561581	1.737167	2.050438	1.810675	1.644733	1.835282	2.070076	1.643538	1.511139	1.741584
se	0.228139	0.275944	0.248221	0.235747	0.241984	0.265468	0.220519	0.242993	0.203464	0.26386	0.19994	0.222421	0.262532	0.231833	0.210587	0.234984	0.265046	0.210433	0.215877	0.230452
Δ47CO2	0.098441	0.072314	0.071797	0.088111	0.079954	0.105647	0.093031	0.099339	0.075239	0.092308	-0.01347	0.051357	0.071775	0.070019	0.087835	0.076543	0.069838	0.094295	0.02126	0.061798
sd	0.077801	0.078464	0.085639	0.093809	0.089724	0.076312	0.076215	0.076264	0.097333	0.095992	0.092386	0.095237	0.08176	0.091053	0.089224	0.087346	0.092666	0.100506	0.108484	0.100552
se	0.009961	0.011463	0.010965	0.012011	0.011488	0.009771	0.009758	0.009765	0.012462	0.012291	0.011829	0.012194	0.010468	0.011658	0.011424	0.011183	0.011865	0.012868	0.015498	0.01341
Δ48CO2	7.744392	6.650095	6.940263	7.636817	7.28854	7.345726	7.406282	7.376004	7.745852	7.428461	4.473316	6.54921	7.137331	8.194962	7.419892	7.584062	7.235182	8.063905	5.01392	6.771003
sd	0.547002	0.537734	0.546708	0.530744	0.538726	0.573108	0.619136	0.596122	0.543981	0.594747	0.530852	0.556527	0.484621	0.607955	0.644434	0.579003	0.640861	0.614006	0.529524	0.594797
se	0.070036	0.078061	0.069999	0.067955	0.068977	0.073379	0.079272	0.076326	0.06965	0.07615	0.067969	0.071256	0.062049	0.077841	0.082511	0.074134	0.082054	0.078615	0.075646	0.078772
Δ49CO2	-0.0262	-0.02351	-0.02254	-0.02747	-0.025	-0.02292	-0.02326	-0.02309	-0.0225	-0.02449	-0.01605	-0.02101	-0.02249	-0.02238	-0.02235	-0.02241	-0.02284	-0.02329	-0.02283	-0.02299
sd	1.781819	1.905381	1.938669	1.841242	1.889955	2.073372	1.722306	1.897839	1.589109	2.060812	1.561581	1.737167	2.050438	1.810675	1.644733	1.835282	2.070076	1.643538	1.511139	1.741584
se	0.228139	0.275944	0.248221	0.235747	0.241984	0.265468	0.220519	0.242993	0.203464	0.26386	0.19994	0.222421	0.262532	0.231833	0.210587	0.234984	0.265046	0.210433	0.215877	0.230452

Run ID	C02402	C02443	Average	C02542	Average	C02450	C02585	Average	C02406	C02451	C02591	Average	C02407	C02457	C02592	Average	C02408	C02458	C02693	Average
Sample	TC 03.02	TC 03.02	TC 03.02	TC 03.03	TC 03.03	TC 03.04	TC 03.04	TC 03.04	TC 03.05	TC 03.05	TC 03.05	TC 03.05	TC 04.01	TC 04.01	TC 04.01	TC 04.01	TC 04.02	TC 04.02	TC 04.02	TC 04.02
Date	03/03/14	03/11/14		03/25/14	03/25/14	03/12/14	03/31/14		03/04/14	03/12/14	04/01/14		03/04/14	03/13/14	04/01/14		03/04/14	03/13/14	05/22/14	
Block	10	10	10	10	10	10	10	10	10	10	10	10	10	10	10	10	10	10	10	10
CC	6	6	6	6	6	6	6	6	6	6	6	6	6	6	6	6	6	6	6	6
	0	0	0	0	0	0	0	0	0	0	0	0	0	0	0	0	0	0	0	0
δ13C	-0.87115	-0.87449	-0.87282	-0.79367	-0.79367	-1.04442	-0.9093	-0.97686	-0.82668	-0.83602	-0.8204	-0.8277	-0.98516	-0.755	-0.92948	-0.88988	-0.72868	-0.76847	-0.63786	-0.71167
sd	0.004944	0.005901	0.005423	0.005298	0.005298	0.005309	0.004504	0.004906	0.005632	0.005153	0.006263	0.005683	0.004734	0.005821	0.004898	0.005151	0.006291	0.005994	0.005625	0.00597
se	0.000633	0.000756	0.000694	0.000678	0.000678	0.00068	0.000577	0.000628	0.000721	0.00066	0.000802	0.000728	0.000606	0.000745	0.000627	0.000659	0.000806	0.000767	0.00072	0.000764
δ18O	3.957883	3.917401	3.937642	4.136086	4.136086	3.930894	3.851874	3.891384	4.116299	4.145985	4.125892	4.129392	4.04156	4.025726	4.032354	4.033213	4.136561	4.049858	4.02262	4.06968
Carbonate	-3.99636	-4.03684	-4.0166	-3.81816	-3.81816	-4.02335	-4.10237	-4.06286	-3.83795	-3.80826	-3.82835	-3.82485	-3.91269	-3.92852	-3.92189	-3.92103	-3.81768	-3.90439	-3.93163	-3.88457
sd	0.008892	0.009285	0.009088	0.009234	0.009234	0.008895	0.009809	0.009352	0.008957	0.009454	0.010027	0.009479	0.007826	0.009522	0.008787	0.008712	0.009018	0.00974	0.009765	0.009507
se	0.001138	0.001189	0.001164	0.001182	0.001182	0.001139	0.001256	0.001197	0.001147	0.001211	0.001284	0.001214	0.001002	0.001219	0.001125	0.001115	0.001155	0.001247	0.00125	0.001217
δ45CO2	2.188522	2.1841	2.186311	2.266949	2.266949	2.024875	2.149324	2.087099	2.235304	2.227471	2.241505	2.23476	2.084051	2.299786	2.13607	2.173302	2.32802	2.287893	2.40975	2.341888
sd	0.004944	0.005901	0.005423	0.005298	0.005298	0.005309	0.004504	0.004906	0.005632	0.005153	0.006263	0.005683	0.004734	0.005821	0.004898	0.005151	0.006291	0.005994	0.005625	0.00597
se	0.000633	0.000756	0.000694	0.000678	0.000678	0.00068	0.000577	0.000628	0.000721	0.00066	0.000802	0.000728	0.000606	0.000745	0.000627	0.000659	0.000806	0.000767	0.00072	0.000764
δ46CO2	9.86936	9.828674	9.849017	10.04859	10.04859	9.84188	9.762757	9.802318	10.02864	10.05845	10.03829	10.04179	9.953207	9.937773	9.944072	9.945017	10.0492	9.961995	9.934894	9.98203
sd	0.008892	0.009285	0.009088	0.009234	0.009234	0.008895	0.009809	0.009352	0.008957	0.009454	0.010027	0.009479	0.007826	0.009522	0.008787	0.008712	0.009018	0.00974	0.009765	0.009507
se	0.001138	0.001189	0.001164	0.001182	0.001182	0.001139	0.001256	0.001197	0.001147	0.001211	0.001284	0.001214	0.001002	0.001219	0.001125	0.001115	0.001155	0.001247	0.00125	0.001217
δ47CO2	12.0611	12.01728	12.03919	12.34085	12.34085	11.85105	11.92821	11.88963	12.26774	12.30198	12.30438	12.29137	12.04884	12.26699	12.07556	12.13046	12.39872	12.29416	12.33508	12.34265
sd	0.104921	0.08969	0.097305	0.081221	0.081221	0.08094	0.088784	0.084862	0.073011	0.078052	0.087666	0.079576	0.07593	0.073897	0.098619	0.082815	0.087766	0.094559	0.075101	0.085809
se	0.013434	0.011484	0.012459	0.010399	0.010399	0.010363	0.011368	0.010865	0.009348	0.009994	0.011224	0.010189	0.009722	0.009462	0.012627	0.010603	0.011237	0.012107	0.009616	0.010987
δ48CO2	27.09582	27.77642	27.43612	27.83984	27.83984	27.27255	26.95148	27.11202	27.63774	27.98416	27.59394	27.73861	27.31686	27.35377	27.29622	27.32228	27.74521	27.59985	25.58524	26.97677
sd	0.625854	0.509826	0.56784	0.58459	0.58459	0.480834	0.59789	0.539362	0.608201	0.517926	0.590694	0.572274	0.546081	0.512874	0.54562	0.534858	0.597401	0.560323	0.454747	0.537491
se	0.080132	0.065277	0.072704	0.074849	0.074849	0.061564	0.076552	0.069058	0.077872	0.066314	0.075631	0.073272	0.069918	0.065667	0.06986	0.068482	0.076489	0.071742	0.058224	0.068819
δ49CO2	-1.33566	-2.06316	-1.69941	-1.78098	-1.78098	-1.38196	-4.20758	-2.79477	-1.03265	-1.11738	-0.98701	-1.04568	-2.00981	-0.75208	0.206935	-0.85165	-4.14094	-1.54843	-3.10856	-2.93264
sd	2.132122	2.111651	2.121887	1.573585	1.573585	1.743411	1.664316	1.703864	1.966032	1.839261	1.965284	1.923526	2.320205	1.911792	2.013571	2.081856	2.179377	1.884171	1.553935	1.872494
se	0.27299	0.270369	0.27168	0.201477	0.201477	0.223221	0.213094	0.218157	0.251725	0.235493	0.251629	0.246282	0.297072	0.24478	0.257811	0.266554	0.279041	0.241243	0.198961	0.239748
Δ47CO2	0.06494	0.065857	0.065399	0.085922	0.085922	0.052463	0.077886	0.065174	0.065696	0.078509	0.086097	0.076767	0.078501	0.08724	0.060318	0.075353	0.079697	0.102697	0.044256	0.07555
sd	0.104921	0.08969	0.097305	0.081221	0.081221	0.08094	0.088784	0.084862	0.073011	0.078052	0.087666	0.079576	0.07593	0.073897	0.098619	0.082815	0.087766	0.094559	0.075101	0.085809
se	0.013434	0.011484	0.012459	0.010399	0.010399	0.010363	0.011368	0.010865	0.009348	0.009994	0.011224	0.010189	0.009722	0.009462	0.012627	0.010603	0.011237	0.012107	0.009616	0.010987
Δ48CO2	7.118467	7.867038	7.492753	7.49037	7.49037	7.346577	7.18957	7.268073	7.332072	7.612159	7.269879	7.404703	7.167958	7.234926	7.165939	7.189608	7.396397	7.42787	5.506765	6.777011
sd	0.625854	0.509826	0.56784	0.58459	0.58459	0.480834	0.59789	0.539362	0.608201	0.517926	0.590694	0.572274	0.546081	0.512874	0.54562	0.534858	0.597401	0.560323	0.454747	0.537491
se	0.080132	0.065277	0.072704	0.074849	0.074849	0.061564	0.076552	0.069058	0.077872	0.066314	0.075631	0.073272	0.069918	0.065667	0.06986	0.068482	0.076489	0.071742	0.058224	0.068819
Δ49CO2	-0.02273	-0.02336	-0.02305	-0.02359	-0.02359	-0.02255	-0.0253	-0.02393	-0.02279	-0.02292	-0.02277	-0.02282	-0.02344	-0.0224	-0.02131	-0.02238	-0.02596	-0.02322	-0.02482	-0.02467
sd	2.132122	2.111651	2.121887	1.573585	1.573585	1.743411	1.664316	1.703864	1.966032	1.839261	1.965284	1.923526	2.320205	1.911792	2.013571	2.081856	2.179377	1.884171	1.553935	1.872494
se	0.27299	0.270369	0.27168	0.201477	0.201477	0.223221	0.213094	0.218157	0.251725	0.235493	0.251629	0.246282	0.297072	0.24478	0.257811	0.266554	0.279041	0.241243	0.198961	0.239748

Run ID	C02415	C02607	C02685	Average	C02416	C02464	C02692	Average	C02422	C02463	C02598	Average	C02423	C02599	Average	C02541	C02600	Average	C02427	C02471
Sample	TC 04.03	TC 04.03	TC 04.03	TC 04.03	TC 04.04	TC 04.04	TC 04.04	TC 04.04	TC 05.01	TC 05.01	TC 05.01	TC 05.01	TC 05.02	TC 05.02	TC 05.02	TC 05.03	TC 05.03	TC 05.03	TC 05.04	TC 05.04
Date	03/06/14	04/03/14	05/21/14		03/06/14	03/14/14	05/22/14		03/07/14	03/14/14	04/02/14		03/07/14	04/02/14		03/25/14	04/02/14		03/08/14	03/15/14
Block	10	10	10	10	10	10	10	10	10	10	10	10	10	10	10	10	10	10	10	10
CC	6	6	6	6	6	6	6	6	6	6	6	6	6	6	6	6	6	6	6	6
	0	0	0	0	0	0	0	0	0	0	0	0	0	0	0	0	0	0	0	0
δ13C	-0.43856	-0.45044	-0.4555	-0.44817	-0.87324	-0.85255	-0.80102	-0.84227	-0.79611	-0.67598	-0.86976	-0.78061	-1.13566	-1.00119	-1.06843	-0.46164	-0.46691	-0.46427	-1.42892	-1.466
sd	0.006677	0.004929	0.005744	0.005783	0.004926	0.00547	0.005299	0.005232	0.005134	0.006223	0.00594	0.005766	0.004617	0.005322	0.004969	0.00733	0.005341	0.006335	0.005037	0.005593
se	0.000855	0.000631	0.000735	0.00074	0.000631	0.0007	0.000678	0.00067	0.000657	0.000797	0.000761	0.000738	0.000591	0.000681	0.000636	0.000938	0.000684	0.000811	0.000645	0.000716
δ18O	4.232733	4.147447	4.138836	4.173005	3.963054	3.956354	3.996937	3.972115	4.235244	4.077216	4.016365	4.109608	3.946084	3.90411	3.925097	4.095574	4.187586	4.14158	3.943353	3.812328
Carbonate	-3.72151	-3.8068	-3.81541	-3.78124	-3.99119	-3.99789	-3.95731	-3.98213	-3.719	-3.87703	-3.93788	-3.84464	-4.00816	-4.05014	-4.02915	-3.85867	-3.76666	-3.81267	-4.01089	-4.14192
sd	0.010903	0.008685	0.009202	0.009596	0.009004	0.010281	0.008778	0.009354	0.008419	0.009752	0.00935	0.009174	0.010294	0.008959	0.009627	0.011525	0.008959	0.010242	0.009288	0.010539
se	0.001396	0.001112	0.001178	0.001229	0.001153	0.001316	0.001124	0.001198	0.001078	0.001249	0.001197	0.001175	0.001318	0.001147	0.001233	0.001476	0.001147	0.001311	0.001189	0.001349
δ45CO2	2.603635	2.589776	2.584751	2.592721	2.186714	2.205949	2.255642	2.216101	2.26779	2.375657	2.191675	2.278374	1.939626	2.064641	2.002133	2.577621	2.575572	2.576596	1.664013	1.625035
sd	0.006677	0.004929	0.005744	0.005783	0.004926	0.00547	0.005299	0.005232	0.005134	0.006223	0.00594	0.005766	0.004617	0.005322	0.004969	0.00733	0.005341	0.006335	0.005037	0.005593
se	0.000855	0.000631	0.000735	0.00074	0.000631	0.0007	0.000678	0.00067	0.000657	0.000797	0.000761	0.000738	0.000591	0.000681	0.000636	0.000938	0.000684	0.000811	0.000645	0.000716
δ46CO2	10.14644	10.06072	10.05205	10.0864	9.874552	9.867862	9.908749	9.883721	10.14822	9.989677	9.928128	10.02201	9.856956	9.815056	9.836006	10.00857	10.10102	10.05479	9.853604	9.721865
sd	0.010903	0.008685	0.009202	0.009596	0.009004	0.010281	0.008778	0.009354	0.008419	0.009752	0.00935	0.009174	0.010294	0.008959	0.009627	0.011525	0.008959	0.010242	0.009288	0.010539
se	0.001396	0.001112	0.001178	0.001229	0.001153	0.001316	0.001124	0.001198	0.001078	0.001249	0.001197	0.001175	0.001318	0.001147	0.001233	0.001476	0.001147	0.001311	0.001189	0.001349
δ47CO2	12.81767	12.70386	12.62172	12.71442	12.07165	12.08255	12.11424	12.08948	12.45202	12.39596	12.14343	12.33047	11.78668	11.88802	11.83735	12.64817	12.72976	12.68896	11.51864	11.32972
sd	0.104701	0.091485	0.063988	0.086724	0.074265	0.080005	0.088622	0.080964	0.078832	0.097897	0.070434	0.082388	0.087799	0.09477	0.091284	0.105717	0.081038	0.093378	0.076629	0.090667
se	0.013406	0.011713	0.008193	0.011104	0.009509	0.010244	0.011347	0.010366	0.010093	0.012534	0.009018	0.010549	0.011241	0.012134	0.011688	0.013536	0.010376	0.011956	0.009811	0.011609
δ48CO2	28.3677	27.94107	25.59443	27.30107	27.18349	27.25854	25.05134	26.49779	27.90747	27.62229	27.39442	27.64139	27.27407	27.0012	27.13764	27.82128	28.0471	27.93419	27.52467	27.07914
sd	0.53411	0.517893	0.509189	0.520397	0.601414	0.597951	0.451838	0.550401	0.589563	0.549812	0.5281	0.555825	0.621432	0.532719	0.577076	0.60324	0.569929	0.586584	0.623904	0.574487
se	0.068386	0.066309	0.065195	0.06663	0.077003	0.07656	0.057852	0.070472	0.075486	0.070396	0.067616	0.071166	0.079566	0.068208	0.073887	0.077237	0.072972	0.075104	0.079883	0.073556
δ49CO2	-6.53033	-2.39971	-9.72008	-6.21671	-0.4365	-1.72178	-1.64473	-1.26767	-0.73556	-0.74454	-0.44986	-0.64332	-3.09002	-3.68813	-3.38907	-3.55396	-6.32959	-4.94178	-10.0544	-3.46258
sd	2.177227	2.185706	1.923179	2.095371	1.928616	1.752185	1.865928	1.84891	1.931197	1.957667	1.651769	1.846878	1.745413	2.154518	1.949966	1.64127	1.946228	1.793749	1.732668	1.980479
se	0.278765	0.279851	0.246238	0.268285	0.246934	0.224344	0.238908	0.236729	0.247264	0.250654	0.211487	0.236468	0.223477	0.275858	0.249668	0.210143	0.249189	0.229666	0.221845	0.253574
Δ47CO2	0.115298	0.100744	0.033239	0.083094	0.072159	0.069673	0.010017	0.050616	0.097739	0.086031	0.085738	0.089836	0.061822	0.074254	0.068038	0.109081	0.101624	0.105352	0.083666	0.065446
sd	0.104701	0.091485	0.063988	0.086724	0.074265	0.080005	0.088622	0.080964	0.078832	0.097897	0.070434	0.082388	0.087799	0.09477	0.091284	0.105717	0.081038	0.093378	0.076629	0.090667
se	0.013406	0.011713	0.008193	0.011104	0.009509	0.010244	0.011347	0.010366	0.010093	0.012534	0.009018	0.010549	0.011241	0.012134	0.011688	0.013536	0.010376	0.011956	0.009811	0.011609
Δ48CO2	7.812505	7.565409	5.282524	6.886813	7.194079	7.281012	5.035355	6.503482	7.357912	7.39464	7.294016	7.348856	7.317999	7.133996	7.225998	7.552028	7.588927	7.570478	7.570409	7.396358
sd	0.53411	0.517893	0.509189	0.520397	0.601414	0.597951	0.451838	0.550401	0.589563	0.549812	0.5281	0.555825	0.621432	0.532719	0.577076	0.60324	0.569929	0.586584	0.623904	0.574487
se	0.068386	0.066309	0.065195	0.06663	0.077003	0.07656	0.057852	0.070472	0.075486	0.070396	0.067616	0.071166	0.079566	0.068208	0.073887	0.077237	0.072972	0.075104	0.079883	0.073556
Δ49CO2	-0.02877	-0.02455	-0.03169	-0.02833	-0.02186	-0.02312	-0.02318	-0.02272	-0.02276	-0.02258	-0.02198	-0.02244	-0.02417	-0.0248	-0.02448	-0.02557	-0.02845	-0.02701	-0.03069	-0.02395
sd	2.177227	2.185706	1.923179	2.095371	1.928616	1.752185	1.865928	1.84891	1.931197	1.957667	1.651769	1.846878	1.745413	2.154518	1.949966	1.64127	1.946228	1.793749	1.732668	1.980479
se	0.278765	0.279851	0.246238	0.268285	0.246934	0.224344	0.238908	0.236729	0.247264	0.250654	0.211487	0.236468	0.223477	0.275858	0.249668	0.210143	0.249189	0.229666	0.221845	0.253574

Run ID	C02601	Average	C02496	C02527	Average	C02495	C02526	C02614	Average	C02494	C02520	C02615	Average	C02493	C02519	C02624	Average	C02487	C02684	C02686	Average
Sample	TC 05.04	TC 05.04	TC 06.01	TC 06.01	TC 06.01	TC 06.02	TC 06.02	TC 06.02	TC 06.02	TC 06.03	TC 06.03	TC 06.03	TC 06.03	TC 06.04	TC 06.04	TC 06.04	TC 06.04	TC 06.05	TC 06.05	TC 06.05	TC 06.05
Date	04/02/14		03/18/14	03/22/14		03/18/14	03/22/14	04/04/14		03/18/14	03/21/14	04/04/14		03/18/14	03/21/14	04/07/14		03/17/14	05/21/14	05/21/14	
Block	10	10	19	10	14.5	10	10	10	10	10	10	10	10	10	10	10	10	10	10	10	10
CC	6	6	6	6	6	6	6	6	6	6	6	6	6	6	6	6	6	6	6	6	6
	0	0	0	0	0	0	0	0	0	0	0	0	0	0	0	0	0	0	0	0	0
δ13C	-1.38772	-1.42755	-0.85411	-0.78006	-0.81708	-1.02178	-0.84825	-0.96333	-0.94445	-0.7674	-0.76748	-0.81849	-0.78446	-0.46859	-0.48859	-0.47865	-0.47861	-0.33673	-0.48301	-0.48076	-0.4335
sd	0.006488	0.005706	0.005103	0.005624	0.005363	0.005212	0.006156	0.005323	0.005564	0.004704	0.00524	0.005306	0.005083	0.005973	0.006057	0.006843	0.006291	0.005545	0.005174	0.00555	0.005423
se	0.000831	0.000731	0.000476	0.00072	0.000598	0.000667	0.000788	0.000682	0.000712	0.000602	0.000671	0.000679	0.000651	0.000765	0.000776	0.000876	0.000806	0.00071	0.000662	0.000711	0.000694
δ18O	3.883786	3.879822	4.02971	4.032475	4.031093	3.826511	3.906775	3.864111	3.865799	3.894151	3.921438	3.929631	3.915073	4.129143	3.996593	4.057584	4.061107	4.117592	4.150303	4.069502	4.112466
Carbonate	-4.07046	-4.07442	-3.92453	-3.92177	-3.92315	-4.12773	-4.04747	-4.09013	-4.08845	-4.06009	-4.03281	-4.02461	-4.03917	-3.8251	-3.95765	-3.89666	-3.89314	-3.83665	-3.80394	-3.88474	-3.84178
sd	0.008596	0.009474	0.009359	0.00885	0.009104	0.009686	0.00883	0.008996	0.009171	0.009143	0.00889	0.008515	0.00885	0.009611	0.010595	0.009841	0.010016	0.009508	0.009478	0.010744	0.00991
se	0.001101	0.001213	0.000873	0.001133	0.001003	0.00124	0.001131	0.001152	0.001174	0.001171	0.001138	0.00109	0.001133	0.001231	0.001357	0.00126	0.001282	0.001217	0.001214	0.001376	0.001269
δ45CO2	1.700842	1.663297	2.206796	2.276459	2.241627	2.042841	2.208417	2.098951	2.116736	2.283978	2.284765	2.237097	2.268614	2.572145	2.549165	2.560438	2.560583	2.695668	2.559268	2.558826	2.604587
sd	0.006488	0.005706	0.005103	0.005624	0.005363	0.005212	0.006156	0.005323	0.005564	0.004704	0.00524	0.005306	0.005083	0.005973	0.006057	0.006843	0.006291	0.005545	0.005174	0.00555	0.005423
se	0.000831	0.000731	0.000476	0.00072	0.000598	0.000667	0.000788	0.000682	0.000712	0.000602	0.000671	0.000679	0.000651	0.000765	0.000776	0.000876	0.000806	0.00071	0.000662	0.000711	0.000694
δ46CO2	9.793833	9.789767	9.941571	9.944503	9.943037	9.737038	9.818051	9.774942	9.776677	9.805533	9.832953	9.841079	9.826522	10.04229	9.90905	9.970358	9.973898	10.03095	10.06352	9.98233	10.0256
sd	0.008596	0.009474	0.009359	0.00885	0.009104	0.009686	0.00883	0.008996	0.009171	0.009143	0.00889	0.008515	0.00885	0.009611	0.010595	0.009841	0.010016	0.009508	0.009478	0.010744	0.00991
se	0.001101	0.001213	0.000873	0.001133	0.001003	0.00124	0.001131	0.001152	0.001174	0.001171	0.001138	0.00109	0.001133	0.001231	0.001357	0.00126	0.001282	0.001217	0.001214	0.001376	0.001269
δ47CO2	11.50019	11.44952	12.16423	12.24866	12.20645	11.77724	12.04127	11.88924	11.90258	12.11557	12.15282	12.12308	12.13049	12.65513	12.49465	12.58641	12.57873	12.79839	12.59344	12.52297	12.63827
sd	0.080406	0.082567	0.09474	0.088875	0.091808	0.092901	0.091104	0.084237	0.089414	0.085216	0.083087	0.088515	0.085606	0.075653	0.086804	0.11139	0.091282	0.072416	0.087557	0.077968	0.079314
se	0.010295	0.010572	0.008835	0.011379	0.010107	0.011895	0.011665	0.010785	0.011448	0.010911	0.010638	0.011333	0.010961	0.009686	0.011114	0.014262	0.011688	0.009272	0.011211	0.009983	0.010155
δ48CO2	28.04917	27.55099	27.58817	27.4579	27.52304	26.89319	27.0124	27.36012	27.08857	27.19486	27.33351	27.39666	27.30834	27.9091	27.4396	27.59825	27.64898	27.83329	25.08553	25.20708	26.04196
sd	0.492908	0.563767	0.539527	0.475775	0.507651	0.609643	0.553563	0.486463	0.54989	0.493525	0.596394	0.476602	0.522173	0.549317	0.599929	0.613775	0.587673	0.596731	0.487224	0.448575	0.510843
se	0.06311	0.072183	0.050311	0.060917	0.055614	0.078057	0.070876	0.062285	0.070406	0.063189	0.07636	0.061023	0.066857	0.070333	0.076813	0.078586	0.075244	0.076404	0.062383	0.057434	0.065407
δ49CO2	-32.0944	-15.2038	-4.08431	-2.13304	-3.10867	-4.54599	-0.78936	-14.3869	-6.57409	-2.88325	-5.61158	-7.2766	-5.25714	-1.32031	-1.9825	-1.25574	-1.51952	-1.81808	-1.69092	-1.69638	-1.73513
sd	1.674504	1.795883	1.642553	1.742574	1.692563	2.513382	2.000351	1.912849	2.142194	1.899651	1.746042	1.631184	1.758959	2.106659	2.036402	1.480084	1.874382	2.364265	1.661238	1.761304	1.928936
se	0.214398	0.229939	0.153169	0.223114	0.188141	0.321806	0.256119	0.244915	0.27428	0.243225	0.223558	0.208852	0.225212	0.26973	0.260735	0.189505	0.23999	0.302713	0.2127	0.225512	0.246975
Δ47CO2	0.085821	0.078311	0.077636	0.086557	0.082096	0.063275	0.074921	0.079292	0.072496	0.082849	0.092107	0.103814	0.092923	0.088714	0.08375	0.103011	0.091825	0.114265	0.020326	0.030336	0.054976
sd	0.080406	0.082567	0.09474	0.088875	0.091808	0.092901	0.091104	0.084237	0.089414	0.085216	0.083087	0.088515	0.085606	0.075653	0.086804	0.11139	0.091282	0.072416	0.087557	0.077968	0.079314
se	0.010295	0.010572	0.008835	0.011379	0.010107	0.011895	0.011665	0.010785	0.011448	0.010911	0.010638	0.011333	0.010961	0.009686	0.011114	0.014262	0.011688	0.009272	0.011211	0.009983	0.010155
Δ48CO2	8.204068	7.723612	7.457161	7.323596	7.390379	7.183704	7.139012	7.566023	7.296246	7.342912	7.424176	7.469886	7.412325	7.570841	7.376376	7.409611	7.452276	7.519136	4.760888	5.041595	5.773873
sd	0.492908	0.563767	0.539527	0.475775	0.507651	0.609643	0.553563	0.486463	0.54989	0.493525	0.596394	0.476602	0.522173	0.549317	0.599929	0.613775	0.587673	0.596731	0.487224	0.448575	0.510843
se	0.06311	0.072183	0.050311	0.060917	0.055614	0.078057	0.070876	0.062285	0.070406	0.063189	0.07636	0.061023	0.066857	0.070333	0.076813	0.078586	0.075244	0.076404	0.062383	0.057434	0.065407
Δ49CO2	-0.0522	-0.03561	-0.02558	-0.02374	-0.02466	-0.02547	-0.02212	-0.03523	-0.02761	-0.02422	-0.02694	-0.02854	-0.02657	-0.02344	-0.02381	-0.02323	-0.02349	-0.02403	-0.02383	-0.02368	-0.02385
sd	1.674504	1.795883	1.642553	1.742574	1.692563	2.513382	2.000351	1.912849	2.142194	1.899651	1.746042	1.631184	1.758959	2.106659	2.036402	1.480084	1.874382	2.364265	1.661238	1.761304	1.928936
se	0.214398	0.229939	0.153169	0.223114	0.188141	0.321806	0.256119	0.244915	0.27428	0.243225	0.223558	0.208852	0.225212	0.26973	0.260735	0.189505	0.23999	0.302713	0.2127	0.225512	0.246975

Run ID	C02486	C02511	C02676	Average	C02485	C02510	C02678	Average	C02479	C02617	C02677	Average	C02503	C02679	Average	C02477	C02502	C02618	Average
Sample	TC 07.01	TC 07.01	TC 07.01	TC 07.01	TC 07.02	TC 07.02	TC 07.02	TC 07.02	TC 07.03	TC 07.03	TC 07.03	TC 07.03	TC 07.04	TC 07.04	TC 07.04	TC 07.05	TC 07.05	TC 07.05	TC 07.05
Date	03/17/14	03/20/14	05/20/14		03/17/14	03/20/14	05/20/14		03/16/14	04/05/14	05/20/14		03/19/14	05/20/14		03/16/14	03/19/14	04/05/14	
Block	10	10	10	10	10	10	10	10	10	10	10	10	10	10	10	10	10	10	10
CC	6	6	6	6	6	6	6	6	6	6	6	6	6	6	6	6	6	6	6
	0	0	0	0	0	0	0	0	0	0	0	0	0	0	0	0	0	0	0
δ13C	-0.51355	-0.52978	-0.42425	-0.48919	-0.79945	-0.67506	-0.72187	-0.73213	-0.43344	-0.3591	-0.329	-0.37385	-1.2287	-1.2057	-1.2172	-0.97734	-0.97583	-0.89111	-0.93347
sd	0.004692	0.005134	0.004224	0.004683	0.004935	0.004963	0.005271	0.005056	0.005365	0.005741	0.005745	0.005617	0.006773	0.00527	0.006021	0.006658	0.006872	0.005339	0.006106
se	0.000601	0.000657	0.000541	0.0006	0.000632	0.000635	0.000675	0.000647	0.000687	0.000735	0.000736	0.000719	0.000867	0.000675	0.000771	0.000852	0.00088	0.000684	0.000782
δ18O	3.989857	4.079959	4.084617	4.051478	3.903407	4.030891	3.987941	3.974079	4.07456	4.073721	4.104555	4.084279	3.961294	3.912698	3.936996	3.906075	4.046162	4.067211	4.056687
Carbonate	-3.96439	-3.87429	-3.86963	-3.90277	-4.05084	-3.92335	-3.9663	-3.98017	-3.87969	-3.88052	-3.84969	-3.86997	-3.99295	-4.04155	-4.01725	-4.04817	-3.90808	-3.88703	-3.89756
sd	0.009174	0.010187	0.010209	0.009857	0.009935	0.009645	0.010314	0.009965	0.009306	0.008659	0.008347	0.008771	0.010411	0.008898	0.009655	0.008431	0.009409	0.007947	0.008678
se	0.001175	0.001304	0.001307	0.001262	0.001272	0.001235	0.001321	0.001276	0.001192	0.001109	0.001069	0.001123	0.001333	0.001139	0.001236	0.001079	0.001205	0.001017	0.001111
δ45CO2	2.525504	2.513107	2.612396	2.550336	2.254158	2.375054	2.329722	2.319645	2.603451	2.673266	2.702518	2.659745	1.852697	1.872767	1.862732	2.087111	2.09296	2.173216	2.133088
sd	0.004692	0.005134	0.004224	0.004683	0.004935	0.004963	0.005271	0.005056	0.005365	0.005741	0.005745	0.005617	0.006773	0.00527	0.006021	0.006658	0.006872	0.005339	0.006106
se	0.000601	0.000657	0.000541	0.0006	0.000632	0.000635	0.000675	0.000647	0.000687	0.000735	0.000736	0.000719	0.000867	0.000675	0.000771	0.000852	0.00088	0.000684	0.000782
δ46CO2	9.90223	9.992736	9.997635	9.9642	9.814767	9.943128	9.899873	9.885923	9.98751	9.986821	10.01787	9.997399	9.872046	9.823262	9.847654	9.81708	9.957851	9.979177	9.968514
sd	0.009174	0.010187	0.010209	0.009857	0.009935	0.009645	0.010314	0.009965	0.009306	0.008659	0.008347	0.008771	0.010411	0.008898	0.009655	0.008431	0.009409	0.007947	0.008678
se	0.001175	0.001304	0.001307	0.001262	0.001272	0.001235	0.001321	0.001276	0.001192	0.001109	0.001069	0.001123	0.001333	0.001139	0.001236	0.001079	0.001205	0.001017	0.001111
δ47CO2	12.4752	12.53047	12.57317	12.52628	12.09715	12.34285	12.1684	12.2028	12.65325	12.72577	12.70765	12.69555	11.70706	11.61761	11.66233	11.91585	12.07149	12.16699	12.11924
sd	0.087617	0.073109	0.082854	0.081193	0.077813	0.076782	0.082778	0.079125	0.089723	0.096051	0.089243	0.091672	0.086512	0.082674	0.084593	0.096283	0.086819	0.072562	0.07969
se	0.011218	0.009361	0.010608	0.010396	0.009963	0.009831	0.010599	0.010131	0.011488	0.012298	0.011426	0.011737	0.011077	0.010585	0.010831	0.012328	0.011116	0.009291	0.010203
δ48CO2	27.3157	27.57871	24.89731	26.59724	27.09234	27.42855	24.88759	26.46949	28.00414	27.89956	25.07698	26.99356	27.13284	24.65754	25.89519	26.89221	27.60213	27.77608	27.68911
sd	0.592429	0.560981	0.478477	0.543962	0.559471	0.498575	0.505592	0.521212	0.473269	0.558138	0.493453	0.508287	0.532412	0.498434	0.515423	0.503823	0.560075	0.581805	0.57094
se	0.075853	0.071826	0.061263	0.069647	0.071633	0.063836	0.064734	0.066734	0.060596	0.071462	0.06318	0.065079	0.068168	0.063818	0.065993	0.064508	0.07171	0.074492	0.073101
δ49CO2	-1.96128	-1.10725	-0.55697	-1.2085	-1.10722	-1.01731	-0.48052	-0.86835	-7.23566	0.859478	-1.1605	-2.51223	-0.6957	-3.37804	-2.03687	7.844638	-3.39892	-5.64052	-4.51972
sd	1.739806	1.700992	1.620956	1.687251	1.868919	2.103102	1.736678	1.9029	1.764505	1.912588	1.637947	1.77168	1.930568	1.610641	1.770605	2.008762	2.241203	1.705458	1.97333
se	0.222759	0.21779	0.207542	0.21603	0.239291	0.269275	0.222359	0.243641	0.225922	0.244882	0.209718	0.22684	0.247184	0.206222	0.226703	0.257196	0.286957	0.218361	0.252659
Δ47CO2	0.095508	0.0746	0.009927	0.060012	0.086299	0.079574	-0.00398	0.053964	0.108078	0.108607	0.030375	0.082353	0.057825	-0.00367	0.027077	0.07668	0.087197	0.078222	0.08271
sd	0.087617	0.073109	0.082854	0.081193	0.077813	0.076782	0.082778	0.079125	0.089723	0.096051	0.089243	0.091672	0.086512	0.082674	0.084593	0.096283	0.086819	0.072562	0.07969
se	0.011218	0.009361	0.010608	0.010396	0.009963	0.009831	0.010599	0.010131	0.011488	0.012298	0.011426	0.011737	0.011077	0.010585	0.010831	0.012328	0.011116	0.009291	0.010203
Δ48CO2	7.2685	7.345813	4.707473	6.440596	7.223951	7.297566	4.89246	6.471326	7.773299	7.672155	4.843338	6.762931	7.149407	4.819339	5.984373	7.023085	7.438364	7.566354	7.502359
sd	0.592429	0.560981	0.478477	0.543962	0.559471	0.498575	0.505592	0.521212	0.473269	0.558138	0.493453	0.508287	0.532412	0.498434	0.515423	0.503823	0.560075	0.581805	0.57094
se	0.075853	0.071826	0.061263	0.069647	0.071633	0.063836	0.064734	0.066734	0.060596	0.071462	0.06318	0.065079	0.068168	0.063818	0.065993	0.064508	0.07171	0.074492	0.073101
Δ49CO2	-0.02375	-0.02308	-0.02265	-0.02316	-0.02247	-0.02275	-0.0221	-0.02244	-0.02915	-0.02131	-0.02337	-0.02461	-0.02176	-0.02431	-0.02304	-0.01354	-0.02482	-0.02714	-0.02598
sd	1.739806	1.700992	1.620956	1.687251	1.868919	2.103102	1.736678	1.9029	1.764505	1.912588	1.637947	1.77168	1.930568	1.610641	1.770605	2.008762	2.241203	1.705458	1.97333
se	0.222759	0.21779	0.207542	0.21603	0.239291	0.269275	0.222359	0.243641	0.225922	0.244882	0.209718	0.22684	0.247184	0.206222	0.226703	0.257196	0.286957	0.218361	0.252659

Run ID	C02562	C02543	C02670	Average	C02561	C02549	C02669	Average	C02570	C02660	Average	C02551	C02661	Average	C02572	C02563	C02662	Average
Sample	TC.08.01	TC 08.01	TC 08.01	TC 08.01	TC.08.02	TC 08.02	TC 08.02	TC 08.02	TC 08.03	TC 08.03	TC 08.03	TC 08.04	TC 08.04	TC 08.04	TC 08.05	TC.08.05	TC 08.05	TC 08.05
Date	03/28/14	03/25/14	05/18/14		03/28/14	03/26/14	05/18/14		03/29/14	05/17/14		03/26/14	05/17/14		03/29/14	03/28/14	05/17/14	
Block	10	10	10	10	7	10	10	9	10	10	10	10	10	10	20	10	10	13.33333
CC	6	6	6	6	6	6	6	6	6	6	6	6	6	6	6	6	6	6
	0	0	0	0	0	0	0	0	0	0	0	0	0	0	0	0	0	0
δ13C	-0.46935	-0.42893	-0.32787	-0.40872	-0.68768	-0.47697	-0.64303	-0.60256	-0.41925	-0.34146	-0.38036	-0.14885	-0.1754	-0.16212	-0.46391	-0.50681	-0.47405	-0.48159
sd	0.005628	0.005743	0.006425	0.005932	0.005367	0.006701	0.005569	0.005879	0.00494	0.004817	0.004878	0.005463	0.005384	0.005424	0.005838	0.006113	0.005818	0.005923
se	0.000721	0.000735	0.000823	0.000759	0.000818	0.000858	0.000713	0.000796	0.000633	0.000617	0.000625	0.000699	0.000689	0.000694	0.000531	0.000783	0.000745	0.000686
δ18O	4.165087	4.029515	4.128647	4.10775	3.948477	3.985907	3.898754	3.94438	4.078931	4.034504	4.056718	4.124136	4.021018	4.072577	3.875562	3.844566	3.934085	3.884738
Carbonate	-3.78916	-3.92473	-3.8256	-3.8465	-4.00577	-3.96834	-4.05549	-4.00987	-3.87531	-3.91974	-3.89753	-3.83011	-3.93323	-3.88167	-4.07868	-4.10968	-4.02016	-4.06951
sd	0.007921	0.007182	0.009281	0.008128	0.010835	0.009412	0.00923	0.009826	0.009605	0.008633	0.009119	0.009304	0.010279	0.009792	0.011405	0.008119	0.01026	0.009928
se	0.001014	0.00092	0.001188	0.001041	0.001652	0.001205	0.001182	0.001346	0.00123	0.001105	0.001168	0.001191	0.001316	0.001254	0.001037	0.00104	0.001314	0.00113
δ45CO2	2.572567	2.606259	2.704343	2.627723	2.360591	2.559744	2.400975	2.440437	2.616915	2.6886	2.652758	2.872393	2.844196	2.858294	2.568533	2.527244	2.56085	2.552209
sd	0.005628	0.005743	0.006425	0.005932	0.005367	0.006701	0.005569	0.005879	0.00494	0.004817	0.004878	0.005463	0.005384	0.005424	0.005838	0.006113	0.005818	0.005923
se	0.000721	0.000735	0.000823	0.000759	0.000818	0.000858	0.000713	0.000796	0.000633	0.000617	0.000625	0.000699	0.000689	0.000694	0.000531	0.000783	0.000745	0.000686
δ46CO2	10.0784	9.942256	10.04208	10.02091	9.860288	9.898337	9.810416	9.856347	9.991932	9.947451	9.969691	10.03792	9.934243	9.98608	9.787482	9.756247	9.846269	9.796666
sd	0.007921	0.007182	0.009281	0.008128	0.010835	0.009412	0.00923	0.009826	0.009605	0.008633	0.009119	0.009304	0.010279	0.009792	0.011405	0.008119	0.01026	0.009928
se	0.001014	0.00092	0.001188	0.001041	0.001652	0.001205	0.001182	0.001346	0.00123	0.001105	0.001168	0.001191	0.001316	0.001254	0.001037	0.00104	0.001314	0.00113
δ47CO2	12.71054	12.61536	12.71354	12.67981	12.27886	12.50868	12.14671	12.31142	12.65468	12.60779	12.63124	12.9829	12.77221	12.87756	12.39306	12.33976	12.36789	12.3669
sd	0.089089	0.091155	0.090533	0.090259	0.094694	0.096488	0.093132	0.094771	0.084085	0.090941	0.087513	0.080154	0.081465	0.080809	0.088472	0.082744	0.078187	0.083134
se	0.011407	0.011671	0.011592	0.011556	0.014441	0.012354	0.011924	0.012906	0.010766	0.011644	0.011205	0.010263	0.01043	0.010347	0.008043	0.010594	0.010011	0.009549
δ48CO2	27.90303	27.73196	24.96963	26.8682	27.41623	27.46072	24.2405	26.37248	26.92725	24.90124	25.91425	27.74805	24.96502	26.35653	26.40992	26.991	24.87542	26.09211
sd	0.606949	0.546886	0.423193	0.525676	0.448605	0.498974	0.419672	0.455751	0.502138	0.490016	0.496077	0.617741	0.509746	0.563743	0.573992	0.601646	0.518672	0.56477
se	0.077712	0.070022	0.054184	0.067306	0.068412	0.063887	0.053734	0.062011	0.064292	0.06274	0.063516	0.079094	0.065266	0.07218	0.052181	0.077033	0.066409	0.065208
δ49CO2	-2.79717	-5.15324	4.461966	-1.16281	-4.8503	-1.5573	5.560581	-0.28234	14.64485	-1.53252	6.556167	-1.01274	-1.06059	-1.03666	15.93279	-1.40193	-0.55514	4.658573
sd	1.63533	1.932042	1.541222	1.702865	1.835843	1.748798	1.787541	1.790727	2.033834	1.685314	1.859574	1.947107	1.904814	1.925961	1.958325	1.758131	1.727375	1.81461
se	0.209383	0.247373	0.197333	0.218029	0.279963	0.223911	0.228871	0.244248	0.260406	0.215782	0.238094	0.249302	0.243886	0.246594	0.17803	0.225106	0.221168	0.208101
Δ47CO2	0.10778	0.111898	0.010709	0.076796	0.112008	0.097176	-0.01144	0.065915	0.091344	0.014726	0.053035	0.108021	0.030057	0.069039	0.082044	0.102297	0.007751	0.06403
sd	0.089089	0.091155	0.090533	0.090259	0.094694	0.096488	0.093132	0.094771	0.084085	0.090941	0.087513	0.080154	0.081465	0.080809	0.088472	0.082744	0.078187	0.083134
se	0.011407	0.011671	0.011592	0.011556	0.014441	0.012354	0.011924	0.012906	0.010766	0.011644	0.011205	0.010263	0.01043	0.010347	0.008043	0.010594	0.010011	0.009549
Δ48CO2	7.492836	7.596767	4.68994	6.593181	7.450744	7.418461	4.435941	6.435049	6.708793	4.811171	5.759982	7.421691	4.899984	6.160837	6.609131	7.24132	4.987214	6.279222
sd	0.606949	0.546886	0.423193	0.525676	0.448605	0.498974	0.419672	0.455751	0.502138	0.490016	0.496077	0.617741	0.509746	0.563743	0.573992	0.601646	0.518672	0.56477
se	0.077712	0.070022	0.054184	0.067306	0.068412	0.063887	0.053734	0.062011	0.064292	0.06274	0.063516	0.079094	0.065266	0.07218	0.052181	0.077033	0.066409	0.065208
Δ49CO2	-0.02496	-0.02704	-0.01792	-0.02331	-0.02633	-0.02339	-0.01609	-0.02194	-0.00778	-0.02359	-0.01568	-0.02344	-0.02326	-0.02335	-0.00607	-0.02293	-0.02231	-0.0171
sd	1.63533	1.932042	1.541222	1.702865	1.835843	1.748798	1.787541	1.790727	2.033834	1.685314	1.859574	1.947107	1.904814	1.925961	1.958325	1.758131	1.727375	1.81461
se	0.209383	0.247373	0.197333	0.218029	0.279963	0.223911	0.228871	0.244248	0.260406	0.215782	0.238094	0.249302	0.243886	0.246594	0.17803	0.225106	0.221168	0.208101

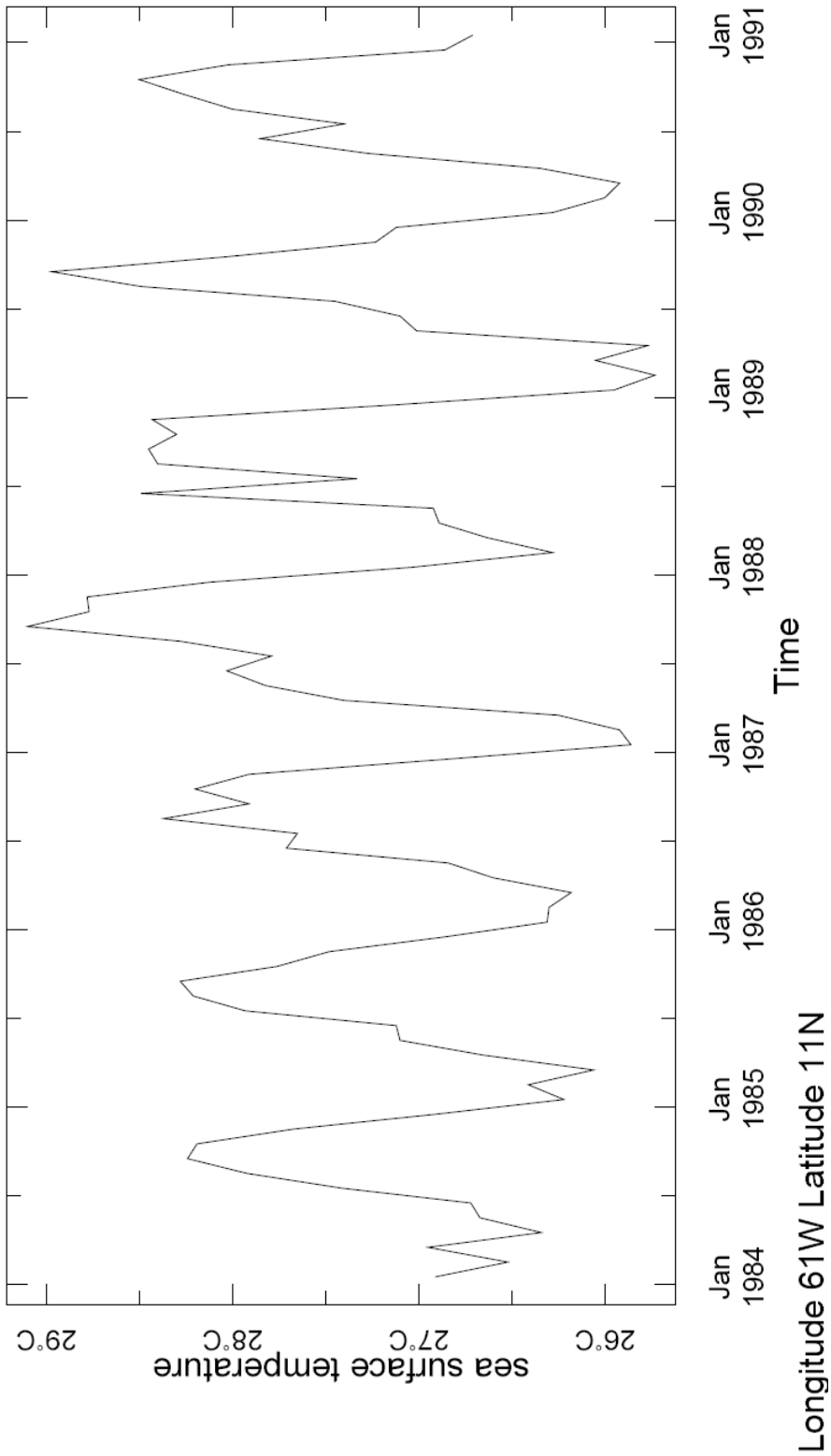
sea surface temperature
26°C
27°C
28°C
29°C
Jan 1984
Jan 1985
Jan 1986
Jan 1987
Jan 1988
Jan 1989
Jan 1990
Jan 1991
Time
Longitude 61W Latitude 11N

APPENDIX 3. Clumped isotope data of the Bahamian calcretes

Run ID	C02804	C02805	C02811	C02812	C02813	C02814	C02819	C02820	C02821	C02822	C02825	C02826	C02830	C02793	C02794	C02795	C02823	C02802	C02803
Sample	CC 01	CC 02	CC 03	CC 04	CC 05	CC 06	CC 07	CC 08	CC 09	CC 10	CC 11	CC 12	CC 13	HC 01	HC 02	HC 03	HC 04	HC 05	HC 06
Date	06/14/14	06/14/14	06/15/14	06/15/14	06/15/14	06/15/14	06/16/14	06/16/14	06/16/14	06/16/14	06/17/14	06/17/14	06/19/14	06/13/14	06/13/14	06/13/14	06/16/14	06/14/14	06/14/14
Block	10	10	10	10	10	10	10	10	20	10	10	10	10	10	10	10	10	10	10
CC	6	6	6	6	6	6	6	6	6	6	6	6	6	6	6	6	6	6	6
	0	0	0	0	0	0	0	0	0	0	0	0	0	0	0	0	0	0	0
δ13C	-5.359277	-8.74096	-8.918272	-8.90326	-9.22837	-9.163125	-8.809495	-9.546161	-8.699688	-8.260122	3.614984	2.408892	2.6426484	-0.658766	-2.6489	-4.88115	-5.220104	-4.25882	-1.06138
sd	0.005272	0.004108	0.00627	0.005152	0.005343	0.00493	0.004861	0.005687	0.005321	0.004633	0.005827	0.005206	0.0050044	0.014441	0.005817	0.005091	0.005207	0.005558	0.005549
se	0.000675	0.000526	0.000803	0.00066	0.000684	0.000631	0.000622	0.000728	0.000484	0.000593	0.000746	0.000667	0.0006408	0.001849	0.000745	0.000652	0.000667	0.000712	0.000711
δ18O	5.163677	5.19612	5.200436	5.209955	4.777397	4.754017	4.985421	5.166205	5.100263	5.26555	7.495381	6.505477	6.6868259	4.984395	5.144484	5.114452	4.792192	4.822509	5.179008
Carbonate	-2.790568	-2.75813	-2.753809	-2.74429	-3.17685	-3.200228	-2.968824	-2.78804	-2.853982	-2.688696	-0.458865	-1.448768	-1.267419	-2.96985	-2.80976	-2.839793	-3.162053	-3.13174	-2.77524
sd	0.008102	0.009652	0.010814	0.010767	0.010041	0.008825	0.008629	0.009695	0.009381	0.011025	0.007834	0.00796	0.0093213	0.019159	0.009419	0.008155	0.01048	0.010265	0.009139
se	0.001037	0.001236	0.001385	0.001379	0.001286	0.00113	0.001105	0.001241	0.000853	0.001412	0.001003	0.001019	0.0011935	0.002453	0.001206	0.001044	0.001342	0.001314	0.00117
δ45CO2	-1.990109	-5.16628	-5.332733	-5.31833	-5.63745	-5.576885	-5.237327	-5.923735	-5.130531	-4.712323	6.51511	5.350704	5.5760502	2.420501	0.55577	-1.542449	-1.871089	-0.96698	2.048378
sd	0.005272	0.004108	0.00627	0.005152	0.005343	0.00493	0.004861	0.005687	0.005321	0.004633	0.005827	0.005206	0.0050044	0.014441	0.005817	0.005091	0.005207	0.005558	0.005549
se	0.000675	0.000526	0.000803	0.00066	0.000684	0.000631	0.000622	0.000728	0.000484	0.000593	0.000746	0.000667	0.0006408	0.001849	0.000745	0.000652	0.000667	0.000712	0.000711
δ46CO2	11.07171	11.0973	11.10127	11.11087	10.67554	10.65218	10.88544	11.06557	11.00106	11.16806	13.43335	12.43613	12.618845	10.9013	11.05804	11.02324	10.69871	10.73116	11.09602
sd	0.008102	0.009652	0.010814	0.010767	0.010041	0.008825	0.008629	0.009695	0.009381	0.011025	0.007834	0.00796	0.0093213	0.019159	0.009419	0.008155	0.01048	0.010265	0.009139
se	0.001037	0.001236	0.001385	0.001379	0.001286	0.00113	0.001105	0.001241	0.000853	0.001412	0.001003	0.001019	0.0011935	0.002453	0.001206	0.001044	0.001342	0.001314	0.00117
δ47CO2	8.724824	5.407824	5.1904	5.23905	4.462221	4.470456	5.052759	4.51135	5.317425	5.900581	20.27448	18.00814	18.449417	13.30578	11.48312	9.177963	8.471986	9.547784	13.1414
sd	0.083084	0.097554	0.071561	0.1004	0.09312	0.091774	0.079227	0.08523	0.084641	0.080304	0.092088	0.081578	0.0751635	0.074677	0.079274	0.089033	0.081994	0.094943	0.090654
se	0.010638	0.01249	0.009162	0.012855	0.011923	0.011751	0.010144	0.010913	0.007695	0.010282	0.011791	0.010445	0.0096237	0.009561	0.01015	0.011399	0.010498	0.012156	0.011607
δ48CO2	26.44984	27.81944	27.24811	27.27172	27.05394	26.45787	26.88636	27.16586	27.13732	28.24819	33.54292	30.50393	35.21606	28.21573	28.08554	28.46347	26.55085	26.05015	27.98872
sd	0.75851	0.637176	0.513914	0.517574	0.495268	0.475505	0.429548	0.502923	0.554399	0.519587	0.501136	0.49307	0.568305	0.580632	0.547827	0.464803	0.441749	1.075451	0.679011
se	0.097117	0.081582	0.0658	0.066269	0.063413	0.060882	0.054998	0.064393	0.0504	0.066526	0.064164	0.063131	0.072764	0.074342	0.070142	0.059512	0.05656	0.137697	0.086938
δ49CO2	-8.758783	-7.65054	-4.33818	-5.70928	-5.47178	-3.441028	-3.14635	-2.500656	-3.327068	-3.102021	-3.490035	-2.669274	-5.58306	-3.227453	-3.34454	-3.025294	-3.050961	-13.7387	-38.8476
sd	2.60495	2.902888	2.862602	2.109412	2.374006	1.965813	2.13007	2.034447	2.114347	1.882225	1.681196	1.77683	1.7806664	1.636467	1.505604	1.922048	1.828558	3.373624	3.266732
se	0.33353	0.371677	0.366519	0.270083	0.30396	0.251697	0.272727	0.260484	0.192213	0.240994	0.215255	0.2275	0.227991	0.209528	0.192773	0.246093	0.234123	0.431948	0.418262
Δ47CO2	-0.102451	-0.1354	-0.183041	-0.15892	-0.17723	-0.209049	-0.208655	-0.211136	-0.168635	-0.184585	0.239239	0.177751	0.2024717	0.049783	0.015699	-0.068354	-0.11273	-0.01135	0.080535
sd	0.083084	0.097554	0.071561	0.1004	0.09312	0.091774	0.079227	0.08523	0.084641	0.080304	0.092088	0.081578	0.0751635	0.074677	0.079274	0.089033	0.081994	0.094943	0.090654
se	0.010638	0.01249	0.009162	0.012855	0.011923	0.011751	0.010144	0.010913	0.007695	0.010282	0.011791	0.010445	0.0096237	0.009561	0.01015	0.011399	0.010498	0.012156	0.011607
Δ48CO2	4.092649	5.381496	4.814742	4.818763	5.471361	4.934262	4.889859	4.80523	4.905546	5.66012	6.32471	5.343276	9.5759297	6.159245	5.719933	6.158896	4.932792	4.378137	5.549682
sd	0.75851	0.637176	0.513914	0.517574	0.495268	0.475505	0.429548	0.502923	0.554399	0.519587	0.501136	0.49307	0.568305	0.580632	0.547827	0.464803	0.441749	1.075451	0.679011
se	0.097117	0.081582	0.0658	0.066269	0.063413	0.060882	0.054998	0.064393	0.0504	0.066526	0.064164	0.063131	0.072764	0.074342	0.070142	0.059512	0.05656	0.137697	0.086938
Δ49CO2	-0.027954	-0.02361	-0.020184	-0.02157	-0.02017	-0.018187	-0.018699	-0.017687	-0.01921	-0.019746	-0.036003	-0.032147	-0.035547	-0.02678	-0.02526	-0.022705	-0.02177	-0.03325	-0.06154
sd	2.60495	2.902888	2.862602	2.109412	2.374006	1.965813	2.13007	2.034447	2.114347	1.882225	1.681196	1.77683	1.7806664	1.636467	1.505604	1.922048	1.828558	3.373624	3.266732
se	0.33353	0.371677	0.366519	0.270083	0.30396	0.251697	0.272727	0.260484	0.192213	0.240994	0.215255	0.2275	0.227991	0.209528	0.192773	0.246093	0.234123	0.431948	0.418262

Sample	Depth	δ13C	sd	δ18O	sd	Δ47	Dennis	Fernandez	Henkes	Tang	Wacker	δ18Ow
Unit	(cm)	(‰)		(‰)			T (°C)	T (°C)	T (°C)	T (°C)	T (°C)	(‰)
C05.01	0	-0.09	0.01	-3.32	0.01	0.76	14.79	6.76	1.41	2.54	-6.35	-3.02
C05.02	4	-3.54	0.01	-3.64	0.01	0.76	15.03	7.12	1.81	2.88	-5.99	-3.29
C05.03	8	-3.77	0.01	-2.92	0.01	0.75	17.02	10.17	5.21	5.78	-2.87	-2.14
C05.04	12	-3.91	0.01	-3.39	0.01	0.75	17.69	11.19	6.35	6.74	-1.83	-2.47
C05.05	16	-2.61	0.01	-3.49	0.01	0.78	10.78	0.74	-5.26	-3.20	-12.48	-4.07
C05.06	20	-0.60	0.01	-3.44	0.01	0.80	8.31	-2.90	-9.25	-6.66	-16.16	-4.59
C05.07	24	-3.15	0.01	-3.99	0.01	0.74	19.35	13.77	9.24	9.19	0.82	-2.72
C05.08	28	-3.05	0.01	-3.87	0.01	0.76	15.94	8.51	3.36	4.20	-4.56	-3.32
C05.09	32	-2.43	0.01	-3.96	0.01	0.75	17.77	11.31	6.49	6.86	-1.70	-3.02
C05.10	36	-3.03	0.01	-4.12	0.01	0.74	19.63	14.21	9.73	9.61	1.27	-2.79
C05.11	40	-0.69	0.01	-3.85	0.01	0.74	19.00	13.22	8.62	8.67	0.25	-2.65
C05.12	44	-2.27	0.01	-4.60	0.01	0.76	16.12	8.78	3.66	4.46	-4.29	-4.01
C05.13	48	-2.46	0.01	-4.47	0.01	0.71	26.18	24.64	21.54	19.47	12.00	-1.78
C05.14	52	-3.66	0.01	-4.92	0.01	0.74	18.24	12.05	7.31	7.56	-0.95	-3.88
C05.15	56	-5.49	0.56	-4.79	0.51	0.66	35.65	40.54	39.91	34.44	28.55	-0.24
C05.16	60	0.01	3.64	-4.31	0.75	16.84	9.89	4.90	5.51	-3.16	-3.16	-3.57

Table: *Calculated δ18O of the fluid values, stable isotope (^{13}C and ^{18}O) isotope analyses and mean temperature estimates using five equations and Δ_{47} values of CO_2 of the LC 05.01(Dominican Republic Project) calcrete complex core samples performed by phosphoric acid digestion at 90°C are summarized including their standard deviations and depth of the measured samples.*